

REGULATION OF SNARE-MEDIATED SYNAPTIC VESICLE RELEASE  
BY SYNAPTOTAGMINS AND COMPLEXINS

APPROVED BY SUPERVISORY COMMITTEE

---

Thomas C. Südhof, M. D. (Mentor)

---

P. Robin Hiesinger, Ph.D. (Committee Chair)

---

Ege T. Kavalali, Ph.D. (Program Chair)

---

Jane E. Johnson, Ph.D.

---

Robert E. Hammer, Ph.D.

---

To my dear grandfather in heaven, Il Seup Han,  
who will be most proud of his little Miss Korea's accomplishment.

REGULATION OF SNARE-MEDIATED SYNAPTIC VESICLE RELEASE  
BY SYNAPTOTAGMINS AND COMPLEXINS

by

YEA JIN KAESER-WOO

DISSERTATION

Presented to the Faculty of the Graduate School of Biomedical Sciences

The University of Texas Southwestern Medical Center at Dallas

In Partial Fulfillment of the Requirements

For the Degree of

DOCTOR OF PHILOSOPHY

The University of Texas Southwestern Medical Center at Dallas

Dallas, Texas

June, 2010

Copyright

by

YEA JIN KAESER-WOO, 2010

All Rights Reserved

## ACKNOWLEDGEMENTS

My deepest gratitude goes to my mentor, Dr. Thomas C. Südhof, for his continuous support and challenging creativity. He is undoubtedly an incredible scientist and I am proud that I could be trained under his mentoring.

The actual 'how-to' for all experiments during my graduate studies were taught by a number of highly skilled scientists in Südhof Lab, especially Drs. Yun Wang, Anton Maximov, Pascal S. Kaeser, Zhiping Pang, Ok-Ho Shin. With their help, I was able to learn various experimental techniques related to molecular and cell biology, biochemistry, mouse genetics, and many more. All the other Südhof lab members, including Drs. Marc F. Bolliger, Manu Sharma, Jacqueline Burré, Antony Boucard, and Peter Bronk and Yingsha Zhang, provided me with trouble-shooting tips and created a stimulating scientific and social environment in the Südhof lab. The technical support staffs Jason Mitchell, Lin Jordan, Iza Kornblum, and Eva Borowicz have provided excellent assistance with mouse colony management and reagent preparations.

Design of synaptotagmin 12 S97A gene targeting would not have been possible without the excellent guidance of Dr. Pascal S. Kaeser. The Transgenic Technology Core at UT Southwestern under the supervision of Dr. Robert E. Hammer has provided outstanding service with the ES cell electroporation and blastocyst injection. With Dr. Pablo E. Castillo and his graduate student Thomas Younts at Albert Einstein College of Medicine we have initiated a fruitful collaboration for the analysis of Syt 12 mutant mice.

The entire electrophysiology data related to complexins have been recorded by Dr. Xiaofei Yang, with whom I shared the fascination for the complexions of complexins over the past years. I also thank Dr. Jiong Tang for providing constructs and for his kind advice on complexin biochemistry.

My thesis committee members, Drs. P. Robin Hiesinger, Jane E. Johnson, Robert E. Hammer, and Ege T. Kavalali, have provided long-term support not only for academic part of my thesis but also for the administrative part of program completion.

Lastly, my beloved parents and my brother Sang In were always there for me in every step of my life to this accomplishment. I deeply thank my husband and colleague, Dr. Pascal S. Kaeser, who has made this scientific journey truly fulfilling with his love and support.

REGULATION OF SNARE-MEDIATED SYNAPTIC VESICLE RELEASE  
BY SYNAPTOTAGMINS AND COMPLEXINS

Publication No. \_\_\_\_\_

YEA JIN KAESER-WOO, Ph.D.

The University of Texas Southwestern Medical Center at Dallas, 2010

ADVISOR: THOMAS C. SÜDHOF, M.D.

In the brain, neurons communicate with each other by synaptic transmission. This process includes release of neurotransmitter from vesicles in the presynaptic neuron into the synaptic cleft, and sensing of these neurotransmitters by the postsynaptic neuron with specific receptors. Long-lasting changes in the strength of synaptic contacts between neurons in the human brain, a process that is referred to as long-term synaptic plasticity, are the cellular correlates that underlie learning and memory.

Synaptic transmission is initiated when an action potential arrives at the presynaptic terminal, and induces  $\text{Ca}^{2+}$  influx through voltage-gated  $\text{Ca}^{2+}$  channels. The SNARE (Soluble *N*-ethylmaleimide-sensitive-factor Attachment Protein Receptors) complex is the core component of the fusion machinery in the presynaptic terminal, as it forms a physical bridge between the vesicular membrane and the presynaptic target membrane that delivers the force to fuse the two membranes. Additional presynaptic proteins are required to activate or suppress neurotransmitter release which allows the presynaptic neuron to tightly control and regulate the process of neurotransmitter release. Among these proteins are synaptotagmins and complexins, two protein families that directly interact with the SNARE complex, and that are interdependent to each other in regulating SNARE-mediated synaptic vesicle release: complexin clamps neurotransmitter release until synaptotagmin is recruited by  $\text{Ca}^{2+}$  influx, and then it activates SNARE-mediated fusion process together with synaptotagmin.

Here I describe the prospective *in vivo* function of synaptotagmin 12, a novel isoform of synaptotagmin, which lacks the typical  $\text{Ca}^{2+}$  binding residues of synaptotagmin, but instead contains a unique sequence motif which can be phosphorylated by cAMP-dependent protein kinase A. By using gene targeting method, I directly examined whether phosphorylation of synaptotagmin 12 is involved in presynaptic forms of long-term plasticity. In parallel, I developed a structure-function approach to functionally dissect how individual domains of

complexin contribute to its dichotomic functions of clamping and activating neurotransmitter release. With this approach, we focused on how the accessory alpha-helix of complexin participates in SNARE-mediated synaptic fusion.

## TABLE OF CONTENTS

COMMITTEE SIGNATURE.....	i
DEDICATION .....	ii
TITLE PAGE .....	iii
COPY RIGHT.....	iv
ACKNOWLEDGEMENTS .....	v
ABSTRACT.. .....	vii
TABLE OF CONTENTS .....	x
LIST OF FIGURES .....	xiv
LIST OF ABBREVIATIONS .....	xix
CHAPTER I: INTRODUCTION	
1.1 Overview of the nervous system.....	1
1.1.1 Neurons and synapses .....	1
1.1.2 Synaptic transmission and the Synaptic vesicle cycle.....	3
1.2 Essential proteins for synaptic vesicle fusion.....	8
1.2.1 SNARE proteins.....	8
1.2.2 Sec1/Munc18-like (SM) proteins.....	11
1.3 Synaptotagmins.....	13
1.3.1 Overview.....	13
1.3.2 Synaptotagmin 12.....	15
1.3.2 Synaptotagmin 12 as a PKA target in Presynaptic long-term plasticity.....	16

1.4 Complexin.....	20
1.4.1 Dual function of complexin in SNARE-mediated vesicle fusion..	20
1.4.2 Functional domains of complexin.....	21
1.4.3 Function of complexin in SNARE-mediated fusion.....	22
1.4.4 Synaptotagmin-switch model of complexin function.....	22
1.5 Major questions.....	26
 CHAPTER II: POTENTIAL FUNCTION OF SYT 12 IN PRESYNAPTIC LONG-TERM PLASTICITY	
2.1 Introduction.....	27
2.2 Materials and Methods.....	29
2.2.1 Molecular cloning of Syt 12 S97A targeting vector.....	29
2.2.2 Southern blotting.....	30
2.2.3 Syt 12 Phospho-specific antibody.....	31
2.2.4 Protein quantification.....	31
2.2.5 Genotyping.....	32
2.2.6 Mouse breeding.....	33
2.2.7 qRT-PCR measurement of mRNA.....	33
2.2.8 Electrophysiology.....	34
2.3 Results.....	36
2.3.1 Generation of Syt 12 S97A knockin and Syt 12 KO.....	36
2.3.2 Survival analysis of Syt 12 S97A knockin and Syt 12 KO mice...41	

2.3.3 Testing of newly generated phospho-specific antibodies in the Syt 12 S97A knockin antibodies.....	42
2.3.4 Assessment of the Syt 12 KO animals by Western blotting and RT-PCR .....	43
2.3.5 Protein composition of brains of Syt 12 mutant mice.....	45
2.3.6 Synaptic transmission in the Syt 12 KO animals.....	48
2.3.7 Basal inhibitory synaptic transmission in Syt 12 KO mice.....	49
2.3.8 Presynaptic forms of long-term plasticity in Syt 12 KO mice.....	49
2.4 Discussion and future perspectives.....	54
CHAPTER III: COMPLEXIN CLAMPS FUSION BY BLOCKING A SECONDARY $Ca^{2+}$ -SENSOR VIA ITS ACCESORY ALPHA-HELIX	
3.1 Introduction.....	58
3.2 Materials and Methods.....	59
3.2.1 Neuronal cultures.....	59
3.2.2 Generation and validation of KD lentiviruses and rescue constructs.....	59
3.2.3 Protein purification and GST-pulldown assay.....	60
3.2.4 Imaging experiments.....	61
3.2.5 Electrophysiology.....	61
3.3 Results.....	62
3.3.1 Complexin clamps an auxiliary $Ca^{2+}$ -sensor .....	62
3.3.2 Mutants in the accessory $\alpha$ -helix of complexin.....	67
3.3.3 Effects of accessory $\alpha$ -helix mutations on mEPSCs release.....	69

3.3.4 Complexin is essential for vesicle priming.....	72
3.3.5 mEPSCs are uniformly activated in all synapses upon complexin KD.....	76
3.3.6 Complexin KD activates delayed release.....	80
3.3.7 Synaptobrevin WW-sequence clamps and activates release similar to complexin.....	84
3.4 Discussion .....	89
3.5 Future perspectives.....	97
3.5.1 Analyzing the function of C-terminal complexin.....	97
3.5.2 Analyzing C-terminal complexin function by flipped SNARE fusion assay.....	99
BIBLIOGRAPHY .....	100

## LIST OF FIGURES

Figure 1.1 A typical vertebrate neuron.....	2
Figure 1.2 Reaction sequence and timing of synaptic transmission.....	3
Figure 1.3 The synaptic vesicle cycle.....	5
Figure 1.4 The ribbon diagrams represent the crystal structure of the core complex and the NMR structure of the amino-terminal Habc domain of syntaxin 1.....	10
Figure 1.5 SM proteins are designed to bind four-helix bundles.....	12
Figure 1.6 Domain structures of synaptotagmins 1–13.....	14
Figure 1.7 Well-described forms of LTP and LTD.....	17
Figure 1.8 Functional domain structure of complexin.....	21
Figure 1.9 Model for complexin and synaptotagmin 1 function in Ca <sup>2+</sup> -triggered release.....	24
Figure 2.1 Cloning of Syt 12 S97A knockin targeting vector.....	29
Figure 2.2 Generation of Syt 12 S97A knockin and constitutive Syt 12 KO mice.....	38
Figure 2.3 Confirmation of homologous recombination by Southern blot and PCR genotyping.....	41
Figure 2.4 Survival analyses of Syt 12 S97A knockin and Syt 12 KO.....	42
Figure 2.5 Measurement of Syt 12 expression by Western blot and RT-PCR.....	45
Figure 2.6 Syt 12 S97A knockin protein quantification.....	47
Figure 2.7 Syt 12 KO protein quantification.....	48
Figure 2.8 Characterization of basal inhibitory synaptic transmission.....	51
Figure 2.9 Presynaptic forms of long-term plasticity in Syt 12 KO mice.....	53

Fig 3.1 Complexin clamps a Ca <sup>2+</sup> -dependent fusion mechanism.....	65
Figure 3.2 Ca <sup>2+</sup> and complexin KD do not affect mEPSC amplitudes, although they control mEPSC frequencies. ....	67
Figure 3.3 Complexin is evolutionarily conserved in all animals.....	69
Figure 3.4 Complexin superclamp- and poorclamp-mutants decrease or increase, respectively, spontaneous but not evoked release.....	71
Figure 3.5 Complexin WW- and AA-mutations increase spontaneous mEPSCs-release without altering evoked release. ....	74
Figure 3.6 Distinct apparent Ca <sup>2+</sup> -affinities and Ca <sup>2+</sup> -cooperativities of spontaneous release in wild-type and complexin mutant synapses .....	76
Figure 3.7 Complexin KD in rat neurons replicates effect of complexin KD in mouse neurons.....	78
Figure 3.8 Synaptotagmin antibody uptake reveals that complexin KD causes uniform activation of spontaneous synaptic fusion. ....	80
Figure 3.9 Effects of complexin and synaptotagmin-1 KDs on delayed release. ....	82
Figure 3.10 Kinetic analysis of evoked NMDA receptor-dependent EPSCs, and validation of the synaptotagmin-1 KD by lentivirally delivered shRNA. ....	84
Figure 3.11 WA-mutation of synaptobrevin/VAMP-2 increases mEPSCs frequency by unclamping secondary Ca <sup>2+</sup> -sensor.....	88

## LIST OF DEFINITIONS

AP	Action potential
Cpx1	complexin 1
DMEM	Dulbecco's Modified Eagle Medium
EPSC	Excitatory postsynaptic current
MEM	minimal essential medium
GST	glutathione-S-transferase
iLTD	endocannabinoid dependent, inhibitory LTD
IPSC	Inhibitory postsynaptic current
KO	Knock-out
LTP	long-term plasticity
LTD	long-term depression
mfLTP	mossy fiber LTP
mIPSC	Miniature inhibitory postsynaptic current
NSF	N-ethylmaleimide-sensitive factor
PAGE	polyacrylamide gel electrophoresis
PCR	polymerase chain reaction
PKA	cyclic AMP dependent protein kinase A
RRP	Readily-releasable pool
SM proteins	Sec1/Munc18 protein family
SNAP	soluble NSF attachment protein
SNAP-25	synaptosome-associated protein of 25 kDa

SNARE	soluble NSF attachment receptor element
SNARE core complex	SNARE complex containing only SNARE motifs
Syb 2	synaptobrevin 2
Syt 1	synaptotagmin 1
Syt 12	synaptotagmin 12
Stx1A	syntaxin 1A

## **CHAPTER 1: INTRODUCTION**

### **1.1 Overview of the nervous system**

#### **1.1.1 Neurons and synapses**

The vertebrate central nervous system contains neurons as the primary functional units and many other cell types for structural, metabolic and immunologic support. The latter include glial cells, microglial cells and blood vessels, and these supportive structures are absolutely required for all functions of the human brain. These functions include cognition, learning and memory, and controlling motor and sensory systems, and they rely on communication between approximately 100 billions of neurons (Kandel, 2001; Williams and Herrup, 1988).

A typical neuron is divided into 3 morphological parts: soma (or cell body), dendrite, and axon (Figure 1.1 and (Bruce Alberts, 2002)). The soma gives rise to several dendrites and to a single axon which can extend over a large distance or project locally. In a prototypical neuron, the axon forms morphological contacts with cell bodies and dendrites of other neurons called “synapses”. At these synaptic sites, neurons send signals from the presynaptic boutons to their postsynaptic targets. Within the axon, the electrical signal called “action potential” propagates into the presynaptic bouton, and this signal is translated into a membrane trafficking reaction where synaptic vesicles fuse in an area called active zone with the presynaptic plasma membrane to release their

neurotransmitters into the synaptic cleft (Akert et al., 1971; Couteaux and Pecot-Dechavassine, 1970; Katz, 1969; Sudhof, 2004). These transmitters are sensed by receptors on dendrites or cell bodies of the postsynaptic neurons, and then translated into graded receptor potential to induce the necessary effects in the postsynaptic compartment of the synapse (Kim and Huganir, 1999; Thomas and Huganir, 2004). In all these processes during neurotransmission,  $\text{Ca}^{2+}$  ions play a fundamental role. Presynaptically,  $\text{Ca}^{2+}$  ions induce fusion and govern a number of regulatory processes that modulate synaptic transmission use-dependently (Neher and Sakaba, 2008). Postsynaptically,  $\text{Ca}^{2+}$  ions are widely involved in intracellular signaling processes that determine how neurotransmitters are sensed.

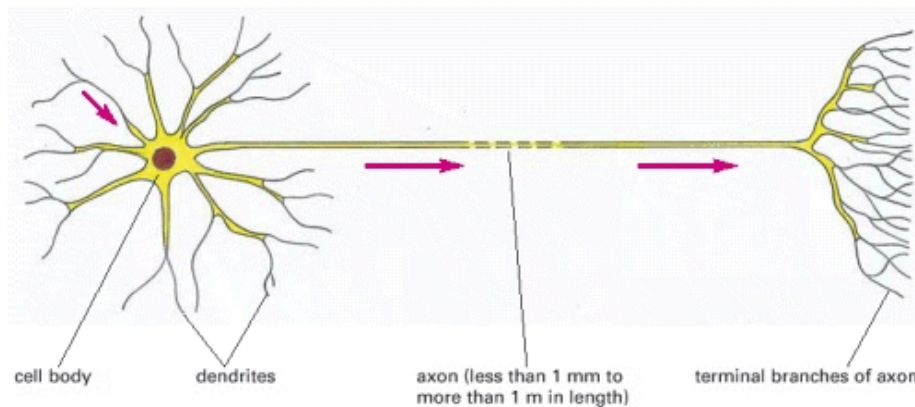


Figure 1.1 A typical vertebrate neuron. The arrows indicate the direction in which signals are conveyed. The single axon conducts signals away from the cell body, while the multiple dendrites receive signals from the axons of other neurons. The nerve terminals end on the dendrites or cell body of other neurons or on other cell types, such as muscle or gland cells (Bruce Alberts, 2002).

### 1.1.2 Synaptic transmission and the synaptic vesicle cycle

The best physiological description of how the arriving action potential induces phasic, synchronous neurotransmitter release was obtained from the synapses formed at the calyx of Held (Meinrenken et al., 2003). When an action potential invades the calyx terminal, voltage gated  $\text{Ca}^{2+}$  channels which are tightly coupled to the active zone open their channel mouth, and  $\text{Ca}^{2+}$  levels in the terminal begin to rise quickly. The increased  $\text{Ca}^{2+}$  levels are sensed by the  $\text{Ca}^{2+}$  sensor synaptotagmin which is located on synaptic vesicles, and the vesicles begin to fuse with the presynaptic membrane (Figure 1.2) (Helmchen et al., 1997). Postsynaptic receptors sense the neurotransmitters, inducing postsynaptic currents which in turn lead to triggering an action potential in the postsynaptic neuron.

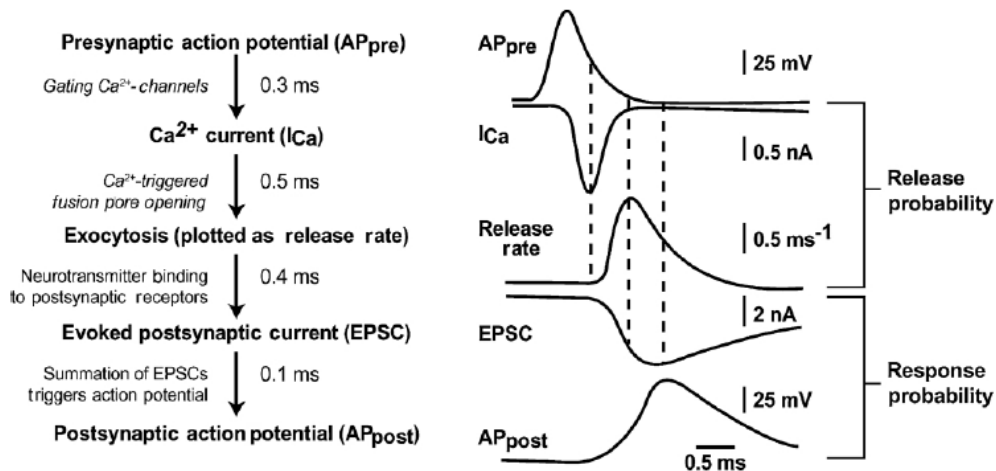


Figure 1.2 Reaction sequence and timing of synaptic transmission. The principal reactions with the associated time constants are shown on the left, and traces from the corresponding reactions in the calyx of Held synapses are illustrated on the right. The time calibration bar at the bottom applies to all traces (Südhof, 2004).

In the presynaptic terminal, neurotransmitter release is a multi-step process of membrane trafficking, which includes the synaptic vesicles and the presynaptic plasma membrane, a process called “synaptic vesicle cycle”. It is absolutely critical for neurons to tightly control synaptic vesicle release in order to maintain the integrity of all functions of the human brain.

During the synaptic vesicle cycle, synaptic vesicles are first filled with neurotransmitters before they dock at the active zone. In a biochemical reaction that consists of multiple protein-protein interactions, synaptic vesicles are then primed to be competent for  $\text{Ca}^{2+}$  triggered fusion-pore opening. When the action potential arrives and the  $\text{Ca}^{2+}$  level rises in the terminal, the vesicles release their content into the synaptic cleft. Recycling of the vesicles occurs presumably by three different pathways; (i) vesicles can remain in the docked stage and are maintained as components of the readily releasable pool (also referred to as “kiss-and-stay”), (ii) or they can be undocked and locally refilled (called “kiss-and-run”). (iii) Alternatively, they are recycled through clathrin-coated pits and either

refilled immediately, or after passing through an endosomal intermediate (Fig 1.3) (Sudhof, 2004).

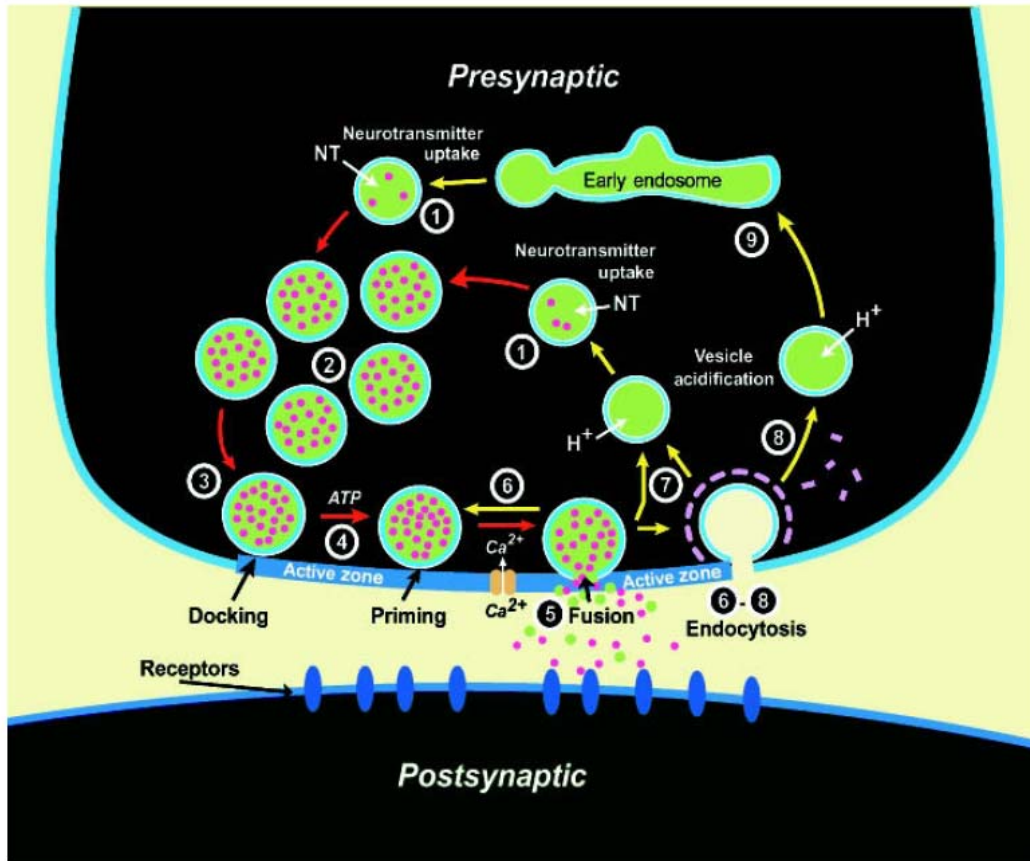


Figure 1.3 The synaptic vesicle cycle. Synaptic vesicles are filled with neurotransmitters by active transport (step 1) and form the vesicle cluster (step 2). Filled vesicles dock at the active zone (step 3), where they undergo a priming reaction (step 4) that makes them competent for  $Ca^{2+}$  triggered fusion-pore opening (step 5). After fusion-pore opening, synaptic vesicles undergo endocytosis and recycle via several routes: local reuse (step 6), fast recycling without an endosomal intermediate (step 7), or clathrin-mediated endocytosis (step 8) with recycling via endosomes (step 9). Steps in exocytosis are

indicated by red arrows and steps in endocytosis and recycling by yellow arrows (adapted from Südhof, 2004).

## **1.2 Essential proteins for synaptic vesicle fusion**

The synaptic vesicle cycle relies on a complex combination of protein interactions that governs exocytosis and endocytosis of the synaptic vesicles. In this cycle, two protein families are absolutely required: the SNARE proteins provide the force required to fuse the two membranes, and the SM proteins govern their fusogenic actions (see below, for a review see (Sudhof and Rothman, 2009)).

Neuronal fusion events are executed at an exquisite speed, and are under tight regulatory control. This requires further molecular processes that prepare synaptic vesicles for fusion. On one side, docking and priming of synaptic vesicles are executed by a number of proteins at the presynaptic active zone and on the synaptic vesicle membrane. Molecules involved in these processes include the neuronal SNARE proteins, the SM protein Munc18, synaptotagmins, RIMs, Munc13s and the vesicular GTPases Rab3/Rab27 (Augustin et al., 1999; Betz et al., 2001; Brose et al., 1995; de Wit et al., 2009; Deak et al., 2009; Fukuda, 2003; Gracheva et al., 2008; Schluter et al., 2004; Schoch et al., 2002; Wang et al., 1997; Young and Neher, 2009). On the other side, when the synaptic vesicles are docked and primed, two families of proteins are essential for fast, synchronized fusion pore opening in concert with the SNARE complexes and the SM proteins: (i) synaptotagmins 1, 2 and 9 act as  $\text{Ca}^{2+}$  sensors (Fernandez-Chacon et al., 2001;

Geppert et al., 1994; Pang et al., 2006b; Sun et al., 2007; Xu et al., 2007), and (ii) complexins act as fusion clamps that activate evoked release when needed (Giraudo et al., 2006; Giraudo et al., 2009; Maximov et al., 2009; McMahon et al., 1995; Tang et al., 2006). Throughout my thesis, I focused on these two families of proteins, both of which interact with the SNARE complexes to govern the precision, accuracy and speed of neurotransmission.

### **1.2.1 SNARE proteins**

In all membrane fusion events, SNARE (soluble *N*-ethylmaleimide-sensitive-factor attachment protein receptor) proteins provide the force for fusion (Sudhof and Rothman, 2009; Ungar and Hughson, 2003). The SNARE protein family has more than sixty members in yeast and mammalian cells, and they have originally been described based on their property to drive fusion *in vitro* (Clary et al., 1990; Malhotra et al., 1988; Wilson et al., 1989). They provide the force for fusion by forming a membrane-bridging complex between the vesicular membrane and the plasmamembrane, a function that has been widely acknowledged as the SNARE hypothesis (Sollner et al., 1993b). Structurally, the shared motif among these members of the SNARE protein family is called SNARE motif which is composed of ~60 amino acids and has a high tendency to form coiled coil domains (Jahn and Sudhof, 1999; Rizo and Sudhof, 2002). Amongst the many SNARE proteins, the membrane bridging complexes are assembled with relatively high specificity, where a specific vesicular SNARE (v-SNARE) only pairs with a limited number of target membrane SNAREs (t-SNAREs), suggesting that SNAREs themselves govern the

specificity of fusion within different compartments of a cell (Fukuda et al., 2000; McNew et al., 2000; Parlati et al., 2000).

Neuronal SNAREs are comprised of three proteins: synaptobrevin/VAMPs (vesicle associated membrane protein) which are localized to synaptic vesicles (v-SNAREs); syntaxin 1 and SNAP-25 (synaptosome-associated protein 25 kDa) are primarily present on the plasma membrane (t-SNAREs) (Sollner et al., 1993a). Together, these neuronal SNAREs form the membrane-bridging SNARE core complex in the synaptic vesicle cycle (Fig 1.4) (Rothman, 1994; Sollner et al., 1993a). In this complex, SNAP-25 provides two alpha-helical coils, whereas Syantxin and synaptobrevin provide one SNARE motif (Chen et al., 2002; Stein et al., 2009; Sutton et al., 1998). Importantly, syntaxin is known exist in two conformations. It contains an N-terminal H<sub>abc</sub> domain that can fold back onto the syntaxin SNARE motif, a state that is referred to as the closed confirmation. Closed syntaxin forms a four-helix bundle on its own without participating in the fusogenic core complex. Conversely, when syntaxin opens, it exposes its SNARE motifs to the other SNAREs, and participates in the membrane bridging core complex that drives synaptic vesicle fusion (Dulubova et al., 2002; Gerber et al., 2008; Richmond et al., 2001).

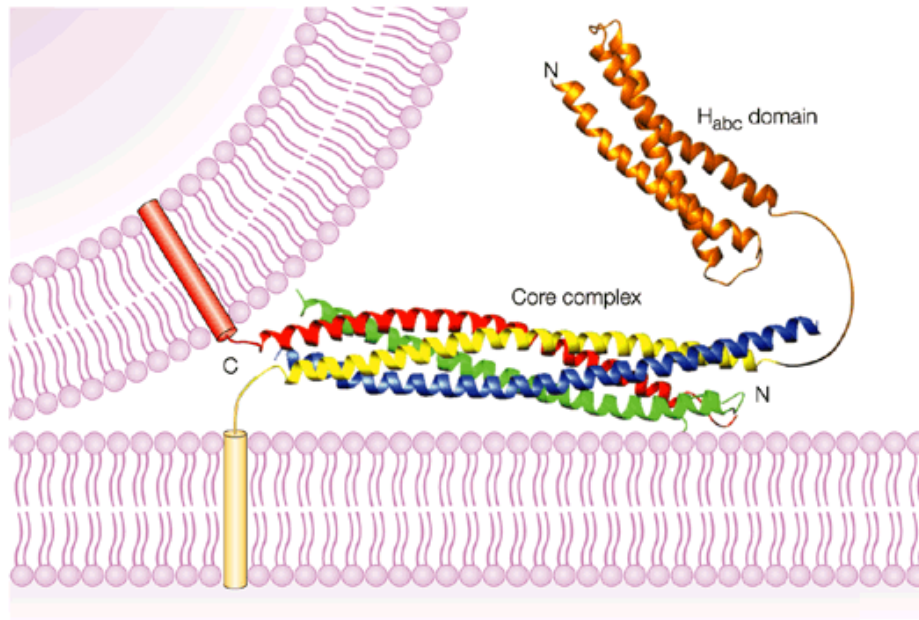


Figure 1.4 The ribbon diagrams represent the crystal structure of the core complex and the NMR structure of the amino-terminal H<sub>abc</sub> domain of syntaxin 1 (Fernandez et al., 1998). The H<sub>abc</sub> domain is coloured in orange and the SNARE (SNAP receptor) motifs are colour coded as follows: synaptobrevin, red; syntaxin 1, yellow; synaptosomal-associated protein of 25 kDa (SNAP-25) amino terminus, blue; SNAP-25 carboxyl terminus, green. The cylinders represent the transmembrane regions of synaptobrevin and syntaxin 1, which are inserted into the synaptic vesicle and plasma membranes, respectively. The curved lines represent short sequences that connect the SNARE motifs and the transmembrane regions, as well as the linker region between the H<sub>abc</sub> domain and the SNARE motif of syntaxin 1 (Rizo and Sudhof, 2002).

### 1.2.2. Sec1/Munc18-like (SM) proteins

Members of Sec1/Munc18 (SM) protein family were originally discovered as *uncoordinated18* (*unc18*) in a screen in the model organism *Caenorhabditis elegans* (Brenner, 1974), and its homologs were later found to be required in the secretory pathway in yeast (Sly1p, Sec1p, Vps45p, and Vps33p) (Novick et al., 1980), and in vertebrate synapses (Hata et al., 1993; Verhage et al., 2000). All SM proteins are hydrophilic proteins of 60–70 kDa that are without recognizable sub-domains. The fundamental importance of SM proteins is best illustrated by its synaptic family member Munc18-1: in the Munc18-1 KO mice, the null allele leads to a complete loss of neurotransmitter release, but brain assembly during embryonic development is normal (Verhage et al., 2000).

Munc18-1 functions in binding of four-helix bundles of SNARE complex, as recently hypothesized by Rothman and Südhof (Sudhof and Rothman, 2009). When they bind to the four-helix bundle of the closed conformation of syntaxin 1 (Dulubova et al., 1999), they inhibit fusion by blocking the interaction between syntaxin and SNAP-25 (Pevsner, 1996). When syntaxin 1 is in ‘open’ conformation, the arch-shaped body of Munc18-1 folds back onto the SNAREpin, binding to the forming four-helix bundle of the membrane-bridging core complex, resulting in the zippering of four-helix bundle to direct the membrane fusion (Fig 1.5 B and C) (Sudhof and Rothman, 2009).

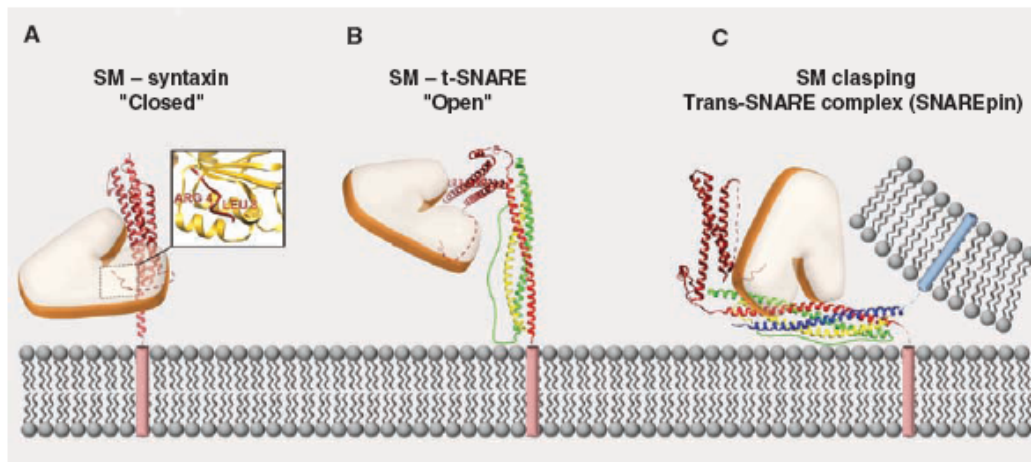


Figure 1.5 SM proteins are designed to bind four-helix bundles. (A) The “closed” conformation of syntaxin-1, in which the SM protein Munc18-1 binds the four-helix bundle composed of syntaxin’s own  $H_{abc}$  domain (three helices, in brown) and its own SNARE motif helix. This closed state has so far only been found with syntaxins involved in exocytosis. Inset: SM proteins are universally attached to  $H_{abc}$  domains by a specialized sequence at the N terminus of  $H_{abc}$ . (B) The “open” conformation of a t-SNARE complex, consisting of a t-SNARE and its cognate SM protein bound to the N-peptide of its syntaxin’s  $H_{abc}$  domain. This is believed to be the universal state in which t-SNAREs are open (i.e., reactive) with cognate v-SNAREs to form trans-SNARE complexes (C), resulting in fusion. Positions of the protein domains in (B) and (C) are arbitrary; (C) illustrates SNAREs and SM proteins, the universal fusion machinery (Sudhof and Rothman, 2009).

## 1.3 Synaptotagmins

### 1.3.1 Overview

Synaptotagmins are a family of transmembrane proteins that act as  $\text{Ca}^{2+}$  sensors for synaptic vesicle release (Fernandez-Chacon et al., 2001; Geppert et al., 1994). Besides their functions as  $\text{Ca}^{2+}$  sensors, they may also be involved in other processes at the synaptic vesicle cycle, as they bind to many other synaptic proteins. Recent studies, for example, have suggested that synaptotagmins may be involved in positioning or docking of synaptic vesicles in various preparations (de Wit et al., 2009; Young and Neher, 2009).

Synaptotagmins are defined by their domain structure, which consist of an N-terminal transmembrane domain, a variable linker region and two C-terminal C2 domains (Fig 1.6). They contain 15 family members (for a review describing the first 13 members, see (Sudhof, 2002)), of which Synaptotagmin 1, 2 and 9 have been shown to be the major  $\text{Ca}^{2+}$  sensors for fast synaptic vesicle release (Fernandez-Chacon et al., 2001; Geppert et al., 1994; Pang et al., 2006a; Sun et al., 2007; Xu et al., 2007). They function as  $\text{Ca}^{2+}$  ion sensors by  $\text{Ca}^{2+}$  dependent phospholipid binding: with their C2 domains, they coordinate 5  $\text{Ca}^{2+}$  ions, whereby phospholipids from the plasmamembrane are suggested to provide additional coordination sites. Their additional binding to the synaptic core complexes puts them at the heart of membrane fusion, where they trigger fusion upon  $\text{Ca}^{2+}$  binding (Shao et al., 1996; Sudhof, 2002; Zhang et al., 1998).

Although the mechanism of  $\text{Ca}^{2+}$  sensing is a fascinating function of synaptotagmins, it is important to note that many of the synaptotagmin family members

do not contain a complete set of Ca<sup>2+</sup> coordination sites (Syt 4, 8, 11, 12 and 13, for example) (Maximov et al., 2007; Sudhof, 2002; von Poser et al., 1997), and thus likely have other functions. Studying these additional functions will be critical to understand the wide involvement of these proteins in the synaptic vesicle cycle and its regulation.

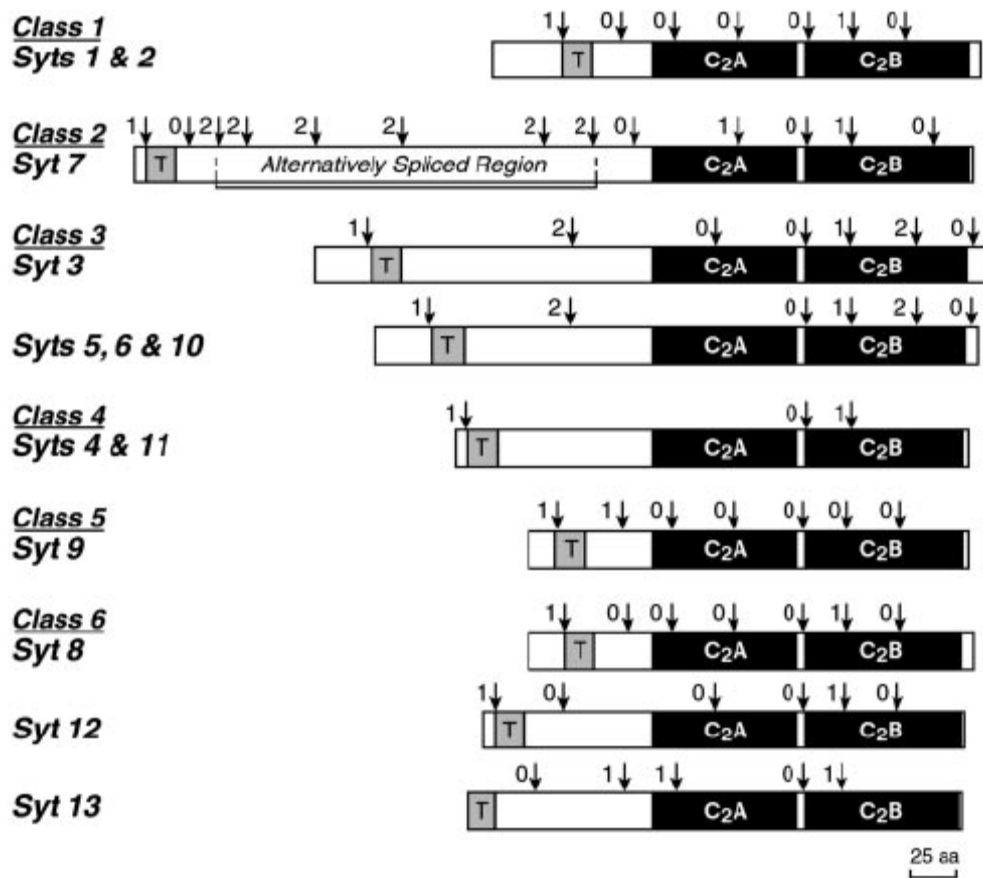


Figure 1.6 Domain structures of synaptotagmins 1–13: relation of protein domains to the intron/exon organization of the human genes. Each diagram shows a single or several

closely related synaptotagmins as identified on the *left*. *Arrows* indicate positions of introns in the corresponding human genes as identified in the human genome sequence.2 the *numbers next to the arrows* describe the position in the codon at which the coding sequence is interrupted by the intron (0, at the codon junction; 1 and 2, after the first and second codon position, respectively). The N-terminal TMR is marked with a *T*, and the C2A and C2B-domains are labeled (Sudhof, 2002).

### 1.3.2 Synaptotamin 12

Synaptotagmin 12 (Syt 12) or synaptotagmin-related gene1 (Srg1), a member of 15 vertebrate synaptotagmin family (Sudhof, 2002), was first found as a thyroid hormone-induced gene in developing rat brain (Thompson, 1996). Syt 12 is expressed throughout the brain including cortex, cerebellum, hippocampus, olfactory bulb, and brainstem (Maximov et al., 2007; Potter et al., 2001; Thompson, 1996). Subcellular fractionation experiments have shown that Syt 12 is enriched in synaptic vesicles like synaptotagmin 1 and synaptobrevin. Further characterization has additionally revealed that overexpressed Syt 12 is distributed in a punctate pattern that resembles a synaptic localization, and immunogold-electron microscopy has confirmed that it is tightly related to synaptic vesicles at the ultra-structural level (Maximov et al., 2007). These initial experiments showed that Syt 12 is a synaptic vesicle protein.

Like other synaptotagmins, Syt 12 is a type 1 transmembrane protein that consists of a short N-terminal tail, a single transmembrane domain, a linker region and two C-terminal C2-domains (Maximov et al., 2007; Sudhof, 2002). Unlike prototypical synaptotagmins, Syt 12 lacks the  $\text{Ca}^{2+}$  binding sequences, and thus cannot function as a

Ca<sup>2+</sup> sensor similar to Syt 1, 2 and 9 (Fig 1.6). Interestingly, Syt 12 has a unique linker sequence between the transmembrane domain and the C2-domains which contains a serine residue at position 97 which is phosphorylated by cAMP-dependent protein kinase A (PKA) *in vitro* (Maximov et al., 2007).

When Syt 12 was overexpressed in cultured neurons, it scaled miniature synaptic transmission (Maximov et al., 2007). This effect was amplified when the adenylate cyclase-PKA pathway was co-activated by forskolin. This suggested that Syt 12 phosphorylation by PKA was involved in enhancing miniature release in cultured neurons. In fact, this function was entirely dependent on the presence of serine residue 97 (serine<sup>97</sup>) in Syt 12 (Maximov et al., 2007). When serine<sup>97</sup> was substituted by alanine, a non-phosphorylatable amino acid, the rate of spontaneous release could not be enhanced by application of forskolin (Maximov et al., 2007).

As introduced below, these experiments led us to hypothesize that Syt 12 may be involved as a target of PKA phosphorylation in presynaptic plasticity.

### **1.3.3 Synaptotagmin 12 as a PKA target in presynaptic long-term plasticity**

Central nervous synapses show use-dependent plasticity, a synaptic function that has been widely associated with learning, memory and other brain functions (Kandel, 2001; Kauer et al., 1990; Nicoll et al., 1988). Synaptic long-term plasticity is bi-directional, it can be either a persistent increase of synaptic transmission (long-term potentiation, LTP), or a lasting decrease in synaptic transmission (long-term depression, LTD).

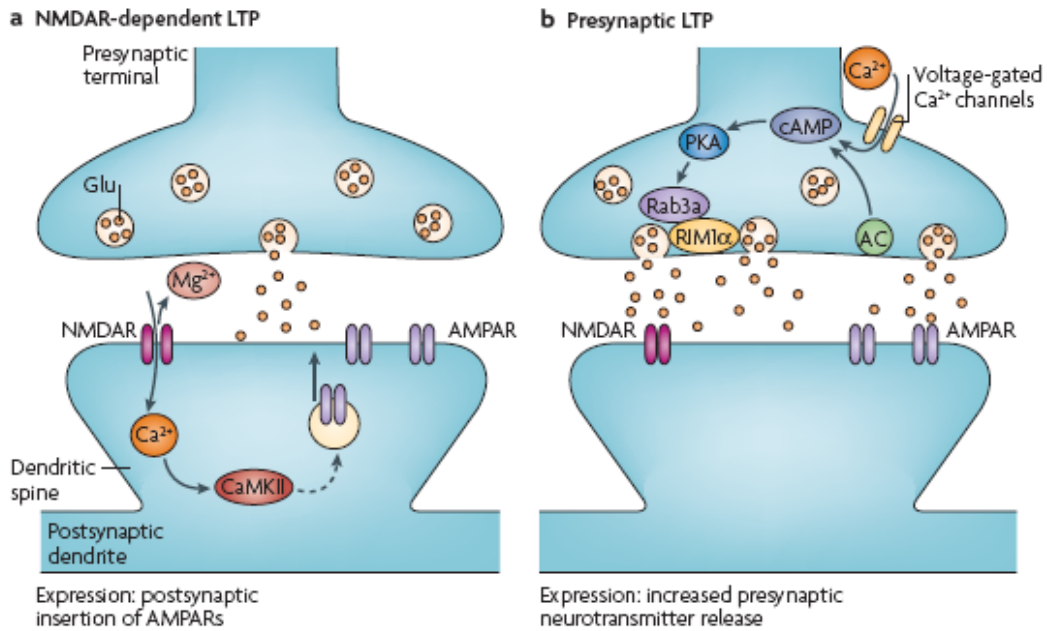


Figure 1.7 Two Well-described forms of LTP. Simplified diagrams of the induction and expression of synaptic plasticity observed in the rodent brain. (a) n-methyl-d-aspartate receptor (NMDAR)-dependent long-term potentiation (LTP) has been observed in many different brain regions and is dependent on postsynaptic NMDAR activation and calcium/calmodulin-dependent protein-kinase II (CaMKII) for its initiation. The voltage-dependent relief of the magnesium block of the NMDAR channel allows the synapse to detect coincident presynaptic release of glutamate and postsynaptic depolarization.  $\alpha$ -amino-3-hydroxy-5-methyl-4-isoxazole propionic acid receptor (AMPAR) insertion into the postsynaptic membrane is a major mechanism underlying LTP expression. (b) Presynaptic LTP has been best characterized at mossy fiber–CA3 hippocampal synapses as well as at parallel fiber–Purkinje cell cerebellar synapses. Repetitive synaptic activity leads to the entry of presynaptic  $\text{Ca}^{2+}$ , which activates a  $\text{Ca}^{2+}$ -sensitive adenylate cyclase (AC) leading to a rise in cAMP and the activation of cyclic AMP-dependent protein

kinase A (PKA). This in turn modifies the functions of Rab3a and RIM1 $\alpha$  leading to a long-lasting increase in glutamate release. (Kauer and Malenka, 2007)

There are two general forms of synaptic long-term plasticity. The more classical form is expressed post-synaptically and includes trafficking of AMPA-type glutamate receptors. On the other hand, there are multiple synapses in brain that encompass a presynaptically expressed form of long-term plasticity (Fig 1.7). These synapses include mossy fiber terminal in the hippocampus (Nicoll and Malenka, 1995; Nicoll and Schmitz, 2005), parallel fiber synapses onto Purkinje cells in the cerebellum (Linden and Ahn, 1999; Salin et al., 1996), cortico-striatal synapses (Spencer and Murphy, 2002), cortico-thalamic synapses (Castro-Alamancos and Calcagnotto, 1999), inhibitory synapses in area CA1 of the hippocampus (Chevalleyre and Castillo, 2003), or synapses in the lateral amygdala (Fourcaudot et al., 2008). Interestingly, these forms of plasticity critically depend on presynaptic activation of adenylate cyclase in response to Ca<sup>2+</sup> entry into the presynaptic terminal when the action potential arrives. Adenylate cyclase produces cyclic AMP, which in turn activates cAMP-dependent protein kinase A (Hirano, 1991; Nguyen and Woo, 2003; Xiang et al., 1994). PKA then acts on an unknown target, and leads to synaptic long-term plasticity which is expressed as a persistent change in the number of synaptic vesicles that fuse with the presynaptic membrane in response to a given stimulus. This form of plasticity critically depends on two presynaptic proteins: the small vesicular GTPase Rab3A (Castillo et al., 1997; Lonart et al., 1998; Weisskopf and Nicoll, 1995), and the large multi-domain active zone protein RIM1 $\alpha$  (Castillo et al., 2002;

Lonart et al., 2003; Schoch et al., 2002; Wang et al., 1997). In KO mice for either of these proteins, forms of presynaptic LTP such as mossy fiber LTP in the hippocampus and parallel fiber LTP in the cerebellum are abolished (Castillo et al., 1997; Castillo et al., 2002). Furthermore, RIM1 $\alpha$  KO mice also lack a form of long-term depression called i-LTD that is induced by postsynaptically, and is expressed in response to transsynaptic endocannabinoid signaling as a presynaptic depression of synaptic vesicle release. These studies provided a first molecular handle on presynaptic forms of long-term plasticity. However, although considerable efforts have been made to determine the specific target for PKA in the presynapse during plasticity, the molecular pathway of this phosphorylation has remained elusive. Specifically, the known PKA phosphorylation sites on Synapsins and Rabphilin are not involved, as these proteins are dispensable for presynaptic long-term plasticity (Schluter et al., 1999; Spillane et al., 1995). In contrast to Rab3s, which are not phosphorylated by PKA, RIMs were an interesting candidate as they are required for presynaptic long-term plasticity, and they can be phosphorylated *in vitro* by PKA (Castillo et al., 2002; Lonart et al., 2003). *In vivo*, however, the protein kinase A phosphorylation sites on RIM were not necessary for RIMs role in presynaptic LTP and LTD (Kaeser et al., 2008a; Yang and Calakos, 2010).

Our initial findings that Syt 12 is a synaptic vesicle protein that is phosphorylated by PKA, and that this phosphorylation potentiates miniature release *in vitro*, prompted us to hypothesize that Syt 12 may be the presynaptic target for PKA-dependent LTP. During my thesis, I generated a set of molecular tools to directly address this hypothesis *in vivo*.

## **1.4 Complexin**

### **1.4.1 Dual function of complexin in SNARE-mediated vesicle fusion**

At a synapse,  $\text{Ca}^{2+}$  induces neurotransmitter release by binding to synaptotagmin, which triggers SNARE-dependent fusion of synaptic vesicles with the plasma membrane (reviewed in (Martens and McMahon, 2008; Rizo and Rosenmund, 2008)). Synaptotagmin functionally cooperates with complexin, a small SNARE-complex binding protein (McMahon et al., 1995; Reim et al., 2001). In most synapses, deletions of synaptotagmin and complexin cause similar phenotypes, i.e., both decrease fast synchronous  $\text{Ca}^{2+}$ -triggered fusion (a process further called “activation”) and increase spontaneous fusion (a function named “clamping”, e.g., see (Littleton et al., 1994; Maximov et al., 2009; Pang et al., 2006c)). The relative size of the activation and clamping functions of complexin, however, differ. In *Drosophila* neuromuscular junctions, the clamping function of complexin predominates, whereas in autapses, its activation function prevails (Huntwork and Littleton, 2007; Reim et al., 2001), leading to the hypothesis of an evolutionary shift in complexin function from clamping to activation (Xue et al., 2009). However, in cellular fusion assays using 'flipped SNAREs', mammalian complexin exerts only a clamping function (Giraud et al., 2006; Giraud et al., 2009; Giraud et al., 2008); whereas in liposomes complexin behaves as an activator of fusion (Yoon et al., 2008). In knockdown (KD) experiments in cultured neurons, finally, complexin acts equally as an activator and a clamp (Maximov et al., 2009), with an effect size that is much larger for both functions than the effect size observed in KO autapses (Xue et al., 2009). Overall, despite the differences of preparations, these results

suggest that complexin functions simultaneously as a clamp and activator in synaptic fusion (Sudhof and Rothman, 2009).

#### 1.4.2 Functional domains of complexin

Complexin contains four functional domains (Fig 1.8): N-terminal and C-terminal unstructured regions, a more N-terminal 'accessory'  $\alpha$ -helix, and a more C-terminal central  $\alpha$ -helix that binds to the groove formed by synaptobrevin and syntaxin in the SNARE complex (Chen et al., 2002). The N-terminal complexin region activates fusion (Maximov et al., 2009; Xue et al., 2007), and its accessory  $\alpha$ -helix clamps fusion (Gerber et al., 2008; Maximov et al., 2009; Xue et al., 2009). The central SNARE-binding  $\alpha$ -helix is required for all of its functions. The C-terminal complexin sequence has been implicated in inhibiting or activating fusion, and binds to phospholipids (Malsam et al., 2009; Seiler et al., 2009; Xue et al., 2009).

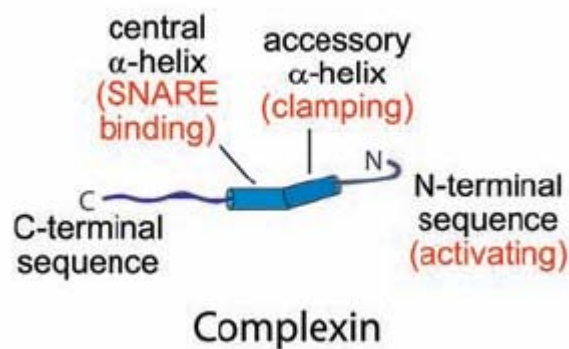


Figure 1.8 Functional domain structure of complexin. Complexin has 2 unstructured C- and N-terminal sequences and 2  $\alpha$ -helices in the center. The central  $\alpha$ -helix binds to

SNARE complex which is essential in regulatory function of complexin during synaptic fusion. The N-terminal domain activates fusion and accessory  $\alpha$ -helix clamps fusion presumably by blocking the SNARE complex zipper. The functions of the C-terminal sequences are largely unknown (Maximov et al., 2009).

#### **1.4.3 Function of complexin in SNARE-mediated fusion**

Apart from the fact that complexin interacts with SNARE complexes (McMahon et al., 1995), two experiments with the SNARE protein synaptobrevin/VAMP functionally link complexin to assembling trans-SNARE complexes. First, mutations in synaptobrevin which block complexin binding but not SNARE-complex assembly exhibit the same phenotype as the complexin KD (Maximov et al., 2009). Since complexin acts upstream of fusion pore opening (Reim et al., 2001), this result demonstrates that complexin functions by binding to trans-SNARE complexes. Second, an alanine substitution of two tryptophans in synaptobrevin (the so-called WA-mutation) phenocopies the complexin KD phenotype (Maximov et al., 2009). Since the WA-mutation is located in the short  $\alpha$ -helical sequence that connects the synaptobrevin SNARE motif (and thus the nascent trans-SNARE complex) to the vesicle membrane, and is outside of the synaptobrevin/complexin interaction site, this result suggests that complexin acts by controlling the transfer of force from assembling trans-SNARE complexes to the fusing membranes.

#### **1.4.4 Synaptotagmin-switch model of complexin function**

Despite much progress in understanding complexin, however, the mechanisms of its activation and clamping functions remain unknown. An exciting recent hypothesis posits that the accessory  $\alpha$ -helix of complexin may clamp fusion by inserting into partially assembled trans-SNARE complexes (Giraudo et al., 2009; Lu et al., 2009). This hypothesis, combined with the finding that  $\text{Ca}^{2+}$ -binding induces synaptotagmin to displace the complexin  $\alpha$ -helices from SNARE complexes (Giraudo et al., 2006; Tang et al., 2006), led the synaptotagmin-switch model of complexin function, which postulates that  $\text{Ca}^{2+}$ -binding to synaptotagmin reverses the complexin-mediated clamp of SNARE-complex assembly by displacing complexin from the clamped SNARE complexes (Fig 1.9) (Tang et al., 2006). The fact that competition of complexin and synaptotagmin for SNARE-complex binding is not absolute, i.e. that complexin and synaptotagmin can be associated both with SNARE complexes at the same time, and may even bind to each other (Chicka and Chapman, 2009; McMahon et al., 1995; Tokumaru et al., 2008), appeared to argue against this model. However, since other complexin sequences besides the SNARE-binding  $\alpha$ -helix may interact with SNARE complexes and/or phospholipids (Malsam et al., 2009; Seiler et al., 2009), and only the  $\alpha$ -helix competes with synaptotagmin for binding (Tang et al., 2006), these findings do not necessarily contradict the synaptotagmin-switch model.

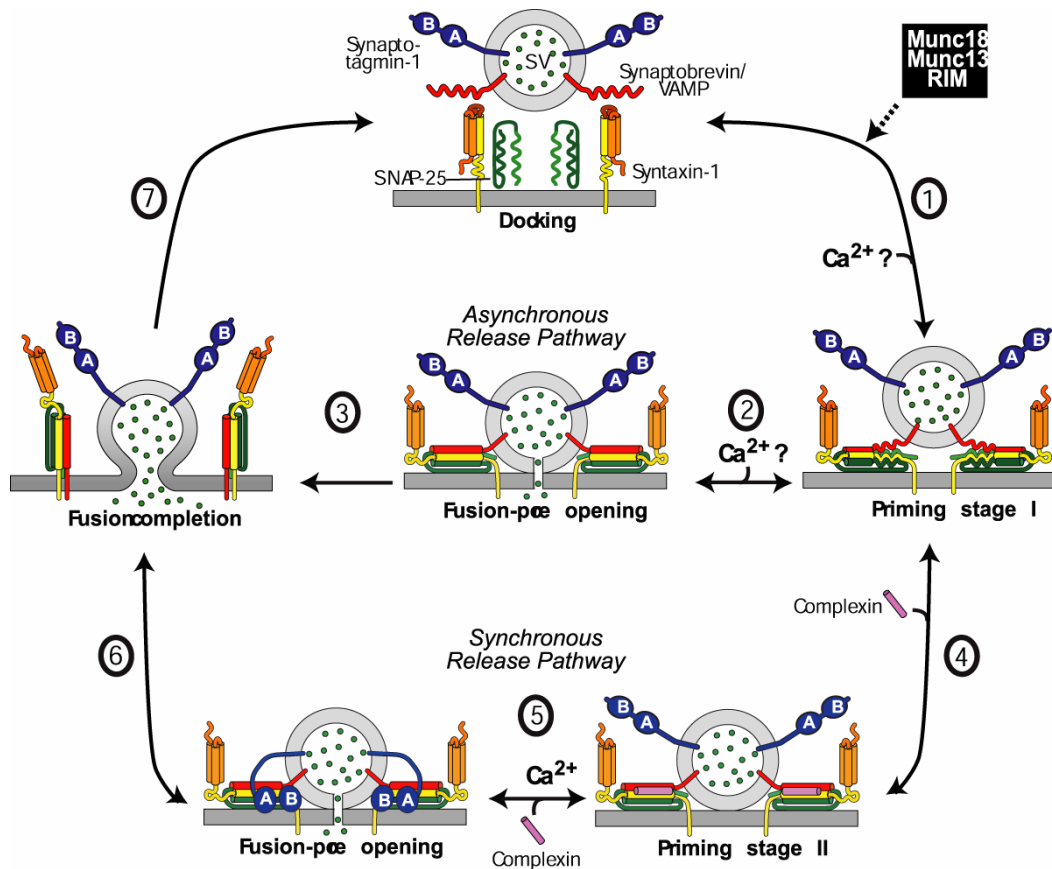


Figure 1.9 Model for complexin and synaptotagmin 1 function in  $\text{Ca}^{2+}$ -triggered release. Docked vesicles containing unassembled SNARE complexes (top) are primed for release by partial SNARE complex assembly catalyzed by Munc18, Munc13, and RIM (step 1). The resulting primed vesicles form the substrate for two release pathways: asynchronous release in which full assembly of the SNARE complexes leads to fusion-pore opening followed by complete fusion (steps 2 and 3), or synchronous release in which 'super-priming' by binding of complexins to assemble SNARE complexes (step 4) activates and freezes SNARE complexes in a metastable state (referred to as priming stage 2). This stage is then substrate for fast  $\text{Ca}^{2+}$ -triggering of release when  $\text{Ca}^{2+}$ -binding to synaptotagmin 1 induces its binding to phospholipids and to SNARE complexes, with

the latter reaction displacing complexin and resulting in fusion pore opening (step 5). Again, opened fusion pores can then dilate to complete fusion (step 6), although both steps 2 and 5 are potentially reversible, i.e. lack of dilation of the fusion pore could lead to 'kiss-and-run' exocytosis in these pathways. Note that steps 1 and 4 are also probably reversible, with a much faster forward than backward speed. It is likely that step 1 is  $\text{Ca}^{2+}$ -dependent, but it is unclear whether or not step 2 is  $\text{Ca}^{2+}$ -dependent since it is possible that asynchronous release is  $\text{Ca}^{2+}$ -dependent solely because  $\text{Ca}^{2+}$  accelerates step 1, and step 2 has a finite probability. Thus the nature of  $\text{Ca}^{2+}$ -triggering of asynchronous release could operate either at the priming or at the actual fusion step (Tang et al., 2006).

## 1.5 Major questions

During my thesis, I focused on synaptotagmins and complexins as protein families that interact with the SNARE complex and regulate its function in synaptic vesicle release.

1) Because of its presynaptic localization, its relationship to synaptic vesicles, and its PKA phosphorylation site in the linker area, we hypothesized that Syt 12 may be the presynaptic target of PKA during presynaptic plasticity. In the second chapter of my thesis, I address this hypothesis *in vivo* by generating mutant knockin animals in which the serine<sup>97</sup> residue is replaced by alanine. Furthermore, using this approach to generate constitutive KO mice for Syt 12 will allow analysis of Syt 12 functions that go beyond the ones of serine<sup>97</sup> phosphorylation.

2) Complexins are proteins that act as inhibitors of spontaneous fusion, and as activators of evoked release. Although this dichotomy of complexin function has been confirmed in different systems, it has to date remained elusive how this works on a molecular level. For this purpose, I generated a series of molecular tools that allow us to biochemically and physiologically dissect complexin functions, and these experiments are described in Chapter III of my thesis. Our findings have led to a first molecular hypothesis of how the accessory  $\alpha$ -helix of complexin interacts with the SNARE complex during the synaptic vesicle cycle to exert its clamping function.

## CHAPTER II: POTENTIAL FUNCTION OF SYT 12 IN PRESYNAPTIC LONG-TERM PLASTICITY

### 2.1 Introduction

All known forms of presynaptic long-term plasticity require a cAMP-dependent PKA phosphorylation event in the presynaptic terminal (Chevalleyre et al., 2007; Huang et al., 1994; Nguyen and Woo, 2003; Tzounopoulos et al., 1998; Villacres et al., 1998; Weisskopf et al., 1994; Weisskopf and Nicoll, 1995). The molecular target of PKA during LTP, however, has remained elusive. Two presynaptic proteins, Rab3a and RIM1, were shown to be required for presynaptic long-term plasticity (Castillo et al., 1997; Castillo et al., 2002; Chevalleyre et al., 2007; Fourcaudot et al., 2008; Kaeser et al., 2008b). Moreover, RIM1 was reported to be directly phosphorylated by PKA (Lonart et al., 2003), and this PKA phosphorylation seemed to be critical for an *in vitro* form of synaptic plasticity (Lonart et al., 2003). However, RIM1 knockin mice with a mutation that abolished PKA phosphorylation (serine 413 to alanine) revealed that major types of presynaptic long-term plasticity are unaffected by the point mutation which abolished PKA phosphorylation, effectively disproving that RIM1 may be the target of PKA phosphorylation in presynaptic forms of long-term plasticity *in vivo* (Kaeser et al., 2008a). Furthermore, this finding has been reproduced by viral mediated rescue of mossy fiber LTP by wild-type and S413A mutant RIM1 $\alpha$ , and these more acute manipulations confirmed that LTP is unaffected in mice that lack the RIM1 S413

phosphorylation site (Kaeser et al., 2008a). Thus, the presynaptic target of PKA during LTP remains unknown.

As described in the overview, it is hypothesized for the following experiments that serine<sup>97</sup> of Syt 12 may be the molecular target of PKA in the presynaptic bouton during long-term plasticity. Here, we directly test the significance of Syt 12 phosphorylation on synaptic transmitter release. This was done by generating a mutant mouse line which expresses a point mutant Syt 12 where the serine residue 97 is replaced by a non-phosphorylatable alanine (Syt 12 S97A). This genetic manipulation is the current gold-standard to test the involvement of a specific protein phosphorylation site in synaptic plasticity (Kaeser et al., 2008a; Lee et al., 2003).

Furthermore, based on GST-protein pull down assays, it was described that Syt 12 may interact with the Ca<sup>2+</sup> sensor synaptotagmin 1. Unlike other synaptotagmins (Sudhof, 2002), Syt 12 does not directly bind to SNARE complexes (Maximov et al., 2007). Thus, our initial hypothesis was that Syt 12 may act in regulating neurotransmitter release via Syt 1 (Maximov et al., 2007). Conversely, however, when miniature excitatory post-synaptic currents (mEPSC) were measured in cultured Syt1 KO cortical neurons, the Syt 12 scaling effect induced by overexpression of Syt 12 was unchanged, arguing that Syt 12 may function in spontaneous neurotransmitter release independent of Syt1 (Maximov et al., 2007). To further assess whether Syt 12 is more broadly involved in synaptic vesicle release, I generated in parallel a mouse line in which Syt 12 is deleted in the germ line. This line will allow testing functions of Syt 12 in neurotransmitter release that go beyond the function of the serine<sup>97</sup> PKA phosphorylation site.

We began to functionally analyze synaptic transmission in these mice in collaboration with the laboratory of Dr. Pablo Castillo at Albert Einstein College of Medicine. Preliminary data suggests that Syt 12 may be involved in expression of presynaptic long-term plasticity.

## 2.2 MATERIALS AND METHODS

### 2.2.1 Molecular cloning of Syt 12 S97A KI targeting vector

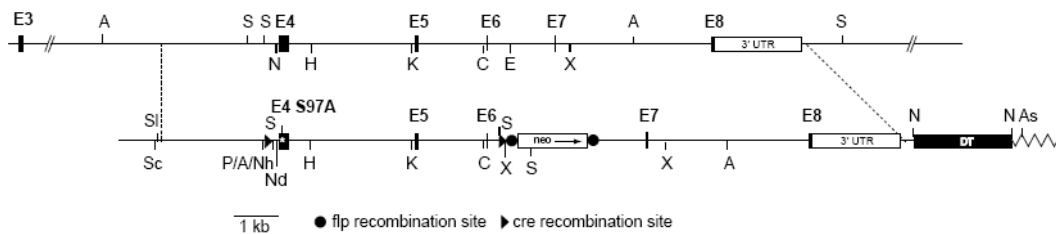


Figure 2.1 Cloning of Syt 12 S97A knockin targeting vector. Syt 12 S97A knocking targeting vector design. A: AseI, S: SpeI, Nd: NdeI, Nh: NheI, H: HpaI, K: KpnI, C: ClaI, E: EcoRI, X: XhoI, P: PacI, Sl: Sall, Sc: SacI, As: AscI. See below for cloning details.

I first performed a genomic screen with a lambda-phage 129SV/J genomic DNA library (Rosahl et al., 1993). Using a 32-P labeled probe from exon 4 of Syt 12 cDNA amplified with primers YJ0601 (GCTGTCACCTAGCGATGGTGCC) and YJ0602 (CACGATCTGTTCGTCTGGCAGC), I isolated a ~15kb genomic clone containing exon 4. Three independent modifications were applied to this genomic clone to generate the targeting vector: First, a fragment between ClaI and XhoI (exon 6~7) was subcloned into a modified multiple cloning site (MCS) of pBluescript (pB-YJ). Then, an SbfI site was

introduced into an intronic non-conserved sequence area (among rat, mouse, and human) by PCR-triple ligation in order to insert an NsiI-neomycin resistance gene (neo) cassette (Kaeser et al., 2008b; Rosahl et al., 1993); second, the Sall-ClaI (exon 4~5) fragment of the Syt 12 genomic clone was subcloned into pB-YJ. At a selected non-conserved sequence area, a PacI-AseI-loxP-NheI sequence was introduced by PCR-triple ligation; third, an NdeI-KpnI (exon 4) fragment was sub-cloned into pB-YJ and Ser-97-Ala was introduced by a site-directed mutagenesis. Finally all three modified fragments were combined and both neomycin gene and diphtheria toxin (DT) expressing cassette (Kaeser et al., 2008b; Rosahl et al., 1993) were inserted at location shown in Figure 2.1.

### **2.2.2 Southern blotting**

Homologously recombined mutant clones were screened by Southern blot following standard protocols (Ho et al., 2006; Rosahl et al., 1993; Southern, 1975). In brief, I extracted DNA from ES cell clones that were electroporated with the Syt 12 S97A targeting vector and subjected to positive selection by G418 and negative selection by a diphtheria toxin expressing cassette for 8 days. The DNA was digested with either AseI or SpeI and separated on 0.8% agarose gel at 30V overnight. The DNA was transferred onto nitrocellulose membrane and incubated with radioactive probes annealing to the genomic sequences outside the 5' and 3' arms of the targeting vector. AseI restriction digests result in a 5' upstream 10.3 kb fragment for wild-type, and 3.6 kb for S97A mutant clones; SpeI digests for with 3' outside probes give rise to a 12.3kb for wild-type and 7.2kb mutant fragments.

### **2.2.3 Syt 12 Phospho-specific antibody**

To generate antibodies against phosphorylated serine<sup>97</sup> of Syt 12, 14 amino acid peptides containing the phosphorylated serine<sup>97</sup> (CPPSRKGS<sup>97</sup>LSIEDT) in the center were synthesized in the Protein Chemistry Technology Center at UT Southwestern. Synthesized peptides were coupled with keyhole limpet hemocyanin (KLH) according to standard protocols (Sudhof et al., 1989) and injected into four rabbits for 3 consecutive times with inter-injection intervals of 1 week. The blood was collected from the rabbits, and the red blood cells were separated from the anti-serum by centrifugation. The anti-sera were tested by standard Western blotting procedures (Burnette, 1981; Ho et al., 2003) on brain homogenates of phosphorylated and non-phosphorylated Syt 12. The patterns of the bands were compared with band patterns of previously generated Syt 12 antibody (U5400), and anti-sera revealing positive signals were used for all experiments. Ultimately, the specificities of antibodies were unequivocally confirmed in the knockin and knock-out animals.

### **2.2.4 Western blot and protein quantification**

Brain tissue from three adult (P30) littermate mice per genotype was isolated and homogenized in PBS, 10 mM EDTA, 1 mM PMSF, and proteinase inhibitor cocktail tablet (Roche). Brain lysates (40 µg) were separated by SDS-PAGE, and immunoblotting was performed with standard methods as described previously (Rosahl et al., 1995). The proteins were then transferred to a nitrocellulose membrane, and were blocked by a blocking buffer containing 10% milk powder and 5% goat serum in TBST (Tris-buffered saline with 0.1% Tween 20). The newly generated antibodies and control antibodies

against Syt 12 (U5400) (Maximov et al., 2007) were then incubated with the nitrocellulose membranes for more than 2 hours in binding solution (5% milk power, 5% goat serum in TBST). After washing 3 times 5 minutes each, the membranes were incubated with secondary, horse-radish peroxidase coupled goat-anti rabbit secondary antibodies for 45 minutes followed by the use of a commercial enhanced chemiluminescence detection kit (ECL, Amersham).

Radioisotope  $^{125}\text{I}$ -labeled secondary antibodies were used for quantitative analyses followed by Typhoon PhosphorImager (GE Health Care Life Sciences) detection with GDP dissociation inhibitor (GDI) or vasolin-containing protein (VCP) as internal controls. The following primary antibodies were used: liprin- $\alpha$ 3 (4396, 1:5000); GDI (81.2 Synaptic Systems, 1:2000); VCP (443B 1:1000); GFAP (172.002 Synaptic Systems, 1:5000); tomosyn (U5403, 1:1000); synapsin (46.1 Synaptic Systems, 1:1000);  $\beta$ -actin Sigma, 1:1000), 14-3-3zeta Santa Cruz biotechnology, 1:1000), complexin-1/2 (122 002 Synaptic Systems, 1:1000); RIM & Raphillin (U1565, 1:2000); Munc13-1 (CL266 B1 Synaptic Systems, 1:1000); ELKS (P224, 1:500); Syt 12 (U5400, 1:250); phospho-Syt 12 (342C, 1:250), Synt 1 (HPC-1 Synaptic Systems, 1:2000), SNAP-25 (71.1 Synaptic Systems, 1:2000), CSP (R809, 1:1000), Syb 2 (69.1 Synaptic Systems, 1:2500); Syt 1 (41.1 Synaptic Systems, 1:2000); Rab3 (42.1 Synaptic Systems, 1:2000).

### **2.2.5 Genotyping**

Crude DNA extraction from mouse tails was prepared as following: (1) cut ~0.5cm of mouse tail; (2) add 250ul quick tail buffer (50mM KCl, 10mM Tris HCl, pH9.0, 0.4% NB40, 0.4% Tween 20) and 4.5ul protease K (14.0mg/ml) per sample; (3)

incubate at least for 6 hr on thermomixer at 55°C 700min<sup>-1</sup>; (4) inactivate protease K for 12 min at 95 °C; (5) centrifuge at full speed for 10 min and use 1 µl of DNA solution for genotyping. For PCR amplification was performed as follows: (1) a denaturation step at 94 °C for 10 min, (2) denaturation at 94 °C for 30 sec, (3) annealing at 60 °C for 45 sec, (4) extension at 65 °C for 3 min, and (5) final extension at 65 °C for 10 min. Steps (2) to (4) were repeated 40 times.

The floxed, flp recombined Syt 12 S97A allele was genotyped by PCR with oligonucleotide primers YJ08109 (TAGGCTGTCAAGTCCAATAGGTCC) and YJ08110 (TACAGAAATAGTCTGTCACCCTGG). This reaction results in a 200 base pair (bp) wild-type band and a 300 bp floxed band. The Syt 12 KO allele was genotyped with YJ0601 (GCTGTCACCTAGCGATGGTGCC) and YJ0602 (CACGATCTGTTCGTCTGGCAGC) to identify a 400 bp wild-type band and with YJ07068 (ATGTCCTAAGTGCTGGTCCC) and YJ08109 to detect a 280 bp mutant band (Fig 2.3 B and C).

### **2.2.6 Mouse breeding**

All mouse husbandries were performed according to institutional guidelines, and were carried out systematically as described in the results section.

### **2.2.7 Quantitative reverse transcriptase PCR**

Total RNA was extracted from dissected mouse brains by a RNAqueous-Micro kit (Ambion INC, TX) following the manufacturer's instructions. The concentration of the total RNA is measured and adjusted to 30-100 ng/µl. The mRNA level of individual

genes was then analyzed by one-step quantitative RT-PCR system with TaqMan gene expression assays (Applied Biosystems, CA). Briefly, 30 -100 ng of RNA samples in 1  $\mu$ l volume is mixed with 10  $\mu$ l of TaqMan fast universal PCR master mix (2x), 0.1  $\mu$ l of reverse transcriptase (50 units/ $\mu$ L), 0.4  $\mu$ l of RNase inhibitor (20 units/ $\mu$ L), 7.5  $\mu$ l of H<sub>2</sub>O and 7  $\mu$ l of pre-made TaqMan gene expression kit of either the target gene (including the forward and reverse PCR primers and the gene-specific TaqMan FAM-MGB probe) or the endogenous control gene. The reaction mixture was loaded onto an ABI7900 fast RT-PCR machine for 30 min of reverse transcription at 48 °C followed by 40 PCR amplification cycles consisting of denaturation at 95°C for 1 s, annealing and extension at 60 °C for 20 s. The amplification curve was collected and analyzed with  $\Delta\Delta$ Ct methods for relative quantification of mRNAs. Briefly, a threshold is set at the exponential region of the amplification curve, and the threshold cycles (Ct) are defined as the number of cycles required for the fluorescent signal to cross this threshold.  $\Delta$ Ct is calculated by subtracting the Ct value of an endogenous control gene from that of the target gene (namely,  $\Delta$ Ct = Ct of target gene – Ct of endogenous control gene).  $\Delta\Delta$ Ct is then determined by subtracting the  $\Delta$ Ct values of the calibrator samples from that of the test samples ( $\Delta\Delta$ Ct =  $\Delta$ Ct of Test –  $\Delta$ Ct of Calibrator). The amount of mRNA of target genes, normalized to that of an endogenous control and relative to the calibrator sample is calculated by  $2^{-\Delta\Delta$ Ct}. We use glyceraldehyde 3-phosphate dehydrogenase (GAPDH) or beta-actin as the endogenous control genes.

### **2.2.8 Electrophysiology**

Hippocampal and cerebellar slices (400  $\mu\text{m}$ ) were prepared from littermate wild-type control and Syt 12 S97A mice (3–6 weeks old). All animal procedures were performed in accordance with the National Institutes of Health Guide for the Care and Use of Laboratory Animals. Slices were prepared on a DTK-2000 vibratome (Dosaka) in ice-cold sucrose-containing cutting solution consisting of 215 mM sucrose, 2.5 mM KCl, 20 mM glucose, 26 mM NaHCO<sub>3</sub>, 1.6 mM NaH<sub>2</sub>PO<sub>4</sub>, 1 mM CaCl<sub>2</sub>, 4 mM MgCl<sub>2</sub>, and 4 mM MgSO<sub>4</sub>. The cutting solution was slowly exchanged ( $\approx$ 30 min) with artificial cerebrospinal fluid (ACSF) containing 124 mM NaCl, 2.5 mM KCl, 10 mM glucose, 26 mM NaHCO<sub>3</sub>, 1.0 mM NaH<sub>2</sub>PO<sub>4</sub>, 2.5 mM CaCl<sub>2</sub>, and 1.3 mM MgCl<sub>2</sub>. Both cutting and ACSF solutions were saturated with 95% O<sub>2</sub> and 5% CO<sub>2</sub> (pH 7.4). The slices were incubated at room temperature for at least 1.5 h before recording. For whole-cell recording, the recording pipette solution was filled with internal solution consisting of 123 mM cesium gluconate, 8 mM NaCl, 1 mM CaCl<sub>2</sub>, 10 mM EGTA, 10 mM Hepes, 10 mM glucose (pH 7.3, 290–295 mOsm). Mossy fiber LTP measurements were performed in the presence of 50  $\mu\text{M}$  D-APV (D-2-amino-5-phosphonovalerate). Field potentials were recorded extracellularly with patch-type pipettes filled with 1 M NaCl. Synaptic responses were evoked with patch pipettes filled with ACSF. Stimulating electrodes were placed in the dentate gyrus cell body layer to activate hippocampal mossy fibers. For mossy fiber LTP, 1  $\mu\text{M}$  (2*S*,2'*R*,3'*R*)-2-(2',3'-dicarboxycyclopropyl)glycine (DCG-IV) was applied at the end of every experiment, and the data were accepted only if synaptic responses were reduced by more than 90%. The synaptic response remaining in DCG-IV was then subtracted from all previous responses before further analysis to isolate mossy fiber-specific synaptic activity. Long-term depression at hippocampal inhibitory synapses

(i-LTD) was elicited by theta-burst stimulation consisting of a series of 10 bursts repeated 4 times. Each burst was comprised of five 100 Hz stimuli and the inter-burst interval was 200 ms. Extracellular and whole-cell patch-clamp recordings were performed using a Multiclamp 700B amplifier (Axon Instruments). Stimulation and acquisition were controlled by custom written software in Igor Pro 4.09A (Wavemetrics). The paired-pulse ratio is defined as the ratio of the amplitude of the second synaptic response to the amplitude of the first synaptic response. The magnitude of mfLTP and i-LTD is calculated as the percentage change between baseline (averaged for 10 min before induction) and post-induction responses (50–60 min post-induction for mf-LTP; 20–30 min for i-LTD). IPSCs were recorded in Normal Ringer from CA1 pyramidal neurons at  $V_{\text{hold}} = -60$  mV by stimulating presynaptic fibers located in strata radiatum while glutamatergic synaptic transmission was blocked using NMDAR and AMPAR/KAR antagonists (50  $\mu$ M AP-5 and 10  $\mu$ M NBQX, respectively). mIPSC was measured similarly, but  $V_{\text{hold}} = +10$  mV and 1  $\mu$ M TTX was bath applied to isolate mIPSCs. All recordings were performed at  $25.0^{\circ}\text{C} \pm 0.1^{\circ}\text{C}$  using a 2-channel temperature controller (TC344B; Warner Instruments). Synaptic responses were acquired using a Multiclamp 700A amplifier (Axon Instruments).

## **2.3 Results**

### **2.3.1 Generation of Syt 12 S97A knockin and Syt 12 KO**

We isolated genomic clones of the murine Syt 12 gene from a 129Sv genomic phage DNA library (Rosahl et al., 1993) by using a radioactive probe directed against exon 4 of the mSyt12 gene. In this genomic screen, 7 clones containing the mSyt12 genes

were isolated and sequenced. Using these genomic DNA fragments, the targeting vector was generated as described in the methods part, and contained the following elements (from 5' to 3') as depicted in Figure 2.1: a loxP recombination site upstream of exon 4, a point mutation in exon four that leads to a replacement of serine residue 97 with alanine (S97A), a cassette containing a loxP site and a neomycin open reading frame driven by the PGK promoter and flanked by *frt* recombination sites, and a diphtheria-toxin expressing cassette at the 3' end (Rosahl et al., 1993). Except the S97A mutation, all elements were inserted in areas of the genome that are non-conserved between rat and mouse sequences, reducing the risk of altering unknown intronic functions of DNA sequences in the *Syt 12* gene.

The finalized vector was extensively mapped with multiple restriction endonucleases to confirm that the assembly of the targeting construct was correct, and was sequenced entirely to exclude that there were any point mutations other than the desired changes as described above. Cre- and flp-recombinase expressing bacteria were used for assessing the functionality of the corresponding recombination sites that were inserted in the targeting vector. For this purpose, the bacterial strains were transformed with the targeting vector, the plasmids were purified from the bacteria, and recombination by cre- or flp recombinase, respectively, was confirmed by restriction mapping and sequencing. The linearized targeting vector was electroporated into R1 embryonic stem (ES) cells (Nagy et al., 1993), and G418 was added to the culture medium to perform a positive selection of clones containing the neomycin resistance cassette and the diphtheria-toxin expressing cassette served as a negative selection maker.

571 resulting ES clones were screened by Southern blotting for homologous recombination as described in the methods section, and 21% of all clones were positive for the 5' loxP site (see Fig 2.3 A). In addition, I screened exon 4 by PCR, DNA sequencing, and SacI digestion in each individual recombined ES cell clone. This procedure confirmed the presence of the S97A mutation. Interestingly, one ES clone (6H1) which was homologously recombined at the 5' and 3' end contained wild-type serine<sup>97</sup>. This repair of the point mutation arose likely by a known mismatch repair mechanism in ES cells (Kaeser et al., 2009; Maximov et al., 2008; Steeg et al., 1990). This clone 6H1 may allow generating a conditional Syt 12 KO line that lacks the serine<sup>97</sup> mutation, a technique that has been previously used to generate conditional KO mice from constructs that were produced to insert a point mutation (Kaeser et al., 2008b).

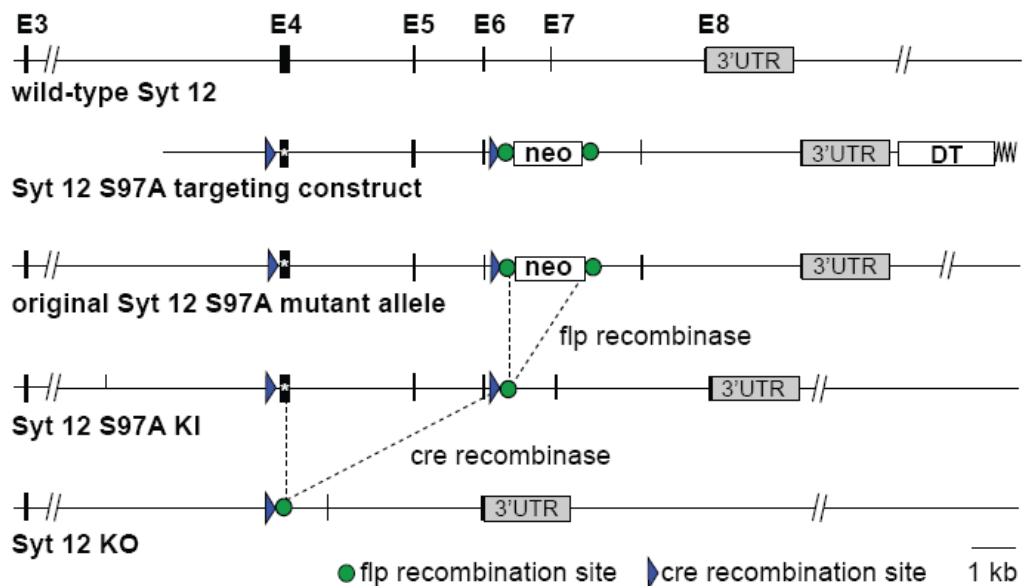


Figure 2.2 Generation of Syt 12 S97A knockin and constitutive Syt 12 KO mice. Knockin strategy for the Syt 12 S97A knockin mice showing (from top to bottom) the wild-type Syt 12 allele, the S97A knockin targeting construct, the Syt 12 mutant allele after homologous recombination, the flp-excised knockin allele, and cre-recombined knockout allele. E 3-8, exons 3-8; UTR, untranslated region; DT, diphtherotoxin-expressing cassette; neo, neomycin resistance cassette; \*, S97A point mutation in exon 4.

6 positive ES clones were then expanded, and Southern screening, S97A SacI digest, and extensive sequencing were used to confirm homologous recombination before selecting the clones for blastocyst injections. Three ES clones were injected into C57Bl/6J blastocysts and male chimeric offsprings were identified by the typical coat color which was used for breeding to achieve germline transmission of the Syt 12 mutant allele. Crossings to transgenic mice expressing flp recombinase in the germline (Dymecki, 1996) were used to remove the neomycin resistance gene, and these mice will be referred to as Syt 12 S97A knockin mice. Cre recombination in the male germ line was achieved by breeding the Syt 12 S97A knockin mice to transgenic mice that express cre recombinase in the male germline (O'Gorman et al., 1997), effectively disrupting the Syt 12 open reading frame by removing exons 4 - 6. This line will be referred to Syt 12 KO mice (Fig 2.2). Both flp- and cre-recombination were assessed by PCR genotyping (Fig 2.3 C), and protein expression in these lines was tested by Western blotting as described below. Finally, by using the 6H1 clone for blastocyst injection, I attempted to generate conditional Syt 12 KO mice according to the breeding scheme outlined above for the S97A knockin mice. Unfortunately, all attempts to breed the flp-recombined allele

of clone 6H1 to homozygosity failed, and homozygote mutant conditional Syt 12 knock-out mice were never obtained. Even several backcrosses to C57BL/6 mice did not solve this problem, and we conclude that it will be impossible to get homozygote mutant Syt 12 conditional KO mice. However, as outlined above and confirmed experimentally below, we succeeded in producing Syt 12 S97A point mutant knockin mice, and Syt 12 constitutive KO mice.

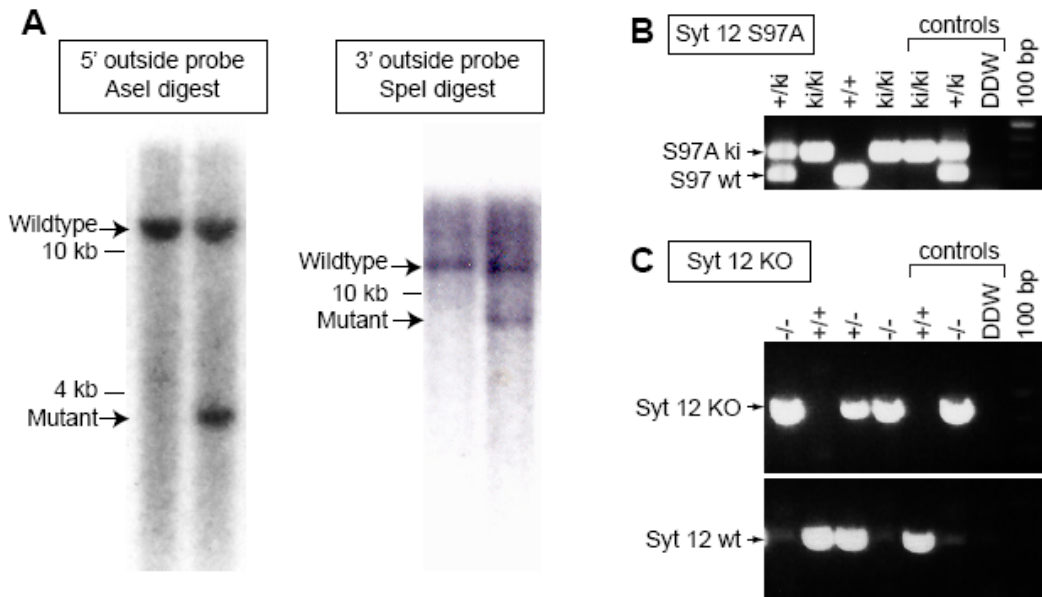


Figure 2.3 Confirmation of homologous recombination by Southern blot and PCR genotyping. (A) Southern blot examples for wildtype and heterozygote mutant embryonic stem cell clones after homologous recombination with the targeting vector. AseI restriction digest results in a 5' upstream 10.3kb fragment for wild-type, and 3.6kb with additional the AseI site that was introduced with loxP and S97A mutation for mutant clones; SpeI digest for 3' downstream gives 12.3kb for wild-type and 7.2kb when additional SpeI with neo cassette is inserted. (B&C) Genotyping Syt 12 S97A knockin and Syt 12 KO by PCR. (B) PCR amplification of the offspring of a Syt 12 S97A heterozygote breeding pair over the loxP site at exon 4 (oligonucleotide primers YJ08109 and YJ08110). (C) PCR amplification of the offspring of a Syt 12 KO heterozygote breeding pair with oligonucleotide primers YJ0601/YJ0602 (top) and YJ07068/YJ08109 (bottom).

### 2.3.2 Survival analysis of Syt 12 S97A knockin and Syt 12 KO mice

We next systematically analyzed survival in the offspring of heterozygote matings of the Syt 12 S97A knockin mice and the Syt 12 KO mice. We found that the genotype distribution amongst the offsprings at postnatal day 21 was unchanged compared to the expected Mendelian distribution for both the Syt 12 S97A knockin and Syt 12 KO mice (Syt 12 S97A knockin, n=110 mice: +/+, 21.8%; +/-, 53.6%; ki/ki, 24.5%; Syt 12 KO n=118 mice): +/+, 28.0%; +/-, 49.1%; -/-, 22.8%) (Fig. 2.4). Furthermore, in both lines, the homozygote mutant animals were viable and fertile, appeared normal, and were indistinguishable from their wild-type littermate.

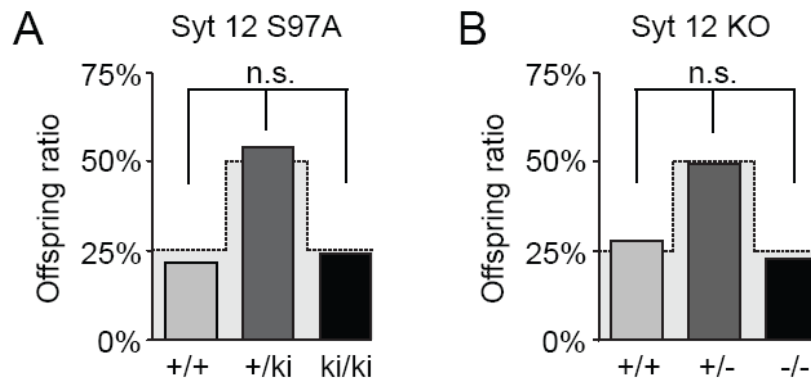


Figure 2.4 Survival analyses. Survival ratios of the offspring of heterozygote matings of Syt 12 S97A knockin (A) and Syt 12 KO mice (B). Normal Mendelian ratios are indicated by grey shaded areas.

### 2.3.3 Testing of phospho-specific antibodies in the Syt 12 S97A knockin animals

To assess the Syt 12 protein expression in the newly generated S97A mice, we generated antibodies with peptides containing a phosphorylated serine<sup>97</sup> and flanking amino acids. Amongst the 4 independent antisera obtained, 1 antiserum (342C) showed a Western signal at the correct molecular weight of Syt 12 that disappears upon mutation of the serine<sup>97</sup> residue to alanine in the mice (Fig 2.5A), confirming that we successfully produced phospho-serine<sup>97</sup> specific Syt 12 antibodies.

Furthermore, the experiments confirm that I successfully generated the Syt S97A mutant animals. When I blotted the same brain homogenates with the previously described antisera against Syt 12 (U5400), I found that in the Syt 12 S97A mutant animals, the Syt 12 band was near normal in intensity, but slightly shifted towards a lower molecular weight (Fig. 2.5A, asterisk). This suggests that mutating serine<sup>97</sup> in mice did not affect the overall expression level, but did induce a change in the migration properties of Syt 12 through an SDS-PAGE gel.

#### **2.3.4 Assessment of the Syt 12 KO animals by Western blotting and RT-PCR**

I have now shown that Syt 12 gene has been successfully targeted by confirming the absence of the serine<sup>97</sup> phosphorylation site in homozygous Syt 12 S97A mutant animals. To confirm that Syt 12 can be effectively deleted by cre recombination, I then assessed Syt 12 protein and mRNA expression in the brain of the Syt 12 KO animals (Fig 2.5 A and B). The Western blotting experiments were done as described above. I found that, in the KO animals, the specific Syt 12 signal was absent (Fig 2.5 A), although some unspecific bands could be observed in longer exposures (arrows, Fig. 2.5A). To reconfirm the absence of Syt 12 in the KO mice, we also used the phospho-specific

antibodies, which showed complete absence of the Syt 12 signal, confirming that Syt 12 had been effectively removed. We thus assume that the light bands in the KO animals are cross-reactive.

To further confirm the gene targeting, I also applied quantitative RT-PCR to test for Syt 12 mRNA levels. mRNA from cortex and hippocampus of Syt 12 KO and wild type littermate brains were prepared and standard RT-PCR procedures were used quantitatively assess the Syt 12 mRNA levels. We found that, in the Syt 12 KO animals, no Syt 12 mRNA could be detected, whereas in the wild-type animals, Syt 12 mRNA was readily detected in both cortical and hippocampal RNA preparations (Fig 2.5 B). Taken together, these experiments confirm that Syt 12 was successfully removed from the KO animals upon cre recombination.

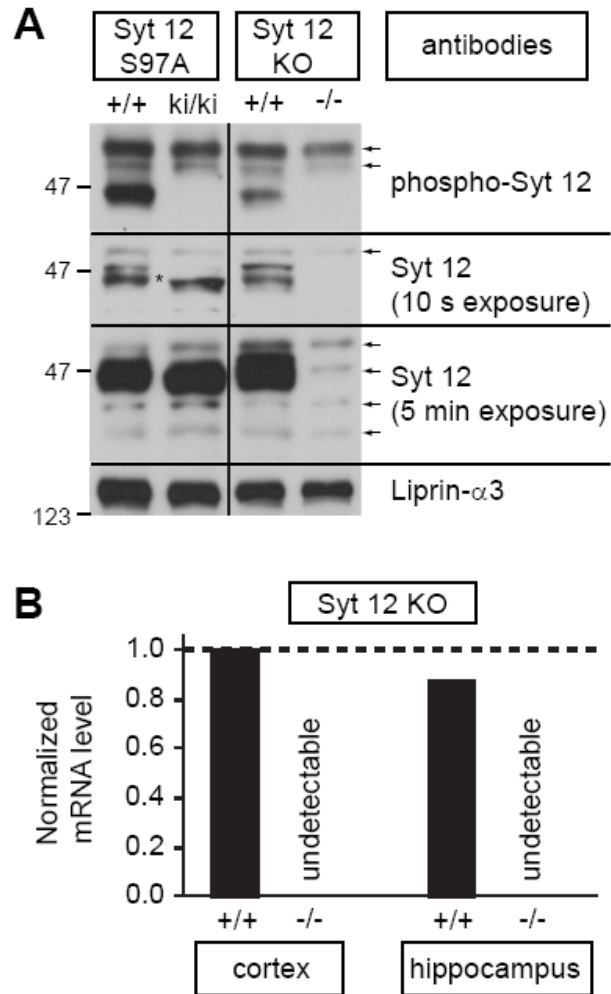


Figure 2.5 Measurement of Syt 12 expression by Western blot and RT-PCR. (A) Western blotting with newly generated phospho-specific Syt 12 antibodies (342C) confirms the absence of phosphorylated Syt 12 in the S97A knockin and Syt 12 KO mice. Slight shift in Syt 12 band detected by Syt 12 antibody (U5400) in the Syt 12 S97A ki animals is marked with an asterisk. (arrows: non-specific bands) (B) Mean expression level of Syt 12 mRNA in Syt KO and wild-type littermates. mRNA level is normalized to

Syt 12 wild-type cortical mRNA. In both Syt 12 KO hippocampus and cortex, Syt 12 mRNA levels were under detection range indicating that Syt 12 expression is abolished in the KO mice.

### **2.3.5 Protein composition of brains of Syt 12 mutant mice**

To assess the protein composition of the brain in mutant mice, I next quantitatively assessed the levels of Syt 12 and related proteins in brains of the newly generated mice. In brief, for both mouse lines we prepared brain homogenates of four pairs of littermate wild-type and mutant mice which were 7 to 8 weeks old at the time of tissue collection. These brain homogenates were then subjected to standard Western blotting procedures as described above, with the difference that <sup>125</sup>I-iodine coupled secondary antibodies were used for signal detection. The signal intensities were then measured and quantified with Typhoon Phosphorimager (GE) and ImageQuant TL software. This method has been widely used for quantitative Western blotting (Ho et al., 2003; Kaeser et al., 2008b; Schoch et al., 2002) , and has a wider linear range for quantitative protein expression assessment compared to other methods such as densitometry measurements of ECL blots or quantitations by use of fluorescently labeled secondary antibodies. The signals for each antibody were normalized to an internal control protein in each lane (antibodies to valosin-containing protein (VCP) or Rab GDP dissociation inhibitor (Rab-GDI) were used for this purpose).

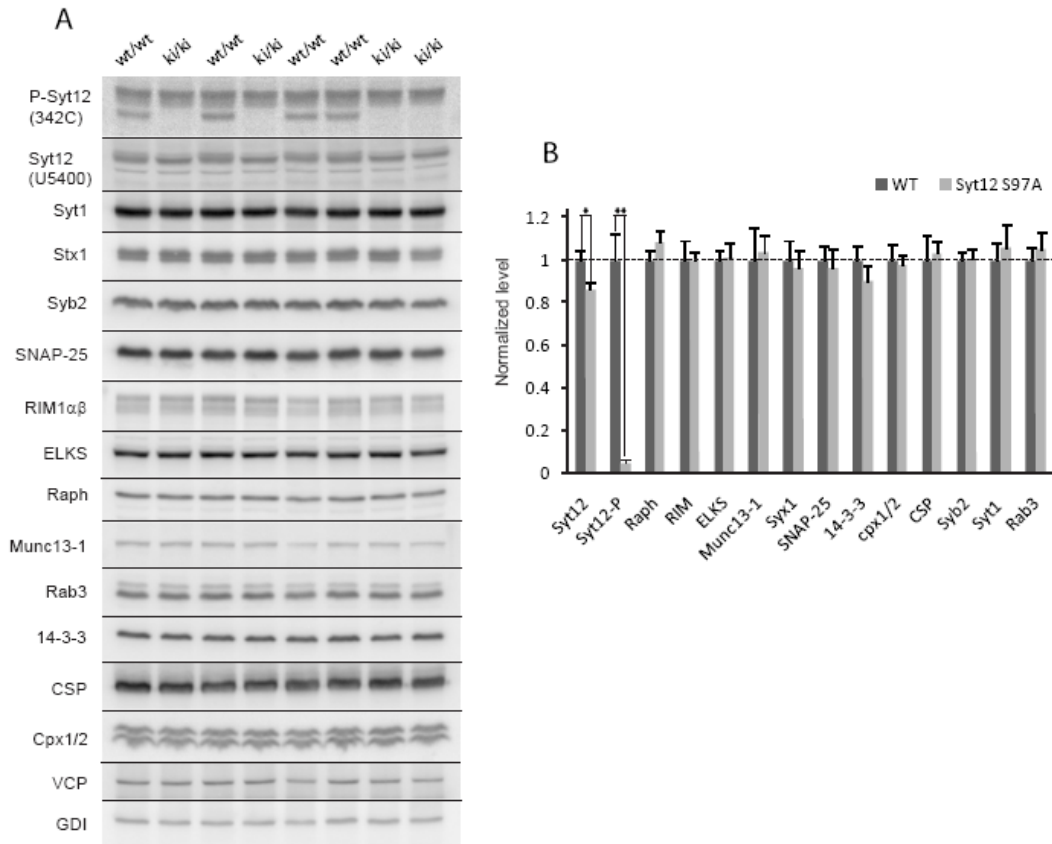


Figure 2.6 Syt 12 S97A knockin protein quantification. (A) Western blotting of whole brain lysates with <sup>125</sup>I iodine labeled secondary antibodies for multiple brain-specific proteins in brains from Syt 12 S97A knockin mice and wild-type littermate controls (n = 4 for each genotype, all at 8-9 weeks of age). GDI and VCP are shown as loading controls and were used for normalization. (B) Quantitative analysis of protein contents normalized to VCP, or GDI (statistical significance in B: \* p < 0.05, \*\* p < 0.01).

In these experiments, Syt 12 S97A knockin animals displayed a near normal protein expression of total Syt 12 levels, whereas phosphorylated Syt 12 (lower band in Fig 2.6 A) was absent. Furthermore, none of the levels of other synaptic proteins that

were tested in this assay were changed, suggesting that the overall brain composition is not changed by removal of the Syt 12 serine<sup>97</sup> phosphorylation.

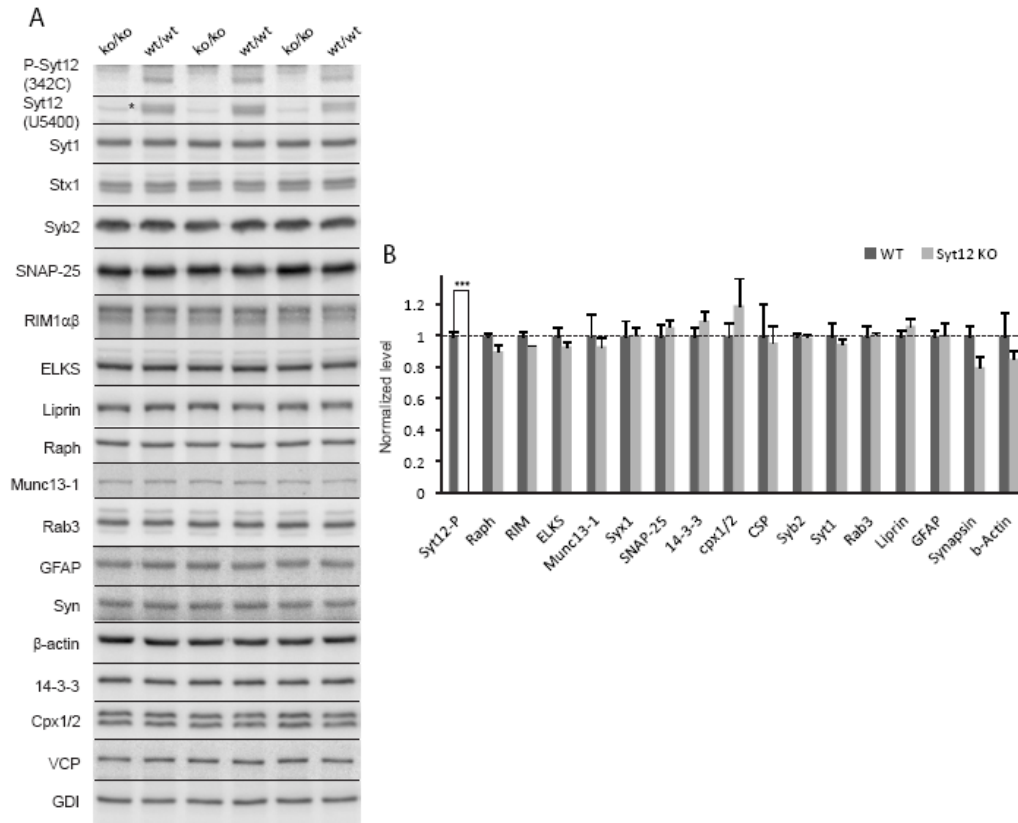


Figure 2.7 Syt 12 KO protein quantification. (A) Western blotting of whole brain lysates with <sup>125</sup>I iodine labeled secondary antibodies for multiple brain-specific proteins in brains from Syt 12 KO mice and wild-type littermate controls (n = 4 for each genotype, all at 8-9 weeks of age). GDI and VCP are shown as loading controls and were used for normalization. (B) Quantitative analysis of protein contents normalized to VCP, or GDI (statistical significance in B: \*\*\*, p < 0.005). Asterisk: non-specific cross-reactive band (see Fig 2.5).

In Syt 12 constitutive KO brains (fig 2.7), Syt 12 protein expression was completely abolished as quantitatively assessed by the p-Syt 12 antibody. Again, of the 15 other proteins tested, none showed a change in levels in the Syt 12 KO animals, suggesting that constitutive removal of Syt 12 during development does not affect the overall composition of the brain.

### **2.3.6 Synaptic transmission in the Syt 12 KO animals**

To functionally characterize the contribution of Syt 12 to synaptic transmission *in vivo*, we initiated collaboration with the laboratory of Dr. Pablo Castillo at Albert Einstein College of Medicine. In this collaboration, we decided to first assess whether synaptic transmission is changed in the Syt 12 KO animals, and once this is completed, we will assess specific questions such as presynaptic long-term and short-term plasticity in the Syt 12 S97A mutant animals.

Functional characterization is currently ongoing, and it includes a wide analysis of synaptic transmission in the hippocampus of Syt 12 KO and littermate control animals. Parameters that are currently being tested are the following: miniature synaptic transmission in excitatory and inhibitory synapses (mEPSC frequencies and amplitudes), forskolin-dependence of miniature synaptic transmission, synaptic input-output curves at inhibitory and excitatory synapses in the hippocampus, short-term synaptic plasticity at inhibitory and excitatory hippocampal synapses (paired-pulse ratios and synaptic depression/facilitation in response to short stimulus trains), presynaptic LTP at excitatory mossy fiber synapses, presynaptic LTD at inhibitory synapses in the CA1 region of the hippocampus. Currently, we do have some analysis of inhibitory synaptic transmission

and presynaptic long-term plasticity, which are included here. The data presented in the following paragraphs are preliminary and incomplete, but they do give us first hints about the function of Syt 12 in synaptic plasticity.

### **2.3.7 Basal inhibitory synaptic transmission in Syt 12 KO mice**

All experiments described here were performed in acute hippocampal slices of Syt 12 KO animals and wild-type littermate controls, and detailed protocols can be found in the methods section. We tested for changes in basal evoked inhibitory synaptic transmission (Fig 2.8 A-C). We found no difference in input/output curves, in paired-pulse responses (PPR), and in synaptic depression in response to short stimulus trains. These data suggest that there is no major change in synaptic strength and in short term plasticity at inhibitory synapses in area CA1 of the hippocampus in the Syt 12 KO mice. Corresponding experiments for excitatory synapses of Schaffer collaterals onto CA1 pyramidal neurons are currently being performed. When we tested mIPSC frequencies and amplitudes, and we found that these parameters were unchanged in the syt 12 KO animals (Fig 2.8 D).

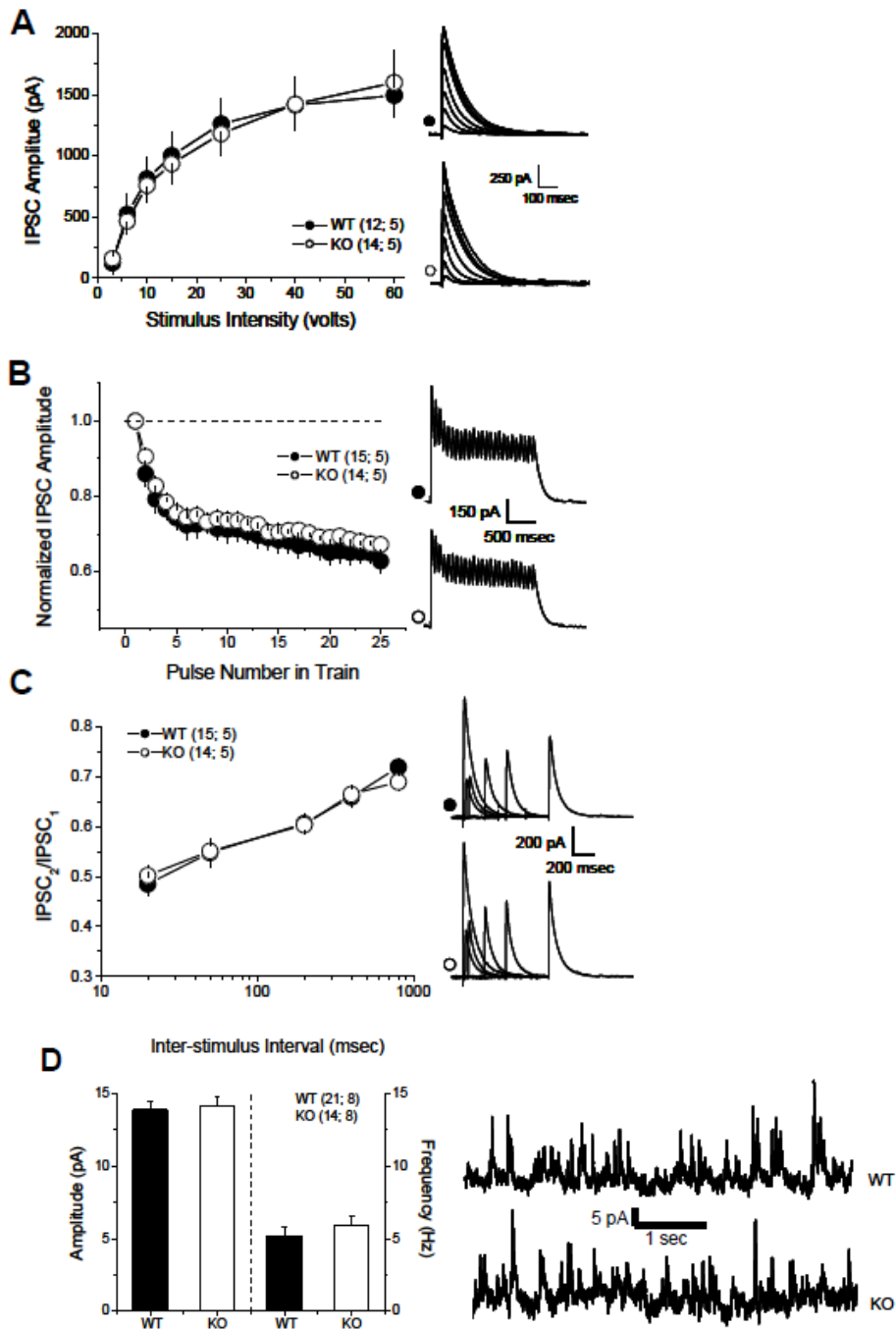


Figure 2.8 Characterization of basal inhibitory synaptic transmission. (A) Left: Input/output summary data. No significant difference between WT (filled circles, here

and subsequently) and KO (open circles, here and subsequently) was detected for evoked IPSC amplitudes plotted as a function of stimulus intensity. Right: Representative example traces averaged for each stimulus intensity (3, 6, 10, 15, 25, 40, and 60 V). (B) Left: Normalized summary data for IPSCs evoked by a burst of 25 pulses at 14 Hz. Each pulse in the burst was normalized to the first pulse. No significant difference between WT and KO was detected. Right: representative synaptic responses. (C) Left: Summary data for paired-pulse responses at 20, 50, 200, 400, and 800 msec inter-stimulus intervals indicating no difference between WT and KO. PPR was determined by subtracting the first pulse from the second pulse and subsequently dividing the peak amplitude of the second pulse by the first. Representative traces are shown at right. (D) Left: Miniature IPSC (mIPSC) summary data from WT and KO indicates no significant differences in amplitude or frequency between groups. Right: Example traces.

### **2.3.8 Presynaptic forms of long-term plasticity in Syt 12 KO mice**

To test our main hypothesis whether Syt 12 is directly involved in presynaptic long-term plasticity, we decided to assess two forms of plasticity in the hippocampus: (1) mossy fiber long-term potentiation (mLTP) (Nicoll and Malenka, 1995) and (2) inhibitory endocannabinoid receptor-mediated long-term depression (iLTD) (Chevalleyre and Castillo, 2003, 2004) in the hippocampus, both of which require cAMP-dependent PKA phosphorylation (Childers and Deadwyler, 1996; Hirano, 1991; Nguyen and Woo, 2003; Xiang et al., 1994).

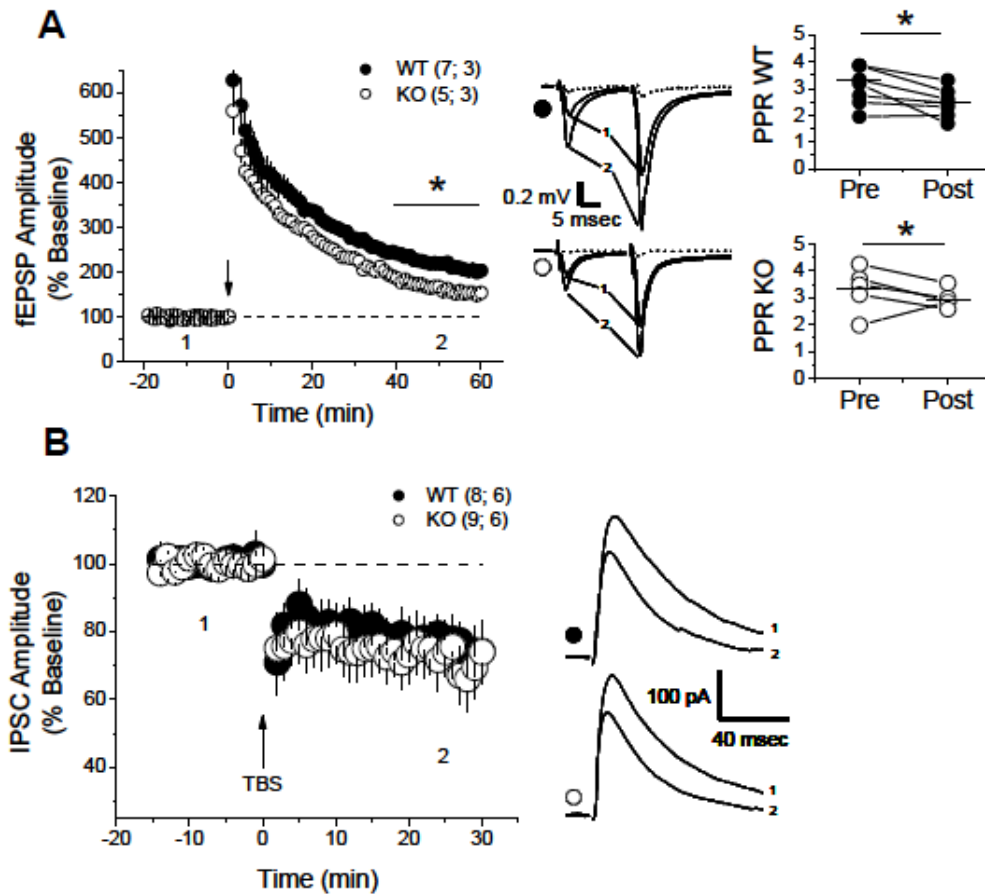


Figure 2.9 Presynaptic forms of long-term plasticity in Syt 12 KO mice. (A) Left: Summary data for mEPSP. fEPSP amplitude is plotted as a function of time and normalized to 20 min baseline period. mEPSP was triggered at time zero as indicated by arrow. Induction consisted of two bursts, each containing 125 pulses at 25 Hz. Number of slices/cells followed by number of animals is indicated in parenthesis here and in subsequent figures. Middle: Representative traces for WT and KO averaged from the times indicated by numbers. DCG-IV was applied at the end of each individual experiment (not shown in summary data), abolishing mossy fiber responses (dashed lines). Right: Consistent with classical mEPSP being expressed presynaptically, both WT

and KO showed significant reductions (\*  $p < 0.05$ , paired t-test) in paired-pulse ratio (PPR). (B) Left: Summary data for iLTD. IPSC amplitude is plotted as a function of time and normalized to 15 min baseline period. iLTD was triggered using theta burst stimulation (TBS) at time zero as indicated by arrow. TBS consisted of a series of 10 bursts (200 msec inter-burst interval), each burst with five stimuli (100 Hz within stimuli) repeated four times (5 sec apart). Right: Representative traces for WT and KO averaged from the times indicated by numbers.

To determine mFLTP, the fEPSP amplitude was plotted as a function of time, normalized to a 20 min baseline period before a LTP inducing stimulus protocol (Fig 2.9 A). mFLTP was then triggered at time zero (indicated by arrow in Fig 2.9 A). Induction consisted of two bursts, each containing 125 pulses at 25 Hz. We observed that the magnitude of mFLTP in Syt 12 KO (open circles) was significantly reduced (\*  $p < 0.05$ , unpaired t-test) compared to wild-type (filled circles) (Fig 2.9 A). To confirm that we stimulated the mossy fiber pathway, we applied DCG-IV (a group-selective agonist for the group II metabotropic glutamate receptors) at the end of each experiment, a method that has been previously used to characterize mossy fiber synaptic transmission (Castillo et al., 1997; Nicoll et al., 1994). To further confirm that the plasticity we induced in these experiments was expressed presynaptically, we measured paired pulse ratios before and after LTP induction. Paired pulse ratios at these terminals are inversely correlated with presynaptic release probability (Castillo et al., 1997; Schoch et al., 2002). We found that, both WT and KO showed significant reductions (\*  $p < 0.05$ , paired t-test) in paired-pulse ratio (PPR), confirming that the plasticity is expressed presynaptically. Again, the KO

animals showed a strong trend towards a reduced change in PPR, suggesting that the overall extent of plasticity may be altered in these animals.

To test presynaptic long-term depression at inhibitory synapses in area CA1 of the hippocampus, we measured the IPSC amplitudes in CA1 pyramidal neurons and plotted them as a function of time normalized to 15 min baseline period. iLTD was triggered using theta burst stimulation (TBS) at time zero as indicated by arrow (Fig 2.9 B). The TBS consisted of a series of 10 bursts (200 msec inter-burst interval) and each burst with five stimuli (100 Hz within stimuli) repeated four times (5 sec apart). The magnitude of iLTD between WT (filled circles) and KO (open circles) animals was not significantly different.

Altogether, these preliminary experiments suggest that Syt 12 may be involved in excitatory presynaptic LTP, but more experiments will be needed to determine the exact function of Syt 12 in synaptic transmission at both inhibitory and excitatory synapses. Furthermore, it will be critical to assess synaptic transmission in the Syt 12 S97A knockin animals in the future, in order to determine whether the presynaptic LTP is mediated by this PKA site of Syt 12, or whether it depends on additional functions of Syt 12.

## **2.4 Discussion and future perspectives**

A recent study suggested that Syt 12 is a synaptic vesicle protein that may regulate miniature neurotransmitter release in cultured neurons in response to phosphorylation of serine residue 97 by cAMP-dependent PKA (Maximov et al., 2007). Based on these findings, we hypothesized that Syt 12 may be the *in vivo* target of PKA

for presynaptic forms of long-term plasticity that depend on presynaptic PKA activation. In this part of my thesis, I generated knockin mice in which I introduced a point mutation of this serine residue to alanine. My experiments to date show that I successfully targeted the gene (Figs 2.4-2.7), and that phosphorylation of Syt 12 is abolished in the mutant mice by use of newly generated S97 phospho-specific antibodies (Fig 2.5 A). Further, I found that the Syt 12 S97A point mutation does not affect survival, and the synaptic protein composition in the brains of these mice appears to be unchanged. This mouse line will allow direct assessment of our hypothesis in acute brain slices of Syt 12 S97A knockin mice.

In parallel, I generated constitutive Syt 12 KO mice by introducing loxP sites surrounding the exon that contains the point mutation, and by crossing the knockin mice to transgenic mice that express cre recombinase in the male germ line (O'Gorman et al., 1997). Again, our current experiments confirm that Syt 12 was constitutively removed, and that deleting Syt 12 constitutively does not affect the survival rate or the protein composition. These mice allow testing the functions of Syt 12 beyond its PKA dependent phosphorylation.

In functional experiments that are currently done in collaboration with the laboratory of Dr. Pablo Castillo at Albert Einstein College of Medicine, we decided to first analyze synaptic transmission in the Syt 12 KO mice, before going into the more specific question of the direct effect of PKA phosphorylation. It is important to note here, that all the data that are derived from the functional experiments are preliminary. Furthermore, important control experiments and also more basic experiments that are

required for this characterization are still not completed. Thus, it is currently too early to draw final conclusions.

However, our preliminary data suggest that basic parameters of inhibitory synaptic transmission are not dramatically changed. Specifically, we found that mIPSC frequencies and amplitudes, input-output curves, and two parameters of short-term synaptic plasticity (paired pulse ratios and synaptic depression in response to short stimulus trains) are likely normal (Fig. 2.8). Furthermore, an inhibitory form of synaptic long-term depression called iLTD also appears normal (Fig 2.9 B). In contrast, it currently appears that mFLTP, an excitatory form of presynaptic long-term plasticity at the large mossy fiber terminals in the hippocampus is attenuated (Fig. 2.9 A). Although these results are exciting, it is important to note that the number of experiments that were performed (5 slices, 3 mice for KO) is still low, and we will do more experiments. In addition, this result is hard to interpret without characterizing basic parameters of excitatory synaptic transmission in the Syt 12 KO mice, because the seemingly reduced mFLTP could be due to either LTP induction or to LTP expression. Thus, it will be important to complete a careful analysis of excitatory synaptic transmission, and this is currently being performed. The parameters that are included in the ongoing analysis are mEPSC measurements, excitatory input-output curves, and excitatory short-term plasticity (paired pulse stimulations and short stimulus trains). These experiments will further determine what will have to be performed.

Finally, if it turns out to be true that mFLTP is affected in the Syt 12 KO animals, we will test mFLTP and other forms of presynaptic long-term plasticity in the Syt 12

S97A KI animals to test whether the phosphorylation of Syt 12 by PKA regulates these events.

A question that will certainly arise if our preliminary findings are true is why mLTP is only attenuated, and not abolished similar to other presynaptic mouse mutant lines of proteins that have been shown to participate in presynaptic LTP (Castillo et al., 1997; Castillo et al., 2002). It is possible that the constitutive deletion leads to an effect of compensation, and it may be that this compensation will not act if Syt 12 present in its non-phosphorylatable S97A mutant form. However, it is currently too early to speculate about the outcome of these experiments, but the analyses of these point mutant mice will certainly be informative, and it will solve the hypothesis of whether PKA phosphorylation of Syt 12 at serine<sup>97</sup> is required for presynaptic, PKA-dependent LTP.

## CHAPTER III: COMPLEXIN CLAMPS FUSION BY BLOCKING A SECONDARY $\text{Ca}^{2+}$ -SENSOR VIA ITS ACCESSORY ALPHA-HELIX

### 3.1 INTRODUCTION

Recent observations with synaptotagmin have cast doubt on the synaptotagmin-switch model. Specifically, using new protocols to deplete presynaptic  $\text{Ca}^{2+}$ , spontaneous fusion in both wild-type and synaptotagmin-deficient synapses was revealed to be largely  $\text{Ca}^{2+}$ -dependent (Xu et al., 2009). Moreover, the apparent  $\text{Ca}^{2+}$ -affinity and  $\text{Ca}^{2+}$ -cooperativity of spontaneous fusion was found to differ between wild-type and synaptotagmin-deficient synapses (which exhibit increased spontaneous fusion), suggesting that synaptotagmin does not actually clamp SNARE complexes to block spontaneous fusion, but instead blocks the action of a secondary  $\text{Ca}^{2+}$ -sensor (Xue et al., 2009). Since the synaptotagmin-switch model of the complexin clamp implies that spontaneous fusion increases in complexin-deficient synapses because of an increased rate of unregulated SNARE-complex assembly, a  $\text{Ca}^{2+}$ -dependent mechanism of spontaneous fusion appears to be inconsistent with the notion that complexin clamps fusion by inserting into the SNARE-complex. Thus, the question arises whether the increase in spontaneous fusion in complexin-deficient synapses, or in synapses containing WA-mutant synaptobrevin, is due to unregulated SNARE-complex assembly, or to the unblocking of a secondary  $\text{Ca}^{2+}$ -sensory. Moreover, if increased spontaneous fusion in complexin-deficient synapses is due to the unblocking of a secondary  $\text{Ca}^{2+}$ -sensor, can this mechanism really be mediated by insertion of the accessory  $\alpha$ -helix of

complexin into the SNARE complex? Finally, how does the clamping function of complexin relate to its activation function?

To address these questions, we have investigated how complexin clamps fusion. We show that the increased spontaneous release in complexin-deficient and in synaptobrevin WA-mutant synapses is indeed  $\text{Ca}^{2+}$ -dependent, with properties suggesting activation of a secondary  $\text{Ca}^{2+}$ -sensor. At the same time, we demonstrate that the accessory  $\alpha$ -helix of complexin mediates its clamping function, likely by inserting into partly assembled SNARE complexes. Moreover, we find that the complexin deficiency dramatically lowers the size of the readily-releasable pool (RRP) of vesicles.

## **3.2 MATERIALS AND METHODS**

### **3.2.1 Neuronal cultures**

Neurons were cultured from the cortex of newborn wild-type mice, synaptobrevin-2 KO mice, or rats (Maximov et al., 2009). Briefly, neurons were dissociated by papain digestion, plated on polylysine-coated glass coverslips, and cultured in Modified Eagle Medium (Invitrogen) supplemented with B27 (Invitrogen), glucose, transferrin, fetal bovine serum, and Ara-C (Sigma, St. Louis, MO).

### **3.2.2 Generation and validation of KD lentiviruses and rescue constructs**

The complexin KD and wild-type complexin ( $\text{Cpx}^{\text{WT}}$ ) rescue constructs were described previously (Maximov et al., 2009).  $\text{Cpx}^{\text{Superclamp}}$  (D27L E34F R37A),  $\text{Cpx}^{\text{Poorclamp}}$  (K26E L41K E47K),  $\text{Cpx}^{\text{WW}}$  (G21W G22W), and  $\text{Cpx}^{\text{AA}}$  (G21A G22A) mutations were generated accordingly. Oligonucleotides encoding the mouse

synaptotagmin-1 shRNA sequence (GAGCAAATCCAGAAAGTGCAA) were cloned into the XhoI/XbaI cloning site downstream of the human H1 promoter in the L309-mCherry lentiviral vector (modified from vector L309 in that the IRES-GFP sequence downstream of the ubiquitin promoter in L309 was altered to mCherry; (Maximov et al., 2009)). The synaptotagmin-1 KD efficiency of this viral vector was verified by measuring the endogenous synaptotagmin-1 mRNA level in cultured cortical neurons using quantitative real-time PCR. Lentiviruses were prepared in transfected 293T cells, and harvested and used immediately two days after transfection. Neurons were infected at DIV6 with control or various KD viruses, and analyzed at DIV14-16.

### 3.2.3 Protein purification and GST-pulldown assay

Wildtype complexin-1 (Cpx<sup>WT</sup>) and point mutants (Cpx<sup>Superclamp</sup>, Cpx<sup>Poorclamp</sup>, Cpx<sup>WW</sup>, and Cpx<sup>AA</sup>; see Fig. 3.3A) were expressed as GST-fusion proteins in pGEX-KG, and recombinant proteins were purified according to standard methods (Okamoto and Sudhof, 1997). Briefly, bacteria containing GST fusion proteins were resuspended in PBS buffer with 2 mM EDTA, and proteases inhibitors (Sigma) before sonication. After centrifugation of lysates at 11,000 rpm for 30 min, supernatant was incubated with glutathione sepharose beads for overnight at 4 °C. Beads were washed with ice-cold PBS three times and resuspended in PBS.

For GST-pulldown, one unstripped rat brain (~1.5 g/brain; Pel-Freez Biologicals, Rogers, AR) was homogenized with a tissuehomogenizer (Thomas Scientific, Philadelphia, PA) in 30 ml of lysate buffer containing 50 mM HEPES-NaOH pH 6.8, 0.1 M NaCl, 4 mM EGTA, protease inhibitor cocktail (Roche, Indianapolis, IN), 1 mM

PMSF, and 1mM DTT. 1% Triton X-100 was added to the homogenate, proteins were extracted for 1 hr at 4 °C with rocking, insoluble proteins were removed by centrifugation (150,000xg for 1 hr), and the supernatant was used for experiments. For 1 ml of brain lysate, I added ~5ng of each GST-fusion proteins for 2hr at 4 °C. Beads were washed with lysate buffer five times and eluted in SDS sample buffer.

### **3.2.4 Imaging experiments**

For measuring synaptic vesicle exo- and endocytosis, infected rat cortical neurons were incubated with synaptotagmin-1 luminal antibodies (CL604.4, 1:25; Matteoli et al., 1992) at 37°C for 30 min in standard medium. Images of randomly chosen neurons were acquired with a confocal microscope (LSM510, Zeiss or TCS2, Leica) at constant settings. Images were analyzed using ImageJ Software (NIH) with intensity of different channels. To quantify the synaptic puncta size, we thresholded all images equally, and measured the average pixel intensities by manually tracing each punctum, with a >2-fold background signal.

### **3.2.5 Electrophysiology**

To monitor synaptic responses, whole-cell patch-clamp recordings were made with neurons at 14–16 d *in vitro*. Synaptic responses were triggered by a 1 ms current pulse (90  $\mu$ A) through a local extracellular electrode (FHC, Bowdoinham, ME), and recorded in whole-cell voltage-clamp mode using a Multiclamp 700A amplifier (Molecular Devices, Union City, CA). Data were digitized at 10 kHz with a 2 kHz low-pass filter. The pipette solution contained the following (in mM): 135 CsCl, 5 NaCl, 1

MgCl<sub>2</sub> 10 HEPES-NaOH pH 7.4, 10 EGTA, 4 Mg-ATP, 0.4 Na-GTP, and 5 QX-314 (lidocaine N-ethyl bromide). The bath solution contained the following (in mM): 140 NaCl, 5 KCl, 2 CaCl<sub>2</sub>, 2 MgCl<sub>2</sub>, 10 HEPES-NaOH pH 7.4 and 10 glucose. NMDA-receptor mediated EPSCs were isolated pharmacologically by including 4 instead of 2 μM MgCl<sub>2</sub>, 20 μM CNQX, 100 μM Picrotoxin and 15 μM glycine in the bath solution. Data were analyzed using Clampfit 9.02 (Molecular Devices) or Igor 5.01 (Wavemetrics, Lake Oswego, OR).

### **3.3 RESULTS**

#### **3.3.1 Complexin clamps an auxiliary Ca<sup>2+</sup>-sensor**

To test whether the increased spontaneous fusion observed after KD of complexin is due to a loss of control over SNARE-mediated fusion, or whether it represents a shift from one mode of Ca<sup>2+</sup>-triggered spontaneous fusion to another, we measured the frequency of miniature excitatory postsynaptic currents (mEPSCs) in complexin KD neurons as a function of Ca<sup>2+</sup> (Fig. 3.1).

The complexin KD increased the mEPSC frequency ~3-fold. In both control and complexin KD neurons, removal of extracellular Ca<sup>2+</sup> decreased the mEPSC frequency ~2-fold, whereas a 30 min preincubation with 10 μM BAPTA-AM in Ca<sup>2+</sup>-free extracellular medium lowered the mEPSC frequency >10-fold (Figs. 3.1A and 3.1B). Thus, the increased mEPSCs observed in complexin KD neurons are Ca<sup>2+</sup>-dependent, analogous to those observed in synaptotagmin KO neurons, in which the deletion of

synaptotagmin unclamps an auxiliary  $\text{Ca}^{2+}$ -sensor with a higher apparent  $\text{Ca}^{2+}$ -affinity and a lower apparent  $\text{Ca}^{2+}$ -cooperativity (Xu et al., 2009).

To characterize the  $\text{Ca}^{2+}$ -dependence of spontaneous fusion in complexin KD neurons, we measured the mEPSC frequency in control and complexin KD neurons as a function of extracellular  $\text{Ca}^{2+}$ , using complexin KD neurons expressing wild-type complexin as a rescue control (Fig. 3.1C). Quantitation of the mEPSC frequency showed that the complexin KD shifted the  $\text{Ca}^{2+}$ -dependence of mEPSCs to the left (Fig. 3.1D). Since we naturally used no BAPTA-AM in these experiments, the mEPSC frequency in the complexin KD neurons is not completely suppressed at low  $\text{Ca}^{2+}$ -concentrations (see Fig. 3.1B for the effect of BAPTA-AM pretreatment). Nevertheless, the overall  $\text{Ca}^{2+}$ -dependence of mEPSCs release can be analyzed by fitting the  $\text{Ca}^{2+}$ -dependence to a Hill function. The data demonstrate that after complexin KD, the apparent  $\text{Ca}^{2+}$ -cooperativity of mEPSC release decreases, whereas their apparent  $\text{Ca}^{2+}$ -affinity increases (Figs. 3.1E and 3.1F). Thus, the effect of the complexin KD on mEPSC release is qualitatively the same as the effect of the synaptotagmin KO (Xu et al., 2009): both unclamp an secondary  $\text{Ca}^{2+}$ -sensor whose properties are similar to that of the  $\text{Ca}^{2+}$ -sensor for asynchronous release (Sun et al., 2007).

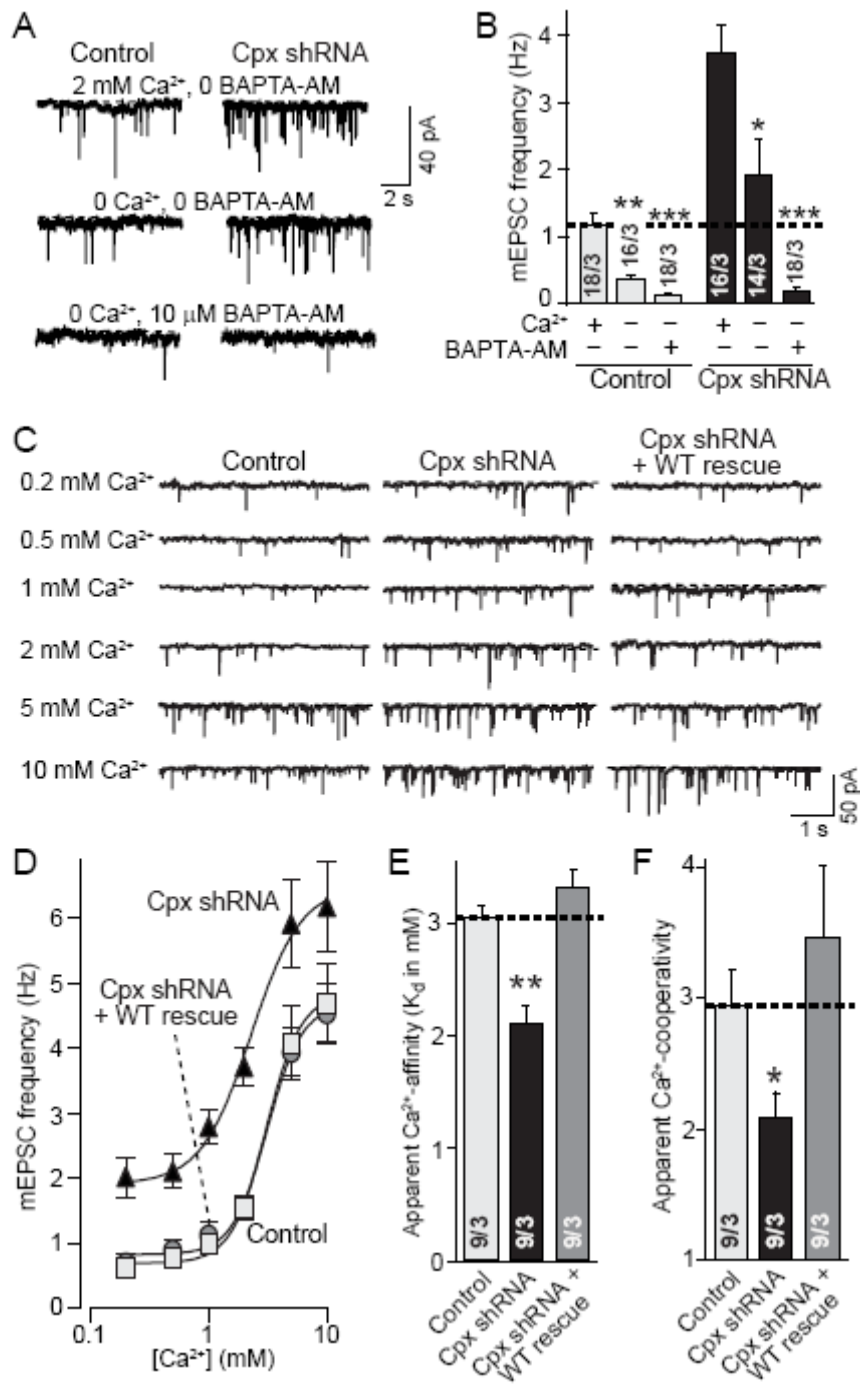


Fig 3.1 Complexin clamps a Ca<sup>2+</sup>-dependent fusion mechanism

A & B, Sample traces (A) and summary graph of the frequency (B) of spontaneous miniature excitatory postsynaptic currents (mEPSC) monitored in control and complexin KD neurons. mEPSCs were recorded in medium containing 2 mM  $\text{Ca}^{2+}$ ,  $\text{Ca}^{2+}$ -free medium, and  $\text{Ca}^{2+}$ -free medium after a 30 mins incubation with 10  $\mu\text{M}$  BAPTA-AM. mEPSC amplitudes did not change significantly (see Fig. 3.6). C & D, Sample traces of mEPSCs (C) and summary graphs of the mEPSC frequency (D) recorded at the indicated concentrations of extracellular  $\text{Ca}^{2+}$  in control neurons and complexin KD neurons expressing either GFP (Cpx shRNA) or wild-type complexin-1 (Cpx shRNA + WT rescue). For mEPSC amplitudes and a plot of the relative mEPSC frequency as a function of  $\text{Ca}^{2+}$ , see Figs. 3.2 B and 3.2 C. E & F, Bar diagram of the apparent  $\text{Ca}^{2+}$ -affinity (E) and  $\text{Ca}^{2+}$ -cooperativity (F) of mEPSCs, calculated by individual Hill function fits to data from multiple independent experiments of the  $\text{Ca}^{2+}$ -dependence of the mEPSC frequency as shown in panel D. Data shown are means  $\pm$  SEMs; number of cells/independent cultures analyzed is depicted in the bars. Statistical significance was analyzed by Student's t-test, comparing the  $\text{Ca}^{2+}$ -free to the control condition separately for control and complexin KD neurons (A and B), or complexin KD conditions to the control (D-F; \*= $p < 0.05$ ; \*\*= $p < 0.01$ ; \*\*\*= $p < 0.001$ ).

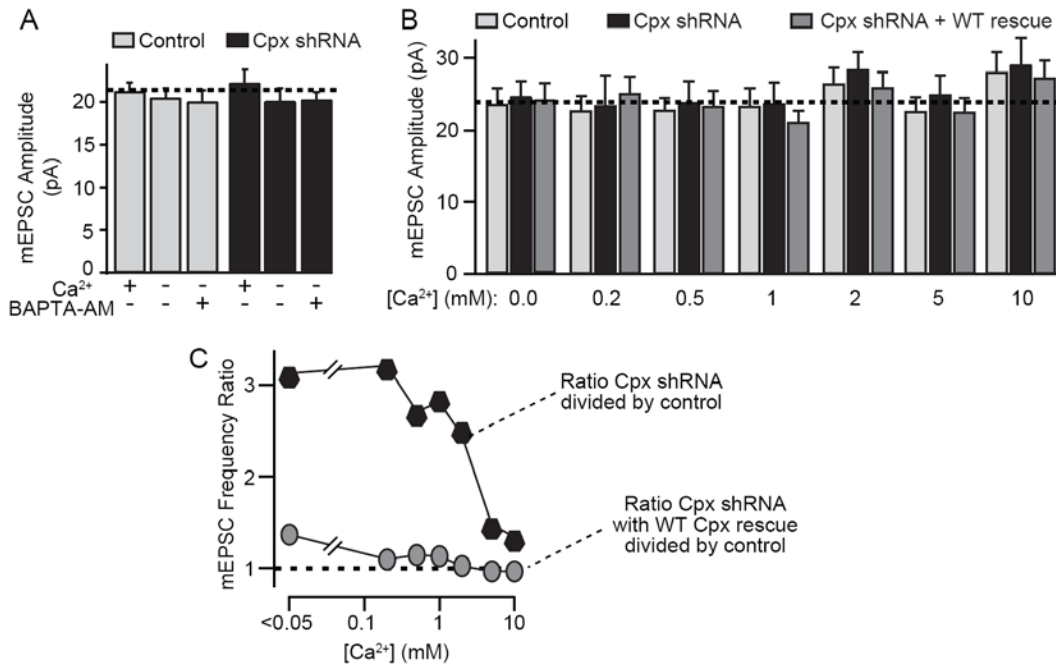


Figure 3.2. Ca<sup>2+</sup> and complexin KD do not affect mEPSC amplitudes, although they control mEPSC frequencies

A, Summary graph of the amplitude of mEPSCs monitored in control and complexin KD neurons in the presence and absence of Ca<sup>2+</sup>. Minis were recorded in medium containing 2 mM Ca<sup>2+</sup>, Ca<sup>2+</sup>-free medium, and Ca<sup>2+</sup>-free medium after a 30 min incubation with 10 μM BAPTA-AM. mEPSC amplitudes did not change significantly, whereas the mEPSC frequency did (see Figs. 3.1A and 3.1B). B. Summary graphs of the mEPSC amplitude recorded at the indicated concentrations of extracellular Ca<sup>2+</sup> in control neurons and complexin KD neurons expressing either GFP (Cpx shRNA) or wild-type complexin-1 (Cpx shRNA + WT rescue). C, Relative mEPSC frequencies in complexin KD neurons without and with rescue as a function of the extracellular Ca<sup>2+</sup>-concentration, determined as the ratio of the mEPSC frequency in complexin KD neurons without (black symbols)

or with rescue with full-length complexin (gray symbols) to the mEPSC frequency in control neurons. For panels B and C, see Figs. 3.1C-3.1F for the primary data and mEPSC frequencies.

### **3.3.2 Mutants in the accessory $\alpha$ -helix of complexin**

The accessory  $\alpha$ -helix of complexin was proposed to clamp exocytosis by inserting into the partially assembled SNARE complex in place of synaptobrevin/VAMP (Giraudo et al., 2009). Databank searches revealed that complexin, along with synaptotagmin, is highly conserved evolutionarily, being even detectable in the most primitive animals such sea anemones and trichoplax (Fig. 3.3A).

To test the role of the accessory  $\alpha$ -helix in clamping mEPSCs, and to specifically examine whether its function is not only required for clamping but also for activation, and whether the accessory  $\alpha$ -helix clamps by inserting into a partially assembled SNARE complex, we generated four point mutants of complexin-1: (i) a 'superclamp' mutant (D27L/E34F/R37A) described by Giraudo et al. (Giraudo et al., 2009) that increases insertion of the complexin accessory  $\alpha$ -helix into the SNARE complex; (ii) a corresponding 'poorclamp' mutant in which we mutated three residues predicted to be essential for insertion of the accessory  $\alpha$ -helix to mimic synaptobrevin into the SNARE complex (K26E/L41K/E47K), and (iii) two substitutions of the tandem glycine residues at the boundary between the N-terminal region and the accessory  $\alpha$ -helix of complexin (G21A/G22A, and G21W/G22W; Fig. 3.3A). To ensure that the accessory  $\alpha$ -helix is not

essential for SNARE binding by the central  $\alpha$ -helix of complexin, we examined whether the four complexin mutants we generated were still able to pull down SNARE complexes from brain homogenates (Fig. 3.3B). We found that all mutants efficiently bound SNARE complexes, suggesting that they do not impair SNARE complex binding by the central  $\alpha$ -helix.

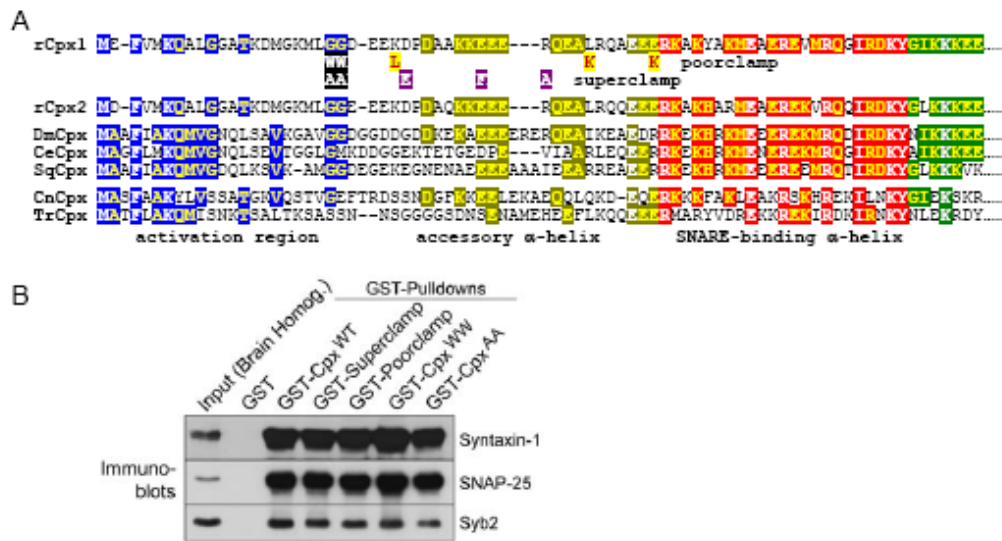


Figure 3.3 Complexin is evolutionarily conserved in all animals: location of mutations in the accessory  $\alpha$ -helix that do not interfere with SNARE binding A, Alignment of the N-terminal 90 residues of rat complexin-1 and -2 with complexin sequences from *Drosophila* (DmCpx), *C. elegans* (CeCpx), squid (SqCpx), *Nomastella* (CnCpx) and *Trichoplax* (TrCpx). Residues present in the majority of sequences are highlighted in a domain-specific color code (blue = activation domain; light green = accessory  $\alpha$ -helix; red = SNARE-binding  $\alpha$ -helix). In addition, the residues of the accessory  $\alpha$ -helix that were mutated in the four point mutants analyzed here are indicated below the complexin-1 sequence (WW-mutant = G21W/G22W; AA-mutant =G21A/G22A; poorclamp =

K26E/L41K/E47K; superclamp = D27L/E34F/R37A). *B*, The complexin accessory  $\alpha$ -helix mutations do not block SNARE protein binding. Solubilized rat brain proteins were bound to immobilized GST-fusion proteins of wild-type or mutant complexins, and bound proteins were analyzed by immunoblotting for the indicated SNARE proteins.

### **3.3.3 Effects of accessory $\alpha$ -helix mutations on mEPSCs release**

We infected neurons with control lentivirus or the complexin KD lentivirus expressing either GFP, superclamp-mutant, or poorclamp-mutant complexin. mEPSC recordings revealed that superclamp complexin rescued both the increased mEPSC frequency – actually suppressed the mEPSC frequency below control levels – and the decreased evoked release in complexin KD neurons (Figs. 3.4A-3.4D). The poorclamp mutant, by contrast, increased the mEPSC frequency even beyond the increase observed in complexin KD neurons, but still fully rescued the decrease in evoked release observed in the complexin KD neurons (Figs. 3.4A-3.4D). Thus, the poorclamp and superclamp mutants of complexin support the notion that complexin clamps fusion by inserting into nascent trans-SNARE complexes, and demonstrate that the clamping and activation functions of complexin are unrelated, i.e. that the complexin clamp is not required for activating synaptotagmin.

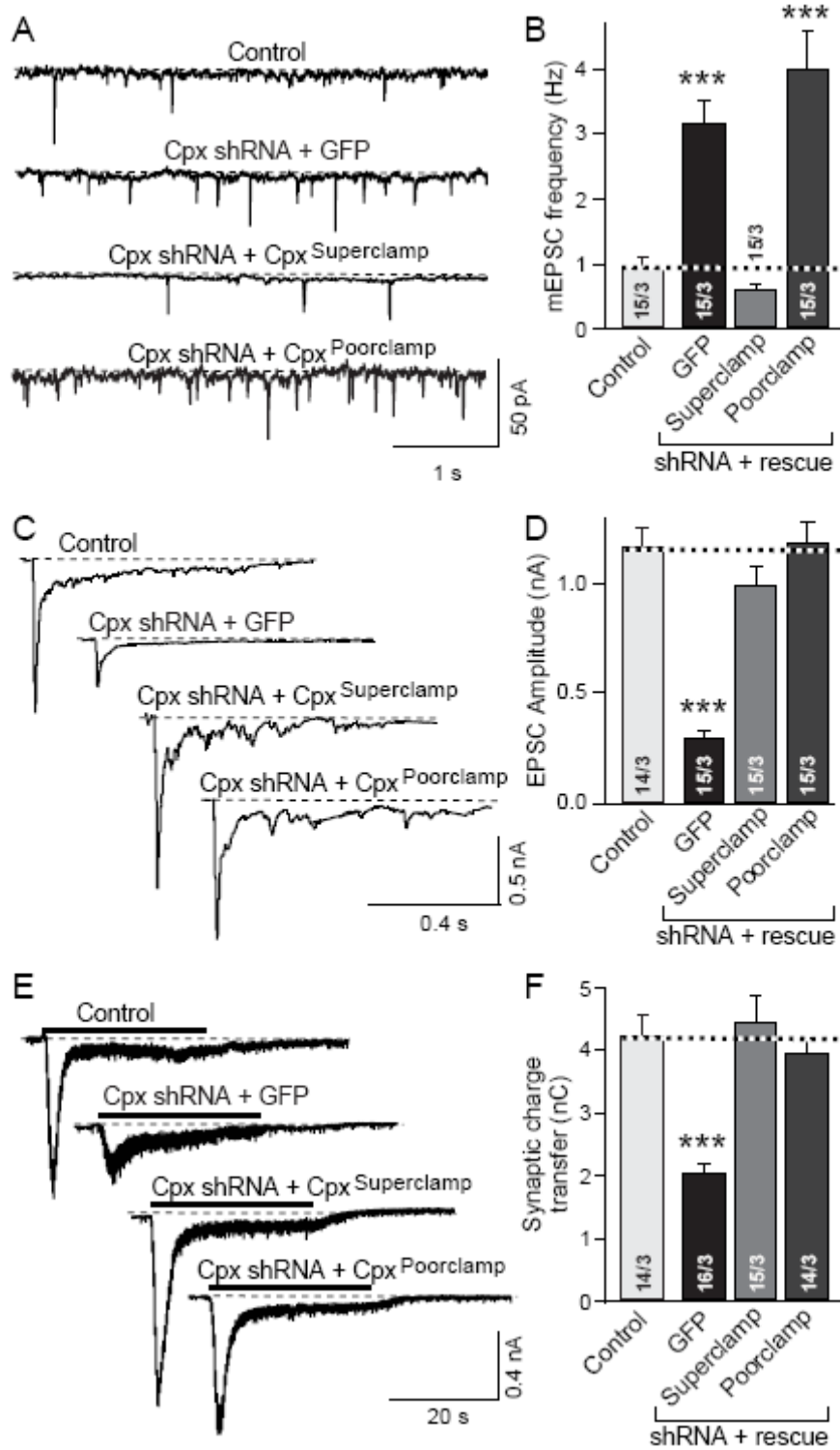


Figure 3.4 Complexin superclamp- and poorclamp-mutants decrease or increase, respectively, spontaneous but not evoked release

A & B, Sample traces of mEPSCs (A) and summary graphs of the mEPSC frequency (B) recorded in control neurons and complexin KD neurons expressing either GFP (Cpx shRNA) or the complexin superclamp or poorclamp mutants (see Fig. 3.3). For  $\text{Ca}^{2+}$ -titration data on the complexin mutants, see Fig. 3.6.C & D, Sample traces of action-potential evoked EPSCs (C) and summary graphs of EPSC amplitudes (D) recorded in control neurons and complexin KD neurons expressing GFP or the complexin superclamp or poorclamp mutants. E & F, Sample traces of sucrose-evoked EPSCs (E) and summary graphs of the charge transfer induced by hypertonic sucrose (F) recorded in control neurons and complexin KD neurons expressing GFP or the complexin superclamp or poorclamp mutants. Release was triggered by a 30 s application of 0.5 M sucrose, and the synaptic charge transfer was integrated over 30 s. For a kinetic analysis of sucrose-induced release, see Fig. 3.6. All data shown are means  $\pm$  SEMs; number of cells/independent cultures analyzed are depicted in the bars. Statistical significance was analyzed by Student's t-test, comparing complexin KD to control neurons (\*\*= $p < 0.001$ ).

We next examined mutations in the di-glycine motif of complexin, using the same experimental paradigm (Fig. 3.5). Alanine substitutions of the di-glycine motif had little effect on the ability of complexin to rescue the increase in mEPSCs and the decrease in evoked release. In contrast, tryptophan substitutions caused a striking increase in

mEPSC frequency that was dramatically more severe than that observed with the complexin KD alone (Figs. 3.5A and 3.5B). Again, the tryptophan substitutions did not impair the ability of complexin to rescue the decrease in evoked release observed in complexin KD neurons (Figs. 3.5C and 3.5D). Thus, two independent mutations (the poorclamp mutation and tryptophan substitution) confirm that the clamping of the auxiliary  $\text{Ca}^{2+}$ -sensor by complexin is separable from its activation function.

### **3.3.4 Complexin is essential for vesicle priming**

In the same experiments in which we studied the effects of various complexin mutations on its clamping and activation functions (Figs. 3.4 and 3.5), we also investigated the role of complexin in the priming of vesicles into the RRP, defined as the vesicle pool whose exocytosis is triggered by hypertonic sucrose (Rosenmund and Stevens, 1996). We found that the complexin KD strongly suppressed the RRP (Figs. 3.4E, 3.4F, 3.5E, and 3.5F). This result was unexpected because in parallel experiments, we found no effect of synaptotagmin KO's on the RRP (Fernandez et al., 2001; Geppert et al., 1994; Pang et al., 2006c; Sun et al., 2007; Xu et al., 2009). The effects of the complexin KD on RRP size and on evoked release were quantitatively similar, suggesting that complexin activates SNARE complexes by superpriming vesicles into the RRP. The decrease in RRP was fully rescued by wild-type complexin and by the four complexin mutants in the accessory  $\alpha$ -helix, demonstrating that the decrease in RRP was not due to an off-target effect (Figs. 3.4 and 3.5). Thus, complexin participates in priming vesicles upstream of synaptotagmin.

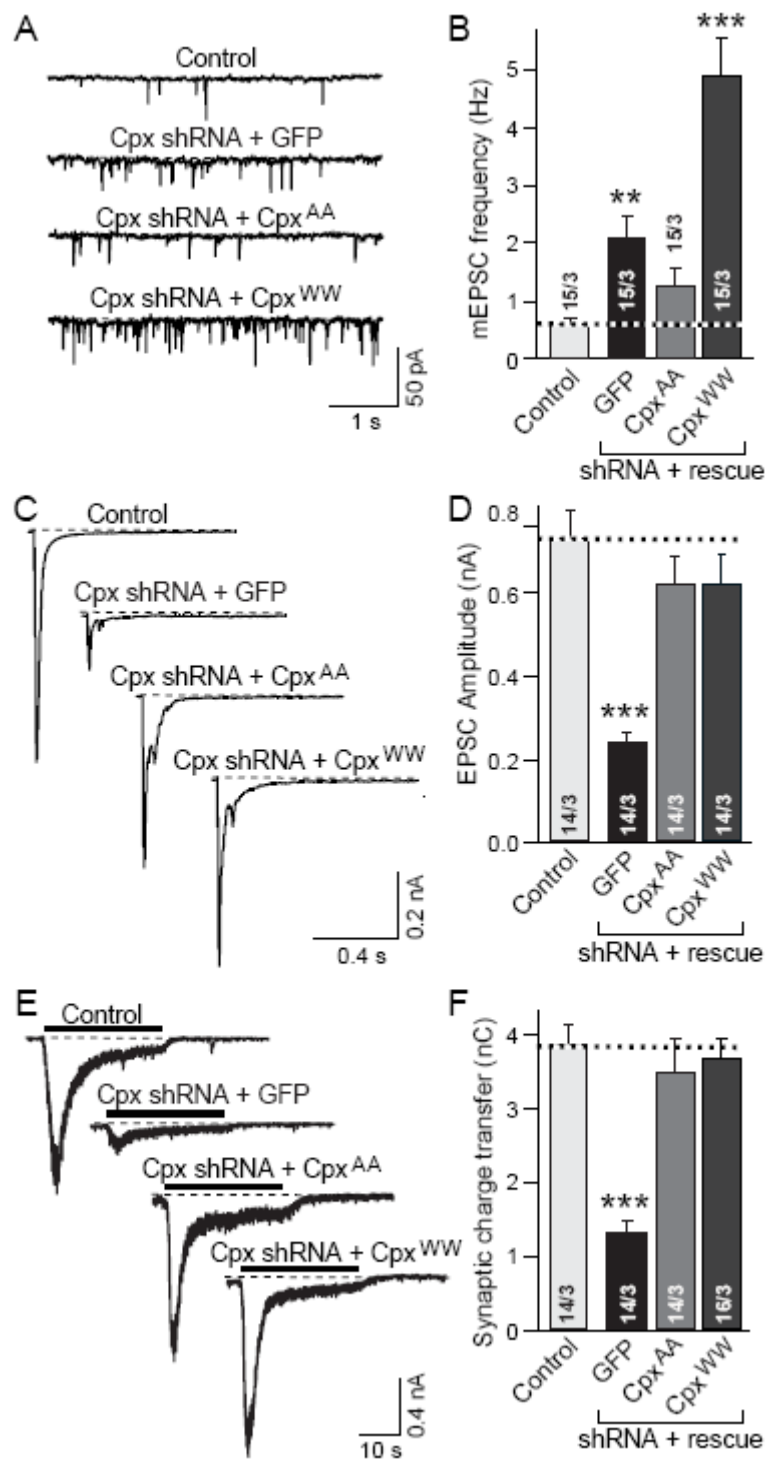


Figure 3.5 Complexin WW- and AA-mutations increase spontaneous mEPSCs-release without altering evoked release

A & B, Sample traces of mEPSCs (A) and summary graphs of the mEPSC frequency (B) recorded in control neurons and complexin KD neurons expressing either GFP (Cpx shRNA) or the complexin 'AA' or 'WW' mutants in which glycines at residue 21 and 22 are replaced by alanine and tryptophan, respectively (see Fig. 3.3). For  $\text{Ca}^{2+}$ -titration data on the complexin mutants see Fig. 3.6. C & D, Sample traces of action-potential evoked EPSCs (C) and summary graphs of EPSC amplitudes (D) recorded in control neurons and complexin KD neurons expressing GFP or the complexin 'AA' or 'WW' mutants. E & F, Sample traces of sucrose-evoked EPSCs (E) and summary graphs of the charge transfer induced by hypertonic sucrose (F) recorded in control neurons and complexin KD neurons expressing GFP or the complexin 'AA' or 'WW' mutants. Release was triggered by a 30 s application of 0.5 M sucrose, and the synaptic charge transfer was integrated over 30 s. For a kinetic analysis of sucrose-induced release, see Fig. 3.6. All data shown are means  $\pm$  SEMs; number of cells/independent cultures analyzed are depicted in the bars. Statistical significance was analyzed by Student's t-test, comparing complexin KD to control neurons (\*\*= $p < 0.01$ , \*\*\*= $p < 0.001$ ).

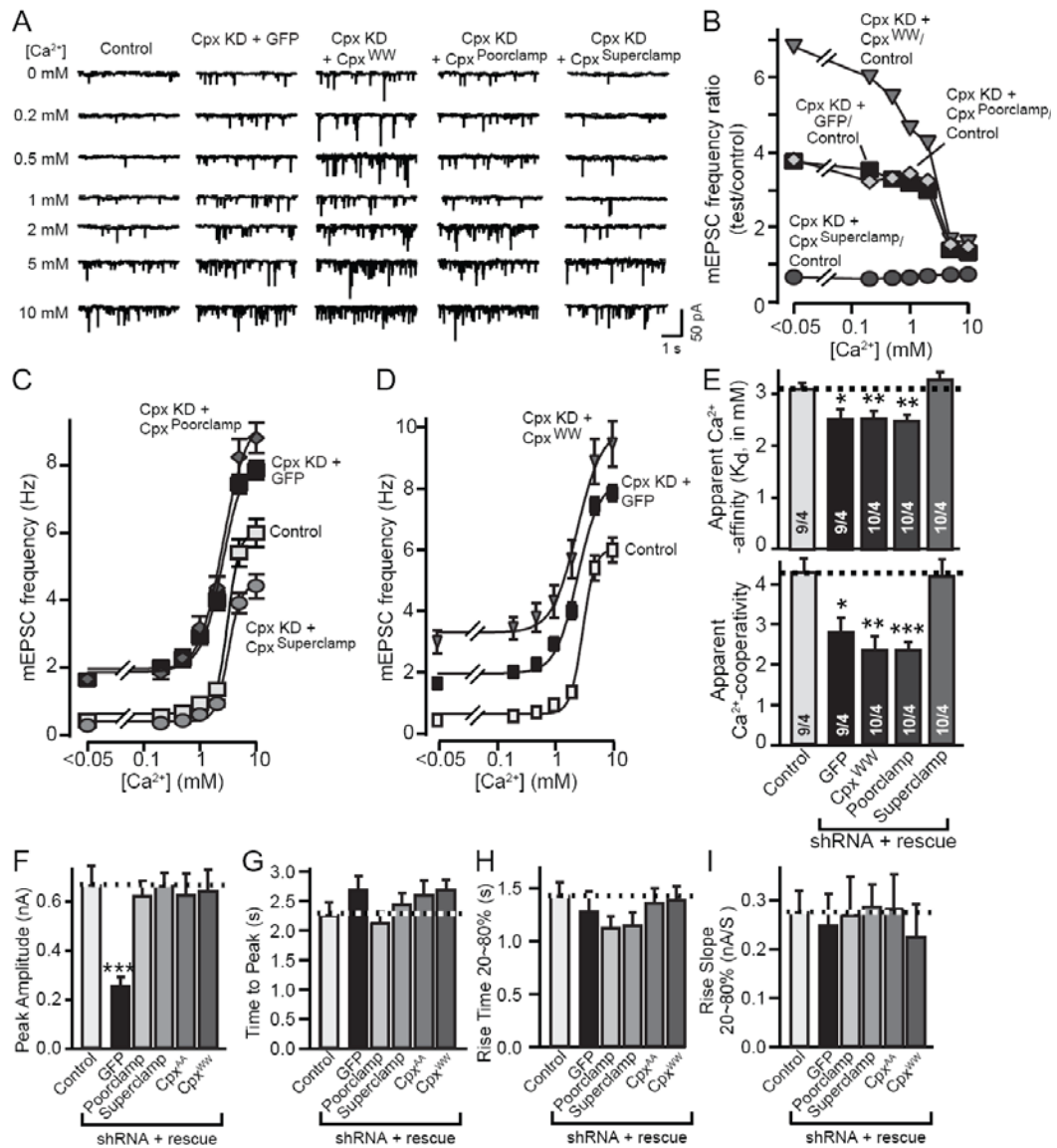


Figure 3.6. Distinct apparent  $\text{Ca}^{2+}$ -affinities and  $\text{Ca}^{2+}$ -cooperativities of spontaneous release in wild-type and complexin mutant synapses (A-E), and effect of the complexin KD and rescues on the kinetics of sucrose-induced release (F-I) A, Sample traces of mEPSCs recorded at the indicated concentrations of extracellular  $\text{Ca}^{2+}$  in control neurons and complexin KD neurons expressing either GFP (Cpx shRNA), the complexin

superclamp or poorclamp mutants, or the complexin 'WW' mutants. B, Relative mEPSC frequency as a function of  $\text{Ca}^{2+}$  (i.e., mEPSC frequency in complexin KD neurons without or with rescue with the various complexin mutant constructs divided by the mEPSC frequency observed under control conditions). C & D, Summary graphs of the mEPSC frequency recorded as a function of the extracellular  $\text{Ca}^{2+}$ -concentration in the neurons described in panels A and B. E, Bar diagrams of the apparent  $\text{Ca}^{2+}$ -affinity (top) and  $\text{Ca}^{2+}$ -cooperativity (bottom) of mEPSCs, calculated by individual Hill function fits to data from multiple independent experiments of the  $\text{Ca}^{2+}$ -dependence of the mEPSC frequency as shown in panels C & D. F – I, Summary graphs of the parameters of sucrose-induced release in the neurons infected with control lentivirus, complexin KD lentivirus without or with various complexin rescue constructs as described for panel A (for sample traces and charge transfer data, see Figures 3.4 and 3.5). The peak amplitude (F), the time to peak (G), the rise time 20-80% (H) and the rise slope 20-80% (I) during the sucrose treatment were shown in bar graphs. All data shown are means  $\pm$  SEMs; number of cells/independent cultures analyzed are depicted in the bars for the mEPSC analyses; for the sucrose induced release, see Figures 3.4 and 3.5. Statistical significance was analyzed by Student's t-test, (\*= $p < 0.05$ ; \*\*= $p < 0.01$ ; \*\*\*= $p < 0.001$ ).

### **3.3.5 mEPSCs are uniformly activated in all synapses upon complexin KD**

Does the complexin KD uniformly increase spontaneous fusion in all synapses, or selectively activate a small subset of synapses? To examine this issue, we chose the synaptotagmin-antibody uptake assay (Matteoli et al., 1992), which measures the

presynaptic uptake of an antibody to the intravesicular N-terminal sequence of synaptotagmin-1 that becomes transiently exposed during exocytosis (Perin et al., 1991). However, the antibody used in the synaptotagmin-uptake assay is specific for rat. Thus, we first established the effectiveness of the complexin KD in rat neurons. We found that the complexin shRNAs caused a similar phenotype in rat and mouse neurons (Fig. 3.7), as expected since the shRNAs used for the KD target 100% conserved sequences, with the same effect of rescue by the wild-type complexin and WW-mutants, suggesting that mouse and rat neurons behave equivalently.

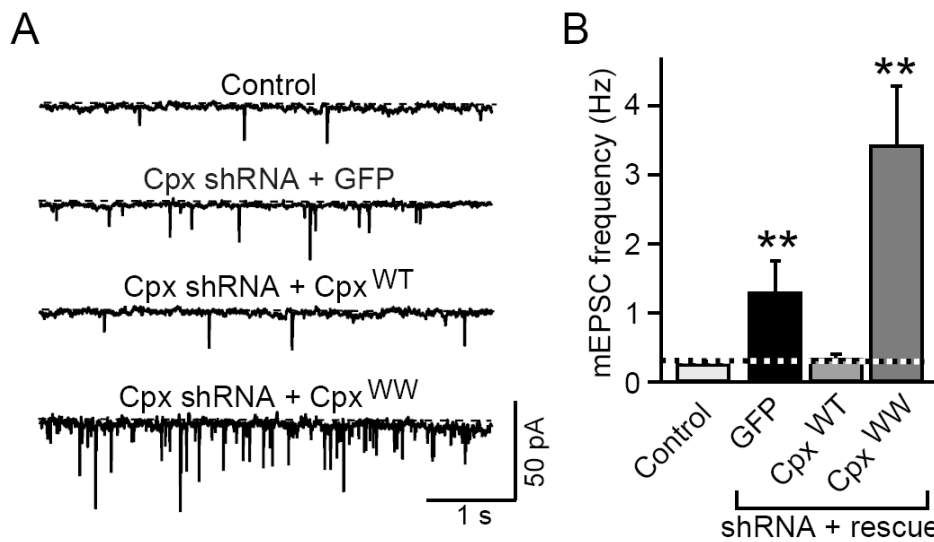


Figure 3.7. Complexin KD in rat neurons replicates effect of complexin KD in mouse neurons. A & B, Sample traces of mEPSCs (A) and summary graphs of the mEPSC frequency (B) recorded in cultured rat cortical neurons that were infected either with a control lentivirus, or the complexin KD lentivirus co-expressing GFP, wild-type

complexin (Cpx<sup>WT</sup>), or the WW-mutant of complexin (Cpx<sup>WW</sup>). Data shown are means  $\pm$  SEMs; statistical significance was analyzed by Student's t-test, (\*\*=p<0.01).

We next incubated control and KD rat neurons with the synaptotagmin-1 antibody, and stained the synapses using antibodies to the internalized antibody and to the vesicular glutamate transporter vGlut1 (to selectively visualize excitatory nerve terminals; Fig. 3.8A). Quantitation of the immunofluorescence signal in three independent experiments showed that the intensity of vGlut1 staining was unchanged in complexin KD neurons, whereas the amount of synaptotagmin-1 antibody uptake was increased >2-fold in the KD neurons (Figs. 3.8B-3.8D). This increase was rescued by expression of wild-type complexin, but not of WW-mutant complexin. Plots of the cumulative probability of the synaptotagmin-1 antibody uptake, normalized for the vGlut1 signal, confirmed that all excitatory synapses exhibited an increase in spontaneous exo- and endocytosis (Fig. 3.8E).

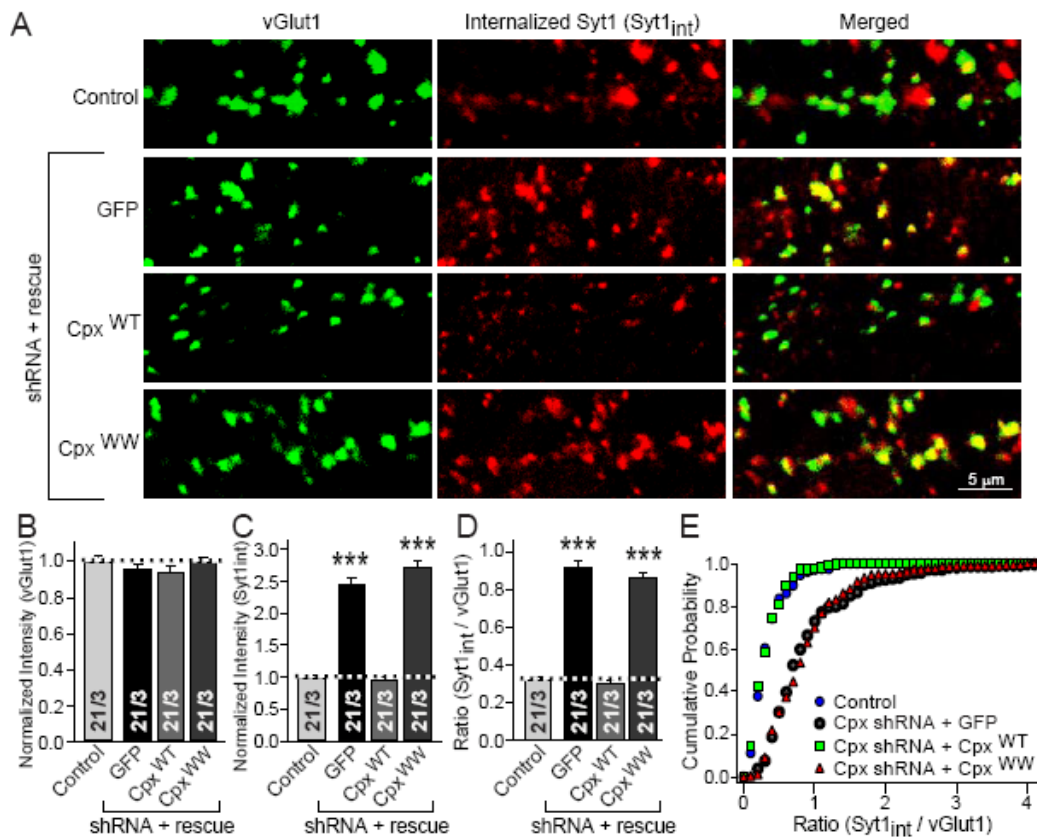


Figure 3.8 Synaptotagmin antibody uptake reveals that complexin KD causes uniform activation of spontaneous synaptic fusion

A, Representative images of cultured rat cortical neurons infected with control lentivirus or with lentivirus expressing the complexin shRNA plus either GFP, wild-type complexin, or WW-mutant complexin. Neurons were infected at DIV6, and incubated with a monoclonal antibody to the N-terminus of synaptotagmin-1 at DIV15, at which point they were fixed and analyzed by double immunofluorescence labeling for vGlut1 (to mark excitatory synapses) and the monoclonal synaptotagmin-1 antibody (to mark synapses which took up the antibody). Scale bar in the right lower corner applies to all images. B-D, Summary graphs of the normalized vGlut1-intensity, normalized

internalized synaptotagmin-1 antibody intensity (Syt1<sub>int</sub>), and their ratio (Syt1<sub>int</sub> divided vGlut1). Data shown are means ± SEMs; number of cells/independent cultures are depicted in the bars. Statistical significance was analyzed by Student's t-test, comparing complexin KD to control neurons (\*\*\*=p<0.001). For documentation that the complexin KD produces the same activation of spontaneous fusion in rat neurons as in mouse neurons, see Fig. 3.7. E, Cumulative distribution of uptake intensities.

### **3.3.6 Complexin KD activates delayed release**

Is the Ca<sup>2+</sup>-sensor that mediates increased spontaneous fusion in complexin-deficient synapses the same as the Ca<sup>2+</sup>-sensor that mediates asynchronous release? Asynchronous release is increased in synaptotagmin-1 KO neurons, consistent with this hypothesis (Maximov and Sudhof, 2005). However, because of network activity, asynchronous release is difficult to measure in excitatory synapses. To circumvent this problem, we selectively analyzed NMDA-receptor mediated EPSCs by recording in the presence of CNQX from postsynaptically depolarized neurons. To confirm that such recordings yield the same results as overall recordings of EPSCs in complexin-deficient synapses, we analyzed the effects of the complexin KD and rescue with poorclamp- and the WW-mutants of complexin on isolated EPSCs measured via the NMDA-receptor component. These results confirmed that the complexin KD decreased evoked release ~3-fold, and that this phenotype was rescued by the two mutant complexins (Figs. 3.9A, 3.9C, and 3.9D). Moreover, to confirm that these effects were similar to those of the synaptotagmin loss-of-function, we generated a synaptotagmin-1 KD, and found that it produced an even larger decrease of release as measured by the NMDA-receptor

dependent EPSC (Figs. 3.9B, 3.9C, and 3.9D). Finally, we measured the kinetics of the NMDA-receptor mediated EPSCs to exclude a postsynaptic effect, but observed no difference between control and complexin KD synapses (Fig. 3.10).

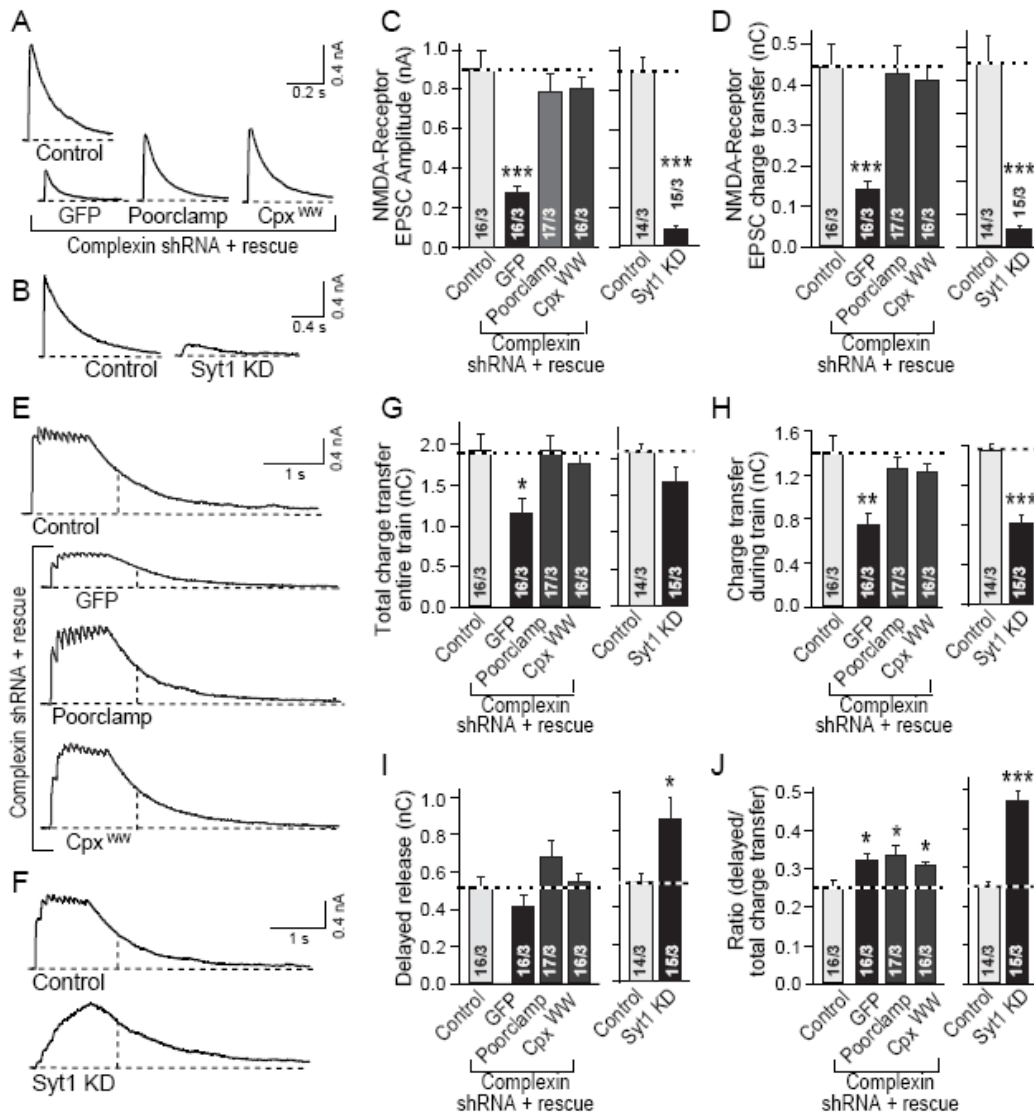


Figure 3.9 Effects of complexin and synaptotagmin-1 KDs on delayed release

A & B, Sample traces of evoked NMDA receptor-dependent EPSCs in control neurons and complexin KD neurons expressing either GFP only, or GFP together with complexin

poorclamp and WW-mutants (A), or in control and synaptotagmin-1 KD (Sy1 KD) neurons (B). For a kinetic analysis of evoked NMDA-receptor EPSCs, see Fig. 3.10 C & D, Summary graphs of the amplitudes (C) and charge transfers of evoked NMDA-receptor EPSCs (D) recorded in multiple experiments as illustrated in panels A and B. For documentation of the efficiency of the synaptotagmin-1 KD, see Fig. 3.10 E & F, Sample traces of NMDA receptor-mediated EPSCs induced by 1s 10 Hz action potential trains in control neurons and complexin KD neurons expressing GFP only, or GFP together with complexin poorclamp and WW-mutants (E), or in control and synaptotagmin-1 KD (Sy1 KD) neurons (F). Vertical dashed line = cutoff time for calculation of delayed release. G-J, Summary graphs of synaptic parameters determined in multiple independent experiments as shown in panels E and F. Panel G depicts the total synaptic charge transfer during and after the train; H depicts the synaptic charge transfer during the train only, I depicts the charge transfer during delayed release starting 500 ms after the last action potential (dashed vertical lines in panels E and F), and J depicts the ratio of delayed release to the total charge transfer.

All data shown are means  $\pm$  SEMs; number of cells/independent cultures analyzed are depicted in the bars. Statistical significance was analyzed by Student's t-test, comparing the various KD conditions to the control condition (\*= $p < 0.05$ ; \*\*= $p < 0.01$ ; \*\*\*= $p < 0.001$ ).

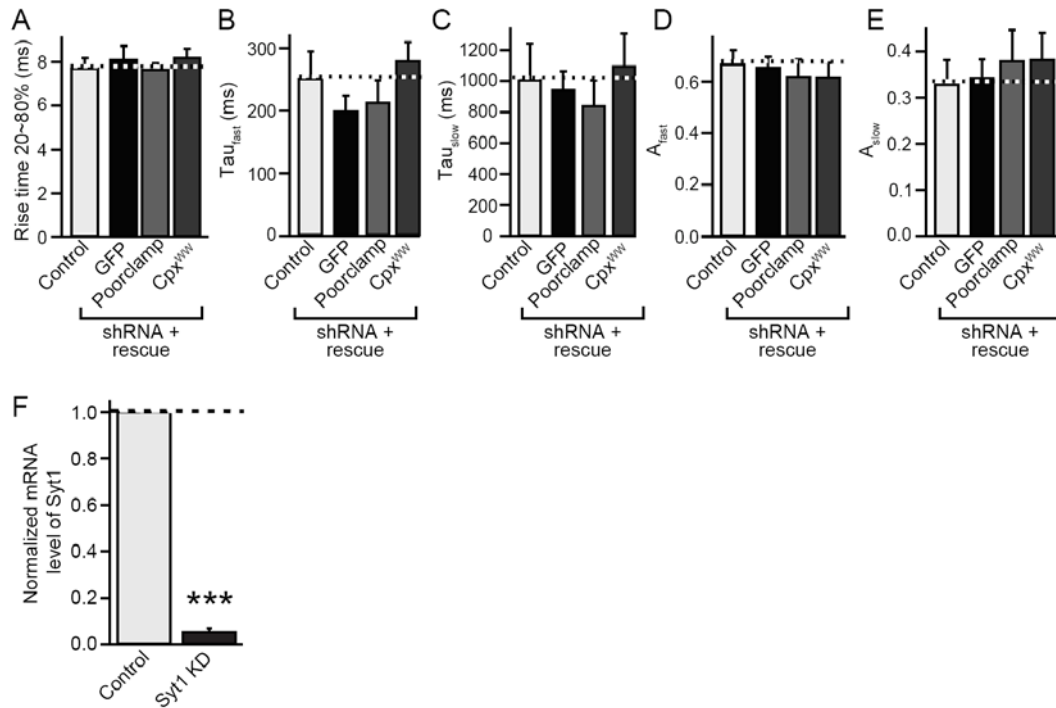


Figure 3.10. Kinetic analysis of evoked NMDA receptor-dependent EPSCs, and validation of the synaptotagmin-1 KD by lentivirally delivered shRNA. A-E, Summary graphs of kinetic parameters determined in evoked NMDA receptor-dependent EPSCs as shown in Figure 3.9. The rise time 20-80% (A), the  $\text{Tau}_{\text{fast}}$  (B), the  $\text{Tau}_{\text{slow}}$  (C), the  $A_{\text{fast}}$  (D) and  $A_{\text{slow}}$  (E) were shown in bar graphs. For the number of experiments, see Figure 3.9. F, Measurements of synaptotagmin-1 mRNA levels in cultured cortical neurons infected with a control lentivirus (Control) or a lentivirus expressing a synaptotagmin-1 shRNA (Syt1<sup>KD</sup>). Neurons from wild-type mice were infected at DIV6, and analyzed at DIV15. Data were obtained by Taqman quantitations of mRNA levels using GAPDH mRNAs as controls and showed a normalization by control neurons (n=3). Data shown are means  $\pm$  SEMs; statistical significance was analyzed by Student's t-test, (\*\*\*)= $p < 0.001$ .

We next examined the effects of the complexin KD and its rescue with the unclamping mutants on release induced by stimulus trains. In these experiments, the first response to a 10 Hz, 1 s stimulus train corresponds to that induced by an isolated action potential, whereas the remaining responses during the train are composed of both synchronous and asynchronous release, and depend on the size of the RRP. Delayed release, which is defined as the continuing release after the stimulus train has ended, is composed purely of asynchronous release (Maximov and Sudhof, 2005).

We found that release during the train was decreased significantly by the complexin KD, and rescued by the unclamping mutants of complexin (Figs. 3.9E, 3.9G, and 3.9H). Delayed release, however, was not decreased by the complexin KD, and the ratio of delayed to total release of significantly increased (Figs. 3.9I and 3.9J). Similar results were obtained with the synaptotagmin-1 KD, except that the synaptotagmin-1 KD does not produce a decrease in release during the stimulus train, presumably because it does not alter the RRP. Interestingly, whereas the unclamping mutants of complexin (the poorclamp- and WW-mutants) rescued the decrease in evoked release during the train, these mutants did not reverse the relative increase in delayed release (Figs. 3.9I and 3.9J).

### **3.3.7 Synaptobrevin WW-sequence clamps and activates release similar to complexin**

The SNARE protein synaptobrevin/VAMP is composed of a SNARE motif that is connected to a C-terminal transmembrane region via a short linker (Sudhof and Rothman, 2009). In the trans-SNARE complex, the entire synaptobrevin sequence from the beginning of the SNARE motif to the end of the transmembrane region forms a continuous  $\alpha$ -helix (Stein et al., 2009). The short linker contains two conserved vicinal tryptophans that project onto the surface of the vesicle membrane. We previously showed that substituting these tryptophans for alanines (the WA-mutation) phenocopies the complexin KD by increasing spontaneous release ~3-fold, and decreasing evoked release ~2-fold, without significantly affecting asynchronous release (Maximov et al., 2009). Based on these findings, we postulated that complexin and synaptotagmin – which bind to assembled SNARE complexes – control the force transfer from the complexes onto the membrane via a mechanism that involves the two tryptophan residues (Maximov et al., 2009).

Our finding that the complexin- and synaptotagmin-deficiencies increase spontaneous release by disinhibiting the actions of a secondary  $\text{Ca}^{2+}$ -sensor is consistent with this model, suggesting that complexin and synaptotagmin normally control the force transfer by blocking a second  $\text{Ca}^{2+}$ -sensor from catalyzing fusion (in addition to their separate activation functions). However, this model posits that the WA-mutation of synaptobrevin acts analogously, i.e., also increases spontaneous release by removing the clamp of the second  $\text{Ca}^{2+}$ -sensor. An alternative interpretation would be that the WA-mutation impairs the effectiveness of the SNARE complex in catalyzing exocytic

membrane fusion, and that the increased spontaneous release observed with the mutation is due to increased 'leakiness'.

To test these hypotheses, we cultured cortical neurons from synaptobrevin-2 KO mice, and infected them with control lentivirus or lentiviruses expressing wild-type or WA-mutant synaptobrevin-2. Recordings of spontaneous inhibitory synaptic events (mIPSCs) confirmed that the WA-mutation caused a large increase in spontaneous release (Figs. 3.11A and 3.11B). Preincubation of the neurons with 10  $\mu$ M BAPTA-AM completely reversed the increase, demonstrating that similar to the increased mEPSCs in synaptotagmin- and complexin-deficient neurons, the increased mIPSCs in WA-mutant neurons is  $\text{Ca}^{2+}$ -dependent (Figs. 3.11A and 3.11B).

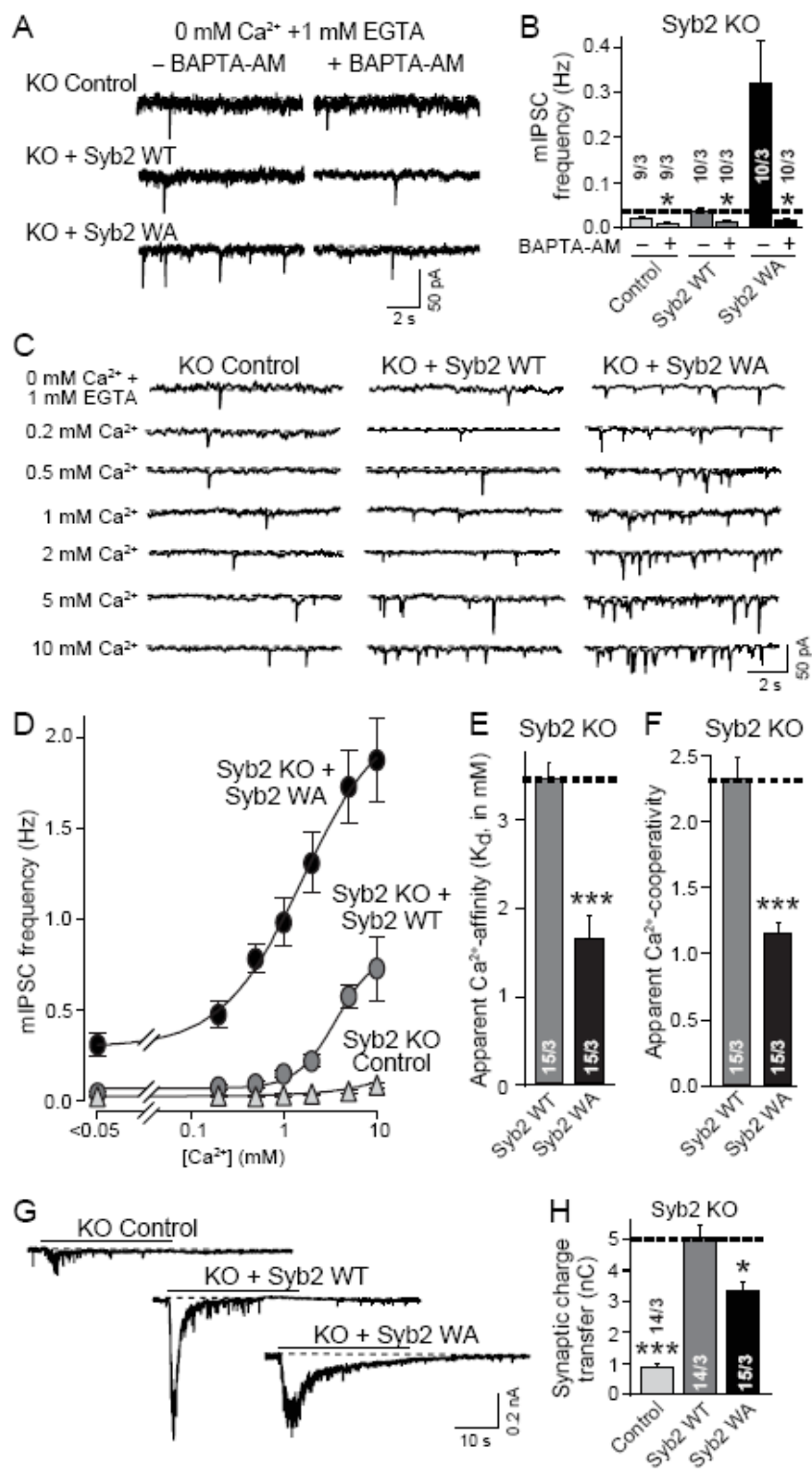


Figure 3.11 WA-mutation of synaptobrevin/VAMP-2 increases mIPSCs frequency by unclamping secondary  $\text{Ca}^{2+}$ -sensor

A & B, Sample traces of mIPSCs (A) and summary graphs of mIPSC frequencies (B) recorded in synaptobrevin-2 KO (Syb2 KO) neurons infected with a control lentivirus, or lentivirus expressing either wild-type synaptobrevin-2 (Syb2 WT) or the WA-mutant of synaptobrevin-2 (Syb2 WA). mIPSCs were recorded in medium lacking extracellular  $\text{Ca}^{2+}$  without or with a 30 min pretreatment with 10  $\mu\text{M}$  BAPTA-AM. C, Sample traces of mIPSCs recorded at the indicated concentrations of extracellular  $\text{Ca}^{2+}$  in synaptobrevin-2 KO (Syb2 KO) neurons infected with a control lentivirus, or lentivirus expressing either wild-type synaptobrevin-2 (Syb2 WT) or the WA-mutant of synaptobrevin-2 (Syb2 WA). D, Plot of the  $\text{Ca}^{2+}$ -dependence of the mIPSC frequency for the three types of neurons described in C. E & F, Bar diagram of the apparent  $\text{Ca}^{2+}$ -affinity (E) and  $\text{Ca}^{2+}$ -cooperativity (F) calculated from fits of the  $\text{Ca}^{2+}$ -dependence of the mIPSC frequency (as shown in D) to a Hill function in individual experiments performed ( $n=3$  independent cultures). G & H, Sample traces of sucrose-evoked IPSCs (G) and summary graphs of the charge transfer induced by hypertonic sucrose (H) recorded in synaptobrevin-2 KO (Syb2 KO) neurons infected with a control lentivirus, or lentivirus expressing either wild-type synaptobrevin-2 (Syb2 WT) or the WA-mutant of synaptobrevin-2 (Syb2 WA). Release was triggered by a 30 s application of 0.5 M sucrose, and the synaptic charge transfer was integrated over 30 s. All data shown are means  $\pm$  SEMs; number of cells/independent cultures analyzed are depicted in the bars. Statistical significance was analyzed by Student's t-test, comparing the  $\text{Ca}^{2+}$ -free to the control condition separately for control and three types of neurons (B), or the two

different WA-rescue and the pure KO condition to the wild-type synaptobrevin rescue neurons (for E, F, and H; \*=p<0.05; \*\*=p<0.01; \*\*\*=p<0.001).

We next titrated the  $\text{Ca}^{2+}$ -dependence of mISPCs release in synapses containing WA-mutant synaptobrevin, using the same approach as described above for complexin (Figs. 3.1C-3.1F). Similar to the complexin KD, the WA-mutation increased the apparent  $\text{Ca}^{2+}$ -affinity and decreased the apparent  $\text{Ca}^{2+}$ -cooperativity of spontaneous release (Figs. 3.11D-3.11F). This effect was not primarily due to a change in the efficiency of the effectiveness of the SNARE-complex containing WA-mutant synaptobrevin because the RRP, measured by hypertonic sucrose, was only marginally impaired (Figs. 3.11G and 3.11H). Thus, the WA-mutation of synaptobrevin in the SNARE complex impairs both aspects of synaptotagmin and complexin function – activation of  $\text{Ca}^{2+}$ -triggered release, and clamping of a secondary  $\text{Ca}^{2+}$ -sensor – despite the fact that complexin is present at wild-type levels and the mutation is not in the complexin-binding site.

### **3.4 Discussion**

Complexins are small SNARE-complex binding proteins that are essential for fast synchronous neurotransmitter release triggered by  $\text{Ca}^{2+}$ -binding to synaptotagmin (Huntwork and Littleton, 2007; Maximov et al., 2009; Reim et al., 2001; Tang et al., 2006; Xue et al., 2007). Complexins perform two major functions in release: they activate SNARE complexes for  $\text{Ca}^{2+}$ -triggered membrane fusion, and clamp spontaneous fusion.

Both functions require complexin-binding to nascent trans-SNARE complexes (Maximov et al., 2009). However, how complexin activates and clamps fusion remained unknown.

Here, we show that complexin activates fusion by promoting the priming of synaptic vesicles into the RRP, and clamps fusion by blocking a secondary  $\text{Ca}^{2+}$ -sensor. We demonstrate that the activation and clamping functions of complexin are encoded by separate complexin sequences, and provide evidence for the hypothesis that the accessory  $\alpha$ -helix of complexin – which was previously shown to mediate its clamping function (Giraud et al., 2009; Maximov et al., 2009; Xue et al., 2009) – inserts into partially assembled SNARE complexes during clamping. Based on these data, we propose that complexins function as molecular switches that are a prerequisite for synaptotagmin action in controlling both spontaneous and evoked release (Xue et al., 2009), but that these actions are mechanistically distinct.

### **Mechanism of complexin activation and clamping.**

Complexin-deficient synapses exhibit a decrease in the size of the RRP that precisely correlates with the decrease in evoked release (Figs. 3.4 and 3.5). Complexin mutants that rescue its activation but not its clamping function equally rescue the decrease in RRP and in evoked release, without a change in kinetics (Figs. 3.4, 3.5, and 3.6). Thus, complexin functions as a 'priming factor', and activates fusion by 'superpriming' secretory vesicles as a prerequisite for synaptotagmin action, consistent with results from chromaffin cells where complexins prime large-dense core vesicles for exocytosis (Cai et al., 2008). In mixed cultured neurons, the effect of the complexin KD on the RRP is the only qualitative difference between complexin- and synaptotagmin-

deficient synapses, in that synaptotagmin-deficient synapses do not exhibit a decrease the size of the RRP (Geppert et al., 1994; Xue et al., 2009).

Elegant biochemical studies suggested that the accessory  $\alpha$ -helix of complexin clamps SNARE complexes by intercalating into partially assembled complexes, thereby preventing full assembly of SNARE complexes (Giraudo et al., 2009; Lu et al., 2009). This hypothesis is consistent with the finding that  $\text{Ca}^{2+}$ -bound synaptotagmin competes for SNARE-complex binding with the central  $\alpha$ -helix of complexin, and disinhibits the complexin clamp by displacing the accessory  $\alpha$ -helix (Tang et al., 2006). We now identify complexin mutations in the accessory  $\alpha$ -helix ( $\text{Cpx}^{\text{poorclamp}}$  and  $\text{Cpx}^{\text{WW}}$ ), designed to decrease its insertion into the SNARE complex, that abolish the clamping function of complexin without affecting activation/priming function of complexin (Figs. 2-5). Thus, consistent with previous observations that the activation function of complexin can be abolished without changing its clamping function (Maximov et al., 2009), the activation and clamping functions of complexin are independent of each other, although both require SNARE-complex binding.

The SNARE-complex insertion mechanism of clamping appears to suggest that KD of complexin increases spontaneous fusion by increasing the rate of non-regulated full SNARE-complex assembly. However, this hypothesis conflicts with the observation that the KO of synaptotagmin increases spontaneous fusion by dis-inhibition of a secondary  $\text{Ca}^{2+}$ -sensor (Xu et al., 2009). This secondary  $\text{Ca}^{2+}$ -sensor operates at lower  $\text{Ca}^{2+}$ -concentrations than synaptotagmin because it has a lower  $\text{Ca}^{2+}$ -cooperativity, raising the question whether the increased spontaneous fusion in complexin-deficient synapses is

indeed due to an increased rate of non-regulated SNARE-complex assembly, or whether it may be due to the same mechanism as the synaptotagmin deficiency. A similar question applies to the WA-mutant in synaptobrevin, which changes the linker sequence of synaptobrevin connecting the assembling SNARE complex to the membrane, and which also increases spontaneous fusion (Maximov et al., 2009).

Using  $\text{Ca}^{2+}$ -chelation and  $\text{Ca}^{2+}$ -titration experiments, we demonstrate that synapses lacking complexin or containing WA-mutant synaptobrevin exhibit the same disinhibition of a secondary  $\text{Ca}^{2+}$ -sensor as synaptotagmin-deficient synapses (Figs. 3.1, 3.4, 3.5, 3.11 and 3.6). Imaging experiments showed that the increased spontaneous release is not restricted to a few hyperactivated synapses, but uniformly affects all synapses (Fig. 5). Thus, deletions of both synaptotagmin and complexin and mutation of the linker sequence connecting the SNARE complex to fusing membranes all disinhibit a secondary  $\text{Ca}^{2+}$ -sensor that resembles the  $\text{Ca}^{2+}$ -sensor for asynchronous release (Sun et al., 2007). Moreover, in complexin- and synaptotagmin-deficient synapses, asynchronous release is disinhibited (Fig. 3.9). This finding supports the notion that the same  $\text{Ca}^{2+}$ -sensor mediates the increased spontaneous and asynchronous release in these synapses, but testing this hypothesis will require identification of the asynchronous  $\text{Ca}^{2+}$ -sensor. The fact that the WA-mutant of synaptobrevin phenocopies the complexin- and synaptotagmin-deficiency states (Fig. 3.11 and (Maximov et al., 2009)) strongly suggests that this secondary  $\text{Ca}^{2+}$ -sensor, similar to synaptotagmin, enables SNARE complexes to translate the energy of assembly into a fusion process.

### **How does complexin work?**

Previously, we proposed a synaptotagmin-switch model that was based on the competition of complexin- and synaptotagmin-binding to SNARE complexes (Tang et al., 2006), and on the complexin-dependent block of fusion in the flipped-SNARE assay, which is released by  $\text{Ca}^{2+}$ -bound synaptotagmin (Giraudo et al., 2006). The synaptotagmin-switch model postulates that complexin clamps and activates SNARE-complexes for fusion, and that  $\text{Ca}^{2+}$  induces two parallel actions of synaptotagmin:  $\text{Ca}^{2+}$ -dependent binding to clamp/activated SNARE complexes to unlodge the complexin clamp, and  $\text{Ca}^{2+}$ -dependent binding to phospholipids to actively promote fusion.

The present data disprove parts of the original synaptotagmin-switch model, but confirm others. The fact that the activation and clamping functions of complexin are encoded by different complexin sequences (Figs. 3.4-3.8) demonstrates that complexin activation and clamping are not simply manifestations of the same activity as we had postulated (Tang et al., 2006). Instead, our data suggest that the activation function of complexin operates upstream of its clamping function at the step of vesicle priming, and is not directly coupled to synaptotagmin. At the same time, however, our data support the notion that complexin clamps fusion by inserting into the SNARE complex, and that synaptotagmin reverses the clamp by displacing it, in parallel to its active promotion of fusion by binding to phospholipids.

The most parsimonious hypothesis accounting for the functions of the six proteins which together mediate fast synchronous exocytosis – the three SNARE proteins, Munc18-1, synaptotagmin, and complexin – is that the Munc18/SNARE-complex assembly catalyzes fusion by forcing membranes together, but that an active

role of a  $\text{Ca}^{2+}$ -sensor is required for fusion-pore opening. For fast synchronous release, this  $\text{Ca}^{2+}$ -sensor is synaptotagmin; for slow asynchronous release, it is an as yet unidentified  $\text{Ca}^{2+}$ -binding protein with a lower  $\text{Ca}^{2+}$ -cooperativity than synaptotagmin (Sun et al., 2007). In a normal synapse, complexin activates SNARE complexes for subsequent synaptotagmin action by superpriming vesicles, and simultaneously clamps the secondary  $\text{Ca}^{2+}$ -sensor.  $\text{Ca}^{2+}$ -binding to synaptotagmin then triggers fusion by actively remodeling the phospholipid membranes (Arac et al., 2006; Hui et al., 2009; Martens et al., 2007; Stein et al., 2009), and by displacing the complexin clamp (Giraudo et al., 2006; Tang et al., 2006). The secondary  $\text{Ca}^{2+}$ -sensor cannot normally trigger fusion because it is unable to displace complexin, explaining how complexin normally inhibits asynchronous release. In the absence of either complexin or synaptotagmin, however, the secondary  $\text{Ca}^{2+}$ -sensor is free to trigger fusion, resulting in an overall increase in spontaneous mEPSCs because the lower  $\text{Ca}^{2+}$ -cooperativity of the second  $\text{Ca}^{2+}$ -sensor renders it active at lower  $\text{Ca}^{2+}$ -concentrations (Sun et al., 2007). This model is supported by the fact that the WA-mutation of synaptobrevin phenocopies the synaptotagmin- and complexin-deficiency state by disinhibiting the secondary  $\text{Ca}^{2+}$ -sensor, indicating that the complexin-clamp can be bypassed by a downstream mutation at the point where the SNARE-complex inserts into the membrane.

Although this model accounts for most observations, it does not explain how synaptotagmin clamps the secondary  $\text{Ca}^{2+}$ -sensor. It is possible that synaptotagmin interacts with the Munc18/SNARE-complex/complexin supramolecular assembly in a  $\text{Ca}^{2+}$ -independent manner, before  $\text{Ca}^{2+}$ -binding to synaptotagmin displaces the complexin

accessory  $\alpha$ -helix from the SNARE complex. This hypothesis is consistent with the  $\text{Ca}^{2+}$ -independent interactions of synaptotagmin with SNARE proteins (Bennett et al., 1992; Li et al., 1995; Pang et al., 2006b). Alternatively, it is possible that without synaptotagmin, vesicles in the Munc18/SNARE-complex/complexin supramolecular assembly state are at a 'dead end', and that filling the slots for this dead end results in an overflow of the remaining vesicles into the second pathway. Again, identification of the secondary  $\text{Ca}$ -sensory will be critical for testing these hypotheses.

### **Discrepancies between KD and KO experiments.**

It is striking that the complexin KD phenotype is significantly more severe than the complexin KO phenotype (e.g., compare (Maximov et al., 2009) with (Xue et al., 2009)). Evoked release is much more impaired after complexin KD than after complexin KO, and can be rescued by increased  $\text{Ca}^{2+}$  in complexin KO but not complexin KD synapses (Maximov et al., 2009; Reim et al., 2001; Xue et al., 2009; Xue et al., 2007). Even more noticeably, spontaneous release is disinhibited in complexin KD synapses (Maximov et al., 2009), whereas only a mild 'inhibitory function' is observed in for complexin in KO synapses (Xue et al., 2009). The mild KO phenotype led to the hypothesis that clamping is an evolutionarily divergent feature of complexins (Xue et al., 2009), but this hypothesis is difficult to reconcile with the clamping function observed for mammalian complexin in various biochemical and electrophysiological experiments (Giraudo et al., 2006; Giraudo et al., 2009; Maximov et al., 2009; Tang et al., 2006). At least three hypotheses may account the discrepancy between the severity of KD and KO phenotypes:

1. The different synapse types examined in complexin KO and KD neurons have distinct intrinsic properties. We analyzed synapses formed by mixed cultures of mouse and rat cortical neurons (Maximov et al., 2009; Tang et al., 2006), whereas most KO analyses were performed in autapses (Reim et al., 2001; Xue et al., 2009). This explanation agrees with the fact that KO or KD of synaptotagmin disinhibits spontaneous fusion in all synapses in cultured neurons and in slices except for autapses, suggesting that autapses may be inherently different from other types of synapses (Geppert et al., 1994; Maximov and Sudhof, 2005; Pang et al., 2006c; Sun et al., 2007; Xue et al., 2009). However, limited slice experiments with complexin KO mice also failed to detect an increase in spontaneous release (Xue et al., 2008).
2. The complexin KD phenotype may be due to off-target effects, a plausible possibility given the fact that the shRNA-mediated KD, in contrast to the KO, is not complete (Maximov et al., 2009). However, the rescue of all complexin KD phenotypes with wild-type complexin, and of specific facets of the phenotype with defined complexin mutants, argues strongly against this explanation. Moreover, the fact that rescue of the KO synapses partly reproduces the complexin KD rescue experiments (Xue et al., 2009) independently corroborates the KD experiments (Maximov et al., 2009).
3. The complexin KO may elicit compensatory effects, a possibility that is consistent with the notion that complexin may have a broader function in exocytosis than synaptotagmin, as evidenced by its priming role (Figs. 3 and 4, and (Cai et al., 2008)).

Independent of which of these explanations will turn out to be correct, there is little doubt that complexin is a major component of  $\text{Ca}^{2+}$ -triggered exocytosis. The fact that this tiny protein can mediate both activation and clamping of SNARE-dependent fusion, and does so by independent sequence modules of 20-30 residues, is amazing. In view of its small size, the selective effect of complexin as a clamp NOT of SNARE-complexes but of the second  $\text{Ca}^{2+}$ -sensor is particularly remarkable, and is consistent with a precise co-evolution of all complexin and synaptotagmin functions as suggested by their sequence conservations (Fig. 3.3A).

### **3.5 Future perspectives**

#### **3.5.1 Analyzing the function of C-terminal complexin**

Currently, we have a working model in which complexin clamps fusion by inserting its accessory  $\alpha$ -helix into SNARE complexes in addition to the SNARE complex binding via the central  $\alpha$ -helix. From our and other experiments, we also know that the N-terminal sequences are required for activation of fusion (Maximov et al., 2009; Xue et al., 2007). The molecular interactions and the functional importance of relatively long C-terminal sequences of complexin (87 -134 a.a), which encompass about 50% of the molecule, however, are not understood.

There have been some speculations that the C-terminal domain of complexin is essential in regulating the synaptic fusion. One biochemical study showed that complexin-1 directly binds to synaptotagmin 1 in a 1:1 stoichiometry at its C-terminal

domain (Tokumaru et al., 2008). Another study suggested that the C-terminus of complexin-1 stimulates SNARE assembly and membrane fusion, and phosphorylation at serine residue 115 may be involved in this function (Malsam et al., 2009). In addition, complexin-1 sequences (1-86 amino acids) lacking the C-terminal domain could not rescue decreased evoked release and increased spontaneous release in complexin KD neurons, suggesting that C-terminal domain plays an important role (Xiaofei Yang, Yea Jin Kaeser-Woo and Thomas C. Südhof, unpublished data). Based on these reports on the function of complexin C-terminus, we began to biochemically analyze the dependence of the interactions between complexin with SNARE complexes and synaptotagmins on the C-terminal sequences of complexin.

We first asked whether there is another ‘player’ in fusion clamping by complexin. Munc18-1, an SM (Sec1/Munc18-like) protein, is known to regulate  $\text{Ca}^{2+}$  - induced synaptic fusion together with synaptotagmins by clasping SNARE complexes (Dulubova et al., 2002; Yamaguchi et al., 2002). Since complexin and Munc18-1 work close to each other, one clamping and the other clasping the SNARE complexes, studying potential direct protein-protein interactions between complexin and Munc18-1 be worthwhile. Indeed, preliminary GST pull-down data showed that complexin-1 and Munc18-1 may bind directly to each other (unpublished data). In the light of these findings, I began to test interaction between complexin-1 and Munc18-1 in the presence and/or absence of C-terminal domain of complexin-1 using GST pull-down experiments.

Unfortunately, the results were inconclusive as different detergents (Triton X-100, CHAPS, sodium deoxycholate) resulted in different affinities between complexin-1, SNARE proteins and Munc18-1. Yet, the *in vitro* binding between Munc18-1 and

complexin-1 was completely abolished by the complexin 4M mutant, suggesting that under these conditions, there is no direct interaction between complexin and Munc18-1 that is independent of SNARE complex binding. Further biochemical and functional experiments will be performed to extend these results.

#### **2.4 Analyzing C-terminal complexin function by flipped SNARE fusion assay**

Alternative cell biological approach to study the mechanism of complexin function in synaptic fusion is the ‘flipped SNARE fusion assay’ developed by James Rothman group (Hu et al., 2003). The paradigm of this method is to express either t-SNARE proteins (SNAP-25 and syntaxin 1A) or v-SNARE protein synaptobrevin 2 on the extracellular surface of two separate groups of cells and to initiate cell-cell fusion by forming SNARE complexes. This elegant method has served to characterize the complexin clamping functions of the accessory  $\alpha$ -helix of complexin in non-neuronal cells (Giraud et al., 2006).

I am currently optimizing this assay in HEK 293T cell system to reproduce the clamping effect of complexin in cell-cell SNARE fusion, and to further evaluate the activating effect of synaptotagmin in fusion *in vitro*. If synaptotagmin fully recovers SNARE fusion from complexin clamping to the control amount, this assay will be considered as a working model system to test the interplay between SNAREs, complexin, synaptotagmin and SM proteins during fusion events, and I will further evaluate complexin with accessory  $\alpha$ -helix mutations (super-, poor-, WW-, and AA- mutants) or C-terminal mutations that change complexin-lipid binding affinities (as described from (Seiler et al., 2009)).

## BIBLIOGRAPHY

Akert, K., Moor, H., and Pfenninger, K. (1971). Synaptic fine structure. *Advances in cytopharmacology* 1, 273-290.

Arac, D., Chen, X., Khant, H.A., Ubach, J., Ludtke, S.J., Kikkawa, M., Johnson, A.E., Chiu, W., Sudhof, T.C., and Rizo, J. (2006). Close membrane-membrane proximity induced by Ca(2+)-dependent multivalent binding of synaptotagmin-1 to phospholipids. *Nat Struct Mol Biol* 13, 209-217.

Augustin, I., Rosenmund, C., Sudhof, T.C., and Brose, N. (1999). Munc13-1 is essential for fusion competence of glutamatergic synaptic vesicles. *Nature* 400, 457-461.

Bennett, M.K., Calakos, N., and Scheller, R.H. (1992). Syntaxin: a synaptic protein implicated in docking of synaptic vesicles at presynaptic active zones. *Science* 257, 255-259.

Betz, A., Thakur, P., Junge, H.J., Ashery, U., Rhee, J.S., Scheuss, V., Rosenmund, C., Rettig, J., and Brose, N. (2001). Functional interaction of the active zone proteins Munc13-1 and RIM1 in synaptic vesicle priming. *Neuron* 30, 183-196.

Brenner, S. (1974). The genetics of *Caenorhabditis elegans*. *Genetics* 77, 71-94.

Brose, N., Hofmann, K., Hata, Y., and Sudhof, T.C. (1995). Mammalian homologues of *Caenorhabditis elegans* unc-13 gene define novel family of C2-domain proteins. *J Biol Chem* 270, 25273-25280.

Bruce Alberts, A.J., Julian Lewis, Martin Raff, Keith Roberts, and Peter Walter (2002). *Molecular biology of the cell*, 4th edn (Garland Science).

Burnette, W.N. (1981). "Western blotting": electrophoretic transfer of proteins from sodium dodecyl sulfate--polyacrylamide gels to unmodified nitrocellulose and radiographic detection with antibody and radioiodinated protein A. *Anal Biochem* 112, 195-203.

Cai, H., Reim, K., Varoqueaux, F., Tapechum, S., Hill, K., Sorensen, J.B., Brose, N., and Chow, R.H. (2008). Complexin II plays a positive role in Ca<sup>2+</sup>-triggered exocytosis by facilitating vesicle priming. *Proc Natl Acad Sci U S A* 105, 19538-19543.

Castillo, P.E., Janz, R., Sudhof, T.C., Tzounopoulos, T., Malenka, R.C., and Nicoll, R.A. (1997). Rab3A is essential for mossy fibre long-term potentiation in the hippocampus. *Nature* 388, 590-593.

Castillo, P.E., Schoch, S., Schmitz, F., Sudhof, T.C., and Malenka, R.C. (2002). RIM1alpha is required for presynaptic long-term potentiation. *Nature* 415, 327-330.

Castro-Alamancos, M.A., and Calcagnotto, M.E. (1999). Presynaptic long-term potentiation in corticothalamic synapses. *J Neurosci* 19, 9090-9097.

Chen, X., Tomchick, D.R., Kovrigin, E., Arac, D., Machius, M., Sudhof, T.C., and Rizo, J. (2002). Three-dimensional structure of the complexin/SNARE complex. *Neuron* 33, 397-409.

Chevaleyre, V., and Castillo, P.E. (2003). Heterosynaptic LTD of hippocampal GABAergic synapses: a novel role of endocannabinoids in regulating excitability. *Neuron* 38, 461-472.

Chevaleyre, V., and Castillo, P.E. (2004). Endocannabinoid-mediated metaplasticity in the hippocampus. *Neuron* 43, 871-881.

Chevaleyre, V., Heifets, B.D., Kaeser, P.S., Sudhof, T.C., and Castillo, P.E. (2007). Endocannabinoid-mediated long-term plasticity requires cAMP/PKA signaling and RIM1alpha. *Neuron* 54, 801-812.

Chicka, M.C., and Chapman, E.R. (2009). Concurrent binding of complexin and synaptotagmin to liposome-embedded SNARE complexes. *Biochemistry* 48, 657-659.

Childers, S.R., and Deadwyler, S.A. (1996). Role of cyclic AMP in the actions of cannabinoid receptors. *Biochem Pharmacol* 52, 819-827.

Clary, D.O., Griff, I.C., and Rothman, J.E. (1990). SNAPs, a family of NSF attachment proteins involved in intracellular membrane fusion in animals and yeast. *Cell* 61, 709-721.

Couteaux, R., and Pecot-Dechavassine, M. (1970). [Synaptic vesicles and pouches at the level of "active zones" of the neuromuscular junction]. *Comptes rendus hebdomadaires des seances de l'Academie des sciences* 271, 2346-2349.

de Wit, H., Walter, A.M., Milosevic, I., Gulyas-Kovacs, A., Riedel, D., Sorensen, J.B., and Verhage, M. (2009). Synaptotagmin-1 docks secretory vesicles to syntaxin-1/SNAP-25 acceptor complexes. *Cell* 138, 935-946.

Deak, F., Xu, Y., Chang, W.P., Dulubova, I., Khvotchev, M., Liu, X., Sudhof, T.C., and Rizo, J. (2009). Munc18-1 binding to the neuronal SNARE complex controls synaptic vesicle priming. *J Cell Biol* 184, 751-764.

Dulubova, I., Sugita, S., Hill, S., Hosaka, M., Fernandez, I., Sudhof, T.C., and Rizo, J. (1999). A conformational switch in syntaxin during exocytosis: role of munc18. *Embo J* 18, 4372-4382.

Dulubova, I., Yamaguchi, T., Gao, Y., Min, S.W., Huryeva, I., Sudhof, T.C., and Rizo, J. (2002). How Tlg2p/syntaxin 16 'snares' Vps45. *EMBO J* 21, 3620-3631.

Dymecki, S.M. (1996). Flp recombinase promotes site-specific DNA recombination in embryonic stem cells and transgenic mice. *Proc Natl Acad Sci U S A* 93, 6191-6196.

Fernandez-Chacon, R., Konigstorfer, A., Gerber, S.H., Garcia, J., Matos, M.F., Stevens, C.F., Brose, N., Rizo, J., Rosenmund, C., and Sudhof, T.C. (2001). Synaptotagmin I functions as a calcium regulator of release probability. *Nature* 410, 41-49.

Fernandez, I., Arac, D., Ubach, J., Gerber, S.H., Shin, O., Gao, Y., Anderson, R.G., Sudhof, T.C., and Rizo, J. (2001). Three-dimensional structure of the synaptotagmin 1 C2B-domain: synaptotagmin 1 as a phospholipid binding machine. *Neuron* 32, 1057-1069.

Fernandez, I., Ubach, J., Dulubova, I., Zhang, X., Sudhof, T.C., and Rizo, J. (1998). Three-dimensional structure of an evolutionarily conserved N-terminal domain of syntaxin 1A. *Cell* 94, 841-849.

Fourcaudot, E., Gambino, F., Humeau, Y., Casassus, G., Shaban, H., Poulain, B., and Luthi, A. (2008). cAMP/PKA signaling and RIM1alpha mediate presynaptic LTP in the lateral amygdala. *Proc Natl Acad Sci U S A* 105, 15130-15135.

Fukuda, M. (2003). Distinct Rab binding specificity of Rim1, Rim2, rabphilin, and Noc2. Identification of a critical determinant of Rab3A/Rab27A recognition by Rim2. *J Biol Chem* 278, 15373-15380.

Fukuda, R., McNew, J.A., Weber, T., Parlati, F., Engel, T., Nickel, W., Rothman, J.E., and Sollner, T.H. (2000). Functional architecture of an intracellular membrane t-SNARE. *Nature* 407, 198-202.

Geppert, M., Goda, Y., Hammer, R.E., Li, C., Rosahl, T.W., Stevens, C.F., and Sudhof, T.C. (1994). Synaptotagmin I: a major Ca<sup>2+</sup> sensor for transmitter release at a central synapse. *Cell* 79, 717-727.

Gerber, S.H., Rah, J.C., Min, S.W., Liu, X., de Wit, H., Dulubova, I., Meyer, A.C., Rizo, J., Arancillo, M., Hammer, R.E., *et al.* (2008). Conformational switch of syntaxin-1 controls synaptic vesicle fusion. *Science* 321, 1507-1510.

Giraudo, C.G., Eng, W.S., Melia, T.J., and Rothman, J.E. (2006). A clamping mechanism involved in SNARE-dependent exocytosis. *Science* 313, 676-680.

Giraudo, C.G., Garcia-Diaz, A., Eng, W.S., Chen, Y., Hendrickson, W.A., Melia, T.J., and Rothman, J.E. (2009). Alternative zippering as an on-off switch for SNARE-mediated fusion. *Science* 323, 512-516.

Giraudo, C.G., Garcia-Diaz, A., Eng, W.S., Yamamoto, A., Melia, T.J., and Rothman, J.E. (2008). Distinct domains of complexins bind SNARE complexes and clamp fusion in vitro. *J Biol Chem* 283, 21211-21219.

Gracheva, E.O., Hadwiger, G., Nonet, M.L., and Richmond, J.E. (2008). Direct interactions between *C. elegans* RAB-3 and Rim provide a mechanism to target vesicles to the presynaptic density. *Neurosci Lett* 444, 137-142.

Hata, Y., Slaughter, C.A., and Sudhof, T.C. (1993). Synaptic vesicle fusion complex contains unc-18 homologue bound to syntaxin. *Nature* 366, 347-351.

Helmchen, F., Borst, J.G., and Sakmann, B. (1997). Calcium dynamics associated with a single action potential in a CNS presynaptic terminal. *Biophys J* 72, 1458-1471.

Hirano, T. (1991). Differential pre- and postsynaptic mechanisms for synaptic potentiation and depression between a granule cell and a Purkinje cell in rat cerebellar culture. *Synapse* 7, 321-323.

Ho, A., Morishita, W., Atasoy, D., Liu, X., Tabuchi, K., Hammer, R.E., Malenka, R.C., and Sudhof, T.C. (2006). Genetic analysis of Mint/X11 proteins: essential

presynaptic functions of a neuronal adaptor protein family. *J Neurosci* 26, 13089-13101.

Ho, A., Morishita, W., Hammer, R.E., Malenka, R.C., and Sudhof, T.C. (2003). A role for Mints in transmitter release: Mint 1 knockout mice exhibit impaired GABAergic synaptic transmission. *Proc Natl Acad Sci U S A* 100, 1409-1414.

Hu, C., Ahmed, M., Melia, T.J., Sollner, T.H., Mayer, T., and Rothman, J.E. (2003). Fusion of cells by flipped SNAREs. *Science* 300, 1745-1749.

Huang, Y.Y., Li, X.C., and Kandel, E.R. (1994). cAMP contributes to mossy fiber LTP by initiating both a covalently mediated early phase and macromolecular synthesis-dependent late phase. *Cell* 79, 69-79.

Hui, E., Johnson, C.P., Yao, J., Dunning, F.M., and Chapman, E.R. (2009). Synaptotagmin-mediated bending of the target membrane is a critical step in Ca(2+)-regulated fusion. *Cell* 138, 709-721.

Huntwork, S., and Littleton, J.T. (2007). A complexin fusion clamp regulates spontaneous neurotransmitter release and synaptic growth. *Nat Neurosci* 10, 1235-1237.

Jahn, R., and Sudhof, T.C. (1999). Membrane fusion and exocytosis. *Annu Rev Biochem* 68, 863-911.

Kaesler, P.S., Deng, L., Chavez, A.E., Liu, X., Castillo, P.E., and Sudhof, T.C. (2009). ELKS2alpha/CAST deletion selectively increases neurotransmitter release at inhibitory synapses. *Neuron* 64, 227-239.

Kaesler, P.S., Kwon, H.B., Blundell, J., Chevaleyre, V., Morishita, W., Malenka, R.C., Powell, C.M., Castillo, P.E., and Sudhof, T.C. (2008a). RIM1alpha phosphorylation at serine-413 by protein kinase A is not required for presynaptic long-term plasticity or learning. *Proc Natl Acad Sci U S A* 105, 14680-14685.

Kaesler, P.S., Kwon, H.B., Chiu, C.Q., Deng, L., Castillo, P.E., and Sudhof, T.C. (2008b). RIM1alpha and RIM1beta are synthesized from distinct promoters of the RIM1 gene to mediate differential but overlapping synaptic functions. *J Neurosci* 28, 13435-13447.

Kandel, E.R. (2001). The molecular biology of memory storage: a dialogue between genes and synapses. *Science* 294, 1030-1038.

Katz, B. (1969). *The Release of Neural Transmitter Substances*. Liverpool Univ Press, Liverpool.

Kauer, J.A., and Malenka, R.C. (2007). Synaptic plasticity and addiction. *Nat Rev Neurosci* 8, 844-858.

Kauer, J.A., Malenka, R.C., Perkel, D.J., and Nicoll, R.A. (1990). Postsynaptic mechanisms involved in long-term potentiation. *Adv Exp Med Biol* 268, 291-299.

Kim, J.H., and Huganir, R.L. (1999). Organization and regulation of proteins at synapses. *Curr Opin Cell Biol* 11, 248-254.

Lee, H.K., Takamiya, K., Han, J.S., Man, H., Kim, C.H., Rumbaugh, G., Yu, S., Ding, L., He, C., Petralia, R.S., *et al.* (2003). Phosphorylation of the AMPA

receptor GluR1 subunit is required for synaptic plasticity and retention of spatial memory. *Cell* 112, 631-643.

Li, C., Davletov, B.A., and Sudhof, T.C. (1995). Distinct Ca<sup>2+</sup> and Sr<sup>2+</sup> binding properties of synaptotagmins. Definition of candidate Ca<sup>2+</sup> sensors for the fast and slow components of neurotransmitter release. *J Biol Chem* 270, 24898-24902.

Linden, D.J., and Ahn, S. (1999). Activation of presynaptic cAMP-dependent protein kinase is required for induction of cerebellar long-term potentiation. *J Neurosci* 19, 10221-10227.

Littleton, J.T., Stern, M., Perin, M., and Bellen, H.J. (1994). Calcium dependence of neurotransmitter release and rate of spontaneous vesicle fusions are altered in *Drosophila* synaptotagmin mutants. *Proc Natl Acad Sci U S A* 91, 10888-10892.

Lonart, G., Janz, R., Johnson, K.M., and Sudhof, T.C. (1998). Mechanism of action of rab3A in mossy fiber LTP. *Neuron* 21, 1141-1150.

Lonart, G., Schoch, S., Kaeser, P.S., Larkin, C.J., Sudhof, T.C., and Linden, D.J. (2003). Phosphorylation of RIM1alpha by PKA triggers presynaptic long-term potentiation at cerebellar parallel fiber synapses. *Cell* 115, 49-60.

Lu, B., Song, S., and Shin, Y.K. (2009). Accessory alpha-helix of complexin I can displace VAMP2 locally in the complexin-SNARE quaternary complex. *J Mol Biol* 396, 602-609.

Malhotra, V., Orci, L., Glick, B.S., Block, M.R., and Rothman, J.E. (1988). Role of an N-ethylmaleimide-sensitive transport component in promoting fusion of transport vesicles with cisternae of the Golgi stack. *Cell* 54, 221-227.

Malsam, J., Seiler, F., Schollmeier, Y., Rusu, P., Krause, J.M., and Sollner, T.H. (2009). The carboxy-terminal domain of complexin I stimulates liposome fusion. *Proc Natl Acad Sci U S A* 106, 2001-2006.

Martens, S., Kozlov, M.M., and McMahon, H.T. (2007). How synaptotagmin promotes membrane fusion. *Science* 316, 1205-1208.

Martens, S., and McMahon, H.T. (2008). Mechanisms of membrane fusion: disparate players and common principles. *Nat Rev Mol Cell Biol* 9, 543-556.

Matteoli, M., Takei, K., Perin, M.S., Sudhof, T.C., and De Camilli, P. (1992). Exo-endocytotic recycling of synaptic vesicles in developing processes of cultured hippocampal neurons. *The Journal of cell biology* 117, 849-861.

Maximov, A., Lao, Y., Li, H., Chen, X., Rizo, J., Sorensen, J.B., and Sudhof, T.C. (2008). Genetic analysis of synaptotagmin-7 function in synaptic vesicle exocytosis. *Proc Natl Acad Sci U S A* 105, 3986-3991.

Maximov, A., Shin, O.H., Liu, X., and Sudhof, T.C. (2007). Synaptotagmin-12, a synaptic vesicle phosphoprotein that modulates spontaneous neurotransmitter release. *J Cell Biol* 176, 113-124.

Maximov, A., and Sudhof, T.C. (2005). Autonomous function of synaptotagmin 1 in triggering synchronous release independent of asynchronous release. *Neuron* 48, 547-554.

Maximov, A., Tang, J., Yang, X., Pang, Z.P., and Sudhof, T.C. (2009). Complexin controls the force transfer from SNARE complexes to membranes in fusion. *Science* 323, 516-521.

McMahon, H.T., Missler, M., Li, C., and Sudhof, T.C. (1995). Complexins: cytosolic proteins that regulate SNAP receptor function. *Cell* 83, 111-119.

McNew, J.A., Parlati, F., Fukuda, R., Johnston, R.J., Paz, K., Paumet, F., Sollner, T.H., and Rothman, J.E. (2000). Compartmental specificity of cellular membrane fusion encoded in SNARE proteins. *Nature* 407, 153-159.

Meinrenken, C.J., Borst, J.G., and Sakmann, B. (2003). Local routes revisited: the space and time dependence of the Ca<sup>2+</sup> signal for phasic transmitter release at the rat calyx of Held. *J Physiol* 547, 665-689.

Nagy, A., Rossant, J., Nagy, R., Abramow-Newerly, W., and Roder, J.C. (1993). Derivation of completely cell culture-derived mice from early-passage embryonic stem cells. *Proc Natl Acad Sci U S A* 90, 8424-8428.

Neher, E., and Sakaba, T. (2008). Multiple roles of calcium ions in the regulation of neurotransmitter release. *Neuron* 59, 861-872.

Nguyen, P.V., and Woo, N.H. (2003). Regulation of hippocampal synaptic plasticity by cyclic AMP-dependent protein kinases. *Progress in neurobiology* 71, 401-437.

Nicoll, R.A., Castillo, P.E., and Weisskopf, M.G. (1994). The role of Ca<sup>2+</sup> in transmitter release and long-term potentiation at hippocampal mossy fiber synapses. *Adv Second Messenger Phosphoprotein Res* 29, 497-505.

Nicoll, R.A., Kauer, J.A., and Malenka, R.C. (1988). The current excitement in long-term potentiation. *Neuron* 1, 97-103.

Nicoll, R.A., and Malenka, R.C. (1995). Contrasting properties of two forms of long-term potentiation in the hippocampus. *Nature* 377, 115-118.

Nicoll, R.A., and Schmitz, D. (2005). Synaptic plasticity at hippocampal mossy fibre synapses. *Nat Rev Neurosci* 6, 863-876.

Novick, P., Field, C., and Schekman, R. (1980). Identification of 23 complementation groups required for post-translational events in the yeast secretory pathway. *Cell* 21, 205-215.

O'Gorman, S., Dagenais, N.A., Qian, M., and Marchuk, Y. (1997). Protamine-Cre recombinase transgenes efficiently recombine target sequences in the male germ line of mice, but not in embryonic stem cells. *Proc Natl Acad Sci U S A* 94, 14602-14607.

Okamoto, M., and Sudhof, T.C. (1997). Mints, Munc18-interacting proteins in synaptic vesicle exocytosis. *J Biol Chem* 272, 31459-31464.

Pang, Z.P., Melicoff, E., Padgett, D., Liu, Y., Teich, A.F., Dickey, B.F., Lin, W., Adachi, R., and Sudhof, T.C. (2006a). Synaptotagmin-2 is essential for survival and contributes to Ca<sup>2+</sup> triggering of neurotransmitter release in central and neuromuscular synapses. *J Neurosci* 26, 13493-13504.

Pang, Z.P., Shin, O.H., Meyer, A.C., Rosenmund, C., and Sudhof, T.C. (2006b). A gain-of-function mutation in synaptotagmin-1 reveals a critical role of Ca<sup>2+</sup>-dependent soluble N-ethylmaleimide-sensitive factor attachment protein receptor complex binding in synaptic exocytosis. *J Neurosci* 26, 12556-12565.

Pang, Z.P., Sun, J., Rizo, J., Maximov, A., and Sudhof, T.C. (2006c). Genetic analysis of synaptotagmin 2 in spontaneous and Ca<sup>2+</sup>-triggered neurotransmitter release. *EMBO J* 25, 2039-2050.

Parlati, F., McNew, J.A., Fukuda, R., Miller, R., Sollner, T.H., and Rothman, J.E. (2000). Topological restriction of SNARE-dependent membrane fusion. *Nature* 407, 194-198.

Perin, M.S., Brose, N., Jahn, R., and Sudhof, T.C. (1991). Domain structure of synaptotagmin (p65). *J Biol Chem* 266, 623-629.

Pevsner, J. (1996). The role of Sec1p-related proteins in vesicle trafficking in the nerve terminal. *J Neurosci Res* 45, 89-95.

Potter, G.B., Facchinetti, F., Beaudoin, G.M., 3rd, and Thompson, C.C. (2001). Neuronal expression of synaptotagmin-related gene 1 is regulated by thyroid hormone during cerebellar development. *J Neurosci* 21, 4373-4380.

Reim, K., Mansour, M., Varoqueaux, F., McMahon, H.T., Sudhof, T.C., Brose, N., and Rosenmund, C. (2001). Complexins regulate a late step in Ca<sup>2+</sup>-dependent neurotransmitter release. *Cell* *104*, 71-81.

Richmond, J.E., Weimer, R.M., and Jorgensen, E.M. (2001). An open form of syntaxin bypasses the requirement for UNC-13 in vesicle priming. *Nature* *412*, 338-341.

Rizo, J., and Rosenmund, C. (2008). Synaptic vesicle fusion. *Nat Struct Mol Biol* *15*, 665-674.

Rizo, J., and Sudhof, T.C. (2002). Snares and Munc18 in synaptic vesicle fusion. *Nat Rev Neurosci* *3*, 641-653.

Rosahl, T.W., Geppert, M., Spillane, D., Herz, J., Hammer, R.E., Malenka, R.C., and Sudhof, T.C. (1993). Short-term synaptic plasticity is altered in mice lacking synapsin I. *Cell* *75*, 661-670.

Rosahl, T.W., Spillane, D., Missler, M., Herz, J., Selig, D.K., Wolff, J.R., Hammer, R.E., Malenka, R.C., and Sudhof, T.C. (1995). Essential functions of synapsins I and II in synaptic vesicle regulation. *Nature* *375*, 488-493.

Rosenmund, C., and Stevens, C.F. (1996). Definition of the readily releasable pool of vesicles at hippocampal synapses. *Neuron* *16*, 1197-1207.

Rothman, J.E. (1994). Mechanisms of intracellular protein transport. *Nature* *372*, 55-63.

Salin, P.A., Malenka, R.C., and Nicoll, R.A. (1996). Cyclic AMP mediates a presynaptic form of LTP at cerebellar parallel fiber synapses. *Neuron* 16, 797-803.

Schluter, O.M., Schmitz, F., Jahn, R., Rosenmund, C., and Sudhof, T.C. (2004). A complete genetic analysis of neuronal Rab3 function. *J Neurosci* 24, 6629-6637.

Schluter, O.M., Schnell, E., Verhage, M., Tzonopoulos, T., Nicoll, R.A., Janz, R., Malenka, R.C., Geppert, M., and Sudhof, T.C. (1999). Rabphilin knock-out mice reveal that rabphilin is not required for rab3 function in regulating neurotransmitter release. *J Neurosci* 19, 5834-5846.

Schoch, S., Castillo, P.E., Jo, T., Mukherjee, K., Geppert, M., Wang, Y., Schmitz, F., Malenka, R.C., and Sudhof, T.C. (2002). RIM1alpha forms a protein scaffold for regulating neurotransmitter release at the active zone. *Nature* 415, 321-326.

Seiler, F., Malsam, J., Krause, J.M., and Sollner, T.H. (2009). A role of complexin-lipid interactions in membrane fusion. *FEBS Lett* 583, 2343-2348.

Shao, X., Davletov, B.A., Sutton, R.B., Sudhof, T.C., and Rizo, J. (1996). Bipartite Ca<sup>2+</sup>-binding motif in C2 domains of synaptotagmin and protein kinase C. *Science* 273, 248-251.

Sollner, T., Bennett, M.K., Whiteheart, S.W., Scheller, R.H., and Rothman, J.E. (1993a). A protein assembly-disassembly pathway in vitro that may correspond to sequential steps of synaptic vesicle docking, activation, and fusion. *Cell* 75, 409-418.

Sollner, T., Whiteheart, S.W., Brunner, M., Erdjument-Bromage, H., Geromanos, S., Tempst, P., and Rothman, J.E. (1993b). SNAP receptors implicated in vesicle targeting and fusion. *Nature* 362, 318-324.

Southern, E.M. (1975). Detection of specific sequences among DNA fragments separated by gel electrophoresis. *Journal of molecular biology* 98, 503-517.

Spencer, J.P., and Murphy, K.P. (2002). Activation of cyclic AMP-dependent protein kinase is required for long-term enhancement at corticostriatal synapses in rats. *Neurosci Lett* 329, 217-221.

Spillane, D.M., Rosahl, T.W., Sudhof, T.C., and Malenka, R.C. (1995). Long-term potentiation in mice lacking synapsins. *Neuropharmacology* 34, 1573-1579.

Stegg, C.M., Ellis, J., and Bernstein, A. (1990). Introduction of specific point mutations into RNA polymerase II by gene targeting in mouse embryonic stem cells: evidence for a DNA mismatch repair mechanism. *Proc Natl Acad Sci U S A* 87, 4680-4684.

Stein, A., Weber, G., Wahl, M.C., and Jahn, R. (2009). Helical extension of the neuronal SNARE complex into the membrane. *Nature* 460, 525-528.

Sudhof, T.C. (2002). Synaptotagmins: why so many? *J Biol Chem* 277, 7629-7632.

Sudhof, T.C. (2004). The synaptic vesicle cycle. *Annu Rev Neurosci* 27, 509-547.

Sudhof, T.C., Czernik, A.J., Kao, H.T., Takei, K., Johnston, P.A., Horiuchi, A., Kanazir, S.D., Wagner, M.A., Perin, M.S., De Camilli, P., *et al.* (1989).

Synapsins: mosaics of shared and individual domains in a family of synaptic vesicle phosphoproteins. *Science* 245, 1474-1480.

Sudhof, T.C., and Rothman, J.E. (2009). Membrane fusion: grappling with SNARE and SM proteins. *Science* 323, 474-477.

Sun, J., Pang, Z.P., Qin, D., Fahim, A.T., Adachi, R., and Sudhof, T.C. (2007). A dual-Ca<sup>2+</sup>-sensor model for neurotransmitter release in a central synapse. *Nature* 450, 676-682.

Sutton, R.B., Fasshauer, D., Jahn, R., and Brunger, A.T. (1998). Crystal structure of a SNARE complex involved in synaptic exocytosis at 2.4 Å resolution. *Nature* 395, 347-353.

Tang, J., Maximov, A., Shin, O.H., Dai, H., Rizo, J., and Sudhof, T.C. (2006). A complexin/synaptotagmin 1 switch controls fast synaptic vesicle exocytosis. *Cell* 126, 1175-1187.

Thomas, G.M., and Huganir, R.L. (2004). MAPK cascade signalling and synaptic plasticity. *Nat Rev Neurosci* 5, 173-183.

Thompson, C.C. (1996). Thyroid hormone-responsive genes in developing cerebellum include a novel synaptotagmin and a hairless homolog. *J Neurosci* 16, 7832-7840.

Tokumaru, H., Shimizu-Okabe, C., and Abe, T. (2008). Direct interaction of SNARE complex binding protein synaphin/complexin with calcium sensor synaptotagmin 1. *Brain Cell Biol* 36, 173-189.

Tzounopoulos, T., Janz, R., Sudhof, T.C., Nicoll, R.A., and Malenka, R.C. (1998). A role for cAMP in long-term depression at hippocampal mossy fiber synapses. *Neuron* 21, 837-845.

Ungar, D., and Hughson, F.M. (2003). SNARE protein structure and function. *Annu Rev Cell Dev Biol* 19, 493-517.

Verhage, M., Maia, A.S., Plomp, J.J., Brussaard, A.B., Heeroma, J.H., Vermeer, H., Toonen, R.F., Hammer, R.E., van den Berg, T.K., Missler, M., *et al.* (2000). Synaptic assembly of the brain in the absence of neurotransmitter secretion. *Science* 287, 864-869.

Villacres, E.C., Wong, S.T., Chavkin, C., and Storm, D.R. (1998). Type I adenylyl cyclase mutant mice have impaired mossy fiber long-term potentiation. *J Neurosci* 18, 3186-3194.

von Poser, C., Ichtchenko, K., Shao, X., Rizo, J., and Sudhof, T.C. (1997). The evolutionary pressure to inactivate. A subclass of synaptotagmins with an amino acid substitution that abolishes Ca<sup>2+</sup> binding. *J Biol Chem* 272, 14314-14319.

Wang, Y., Okamoto, M., Schmitz, F., Hofmann, K., and Sudhof, T.C. (1997). Rim is a putative Rab3 effector in regulating synaptic-vesicle fusion. *Nature* 388, 593-598.

Weisskopf, M.G., Castillo, P.E., Zalutsky, R.A., and Nicoll, R.A. (1994). Mediation of hippocampal mossy fiber long-term potentiation by cyclic AMP. *Science* 265, 1878-1882.

Weisskopf, M.G., and Nicoll, R.A. (1995). Presynaptic changes during mossy fibre LTP revealed by NMDA receptor-mediated synaptic responses. *Nature* 376, 256-259.

Williams, R.W., and Herrup, K. (1988). The control of neuron number. *Annu Rev Neurosci* 11, 423-453.

Wilson, D.W., Wilcox, C.A., Flynn, G.C., Chen, E., Kuang, W.J., Henzel, W.J., Block, M.R., Ullrich, A., and Rothman, J.E. (1989). A fusion protein required for vesicle-mediated transport in both mammalian cells and yeast. *Nature* 339, 355-359.

Xiang, Z., Greenwood, A.C., Kairiss, E.W., and Brown, T.H. (1994). Quantal mechanism of long-term potentiation in hippocampal mossy-fiber synapses. *J Neurophysiol* 71, 2552-2556.

Xu, J., Mashimo, T., and Sudhof, T.C. (2007). Synaptotagmin-1, -2, and -9: Ca<sup>2+</sup> sensors for fast release that specify distinct presynaptic properties in subsets of neurons. *Neuron* 54, 567-581.

Xu, J., Pang, Z.P., Shin, O.H., and Sudhof, T.C. (2009). Synaptotagmin-1 functions as a Ca<sup>2+</sup> sensor for spontaneous release. *Nat Neurosci* 12, 759-766.

Xue, M., Lin, Y.Q., Pan, H., Reim, K., Deng, H., Bellen, H.J., and Rosenmund, C. (2009). Tilting the balance between facilitatory and inhibitory functions of mammalian and *Drosophila* Complexins orchestrates synaptic vesicle exocytosis. *Neuron* *64*, 367-380.

Xue, M., Reim, K., Chen, X., Chao, H.T., Deng, H., Rizo, J., Brose, N., and Rosenmund, C. (2007). Distinct domains of complexin I differentially regulate neurotransmitter release. *Nat Struct Mol Biol* *14*, 949-958.

Xue, M., Stradomska, A., Chen, H., Brose, N., Zhang, W., Rosenmund, C., and Reim, K. (2008). Complexins facilitate neurotransmitter release at excitatory and inhibitory synapses in mammalian central nervous system. *Proc Natl Acad Sci U S A* *105*, 7875-7880.

Yamaguchi, T., Dulubova, I., Min, S.W., Chen, X., Rizo, J., and Sudhof, T.C. (2002). Sly1 binds to Golgi and ER syntaxins via a conserved N-terminal peptide motif. *Dev Cell* *2*, 295-305.

Yang, Y., and Calakos, N. (2010). Acute in vivo genetic rescue demonstrates that phosphorylation of RIM1alpha serine 413 is not required for mossy fiber long-term potentiation. *J Neurosci* *30*, 2542-2546.

Yoon, T.Y., Lu, X., Diao, J., Lee, S.M., Ha, T., and Shin, Y.K. (2008). Complexin and Ca<sup>2+</sup> stimulate SNARE-mediated membrane fusion. *Nat Struct Mol Biol* *15*, 707-713.

Young, S.M., Jr., and Neher, E. (2009). Synaptotagmin has an essential function in synaptic vesicle positioning for synchronous release in addition to its role as a calcium sensor. *Neuron* 63, 482-496.

Zhang, X., Rizo, J., and Sudhof, T.C. (1998). Mechanism of phospholipid binding by the C2A-domain of synaptotagmin I. *Biochemistry* 37, 12395-12403.